Trend, Cycle and Expectation Formation*

HENG CHEN
University of Hong Kong
YICHENG LIU
University of Hong Kong

October 4, 2024

Abstract. We document a set of empirical patterns in forecasting behaviors across different horizons that are inconsistent with the common assumption in the expectation formation literature that trends are observable. To address this, we propose a model characterizing how forecasters form expectations when they cannot perfectly distinguish between trends and cycles. Our model not only organizes these empirical patterns well but also accounts for changes in forecasting behavior following the introduction of explicit inflation targeting in 2012. Furthermore, we demonstrate that overlooking this friction can lead policymakers to design sub-optimal policies, underscoring its relevance for policy design.

Keywords. trend, cycle, expectation formation, inflation expectation.

JEL Classification. D83, D84,E37

*Heng CHEN: hengchen@hku.hk; Yicheng LIU: Yicheng@connect.hku.hk.

1 Introduction

There is a growing interest in understanding how forecasters form expectations and make forecasts on macroeconomic variables. The literature on expectation formation primarily focuses on how forecasters make predictions for macroeconomic variables following a stationary process, with fewer studies investigating how they deal with trends and cycles in their expectation formation process. In this paper, we introduce a simple framework to characterize how forecasters update their beliefs, form expectations and make forecasts when macroeconomic variables consist of trends and forecasters cannot perfectly distinguish between trends and cycles.

This paper makes three key contributions. First, we develop a theoretical framework demonstrating that when trends and cycles are not perfectly distinguishable, forecasting behaviors can deviate qualitatively from the predictions of standard models with stable or stochastic but observable trends. In some cases, our model predicts forecasting patterns opposite to those of standard models. Second, we present empirical evidence on how forecasting behaviors vary across different forecast horizons, shedding light on the process of expectation formation. Our findings are inconsistent with the assumption of stable or observable trends, instead supporting our framework with additional friction in distinguishing trends and cycles. Third, we demonstrate the policy relevance of this novel information friction in a policy game where policymakers have a superior ability to distinguish between trends and cycles compared to private sector agents. We show that if policymakers overlook this discrepancy in information friction when designing optimal policies, the resulting policies may be sub-optimal.

We begin with our empirical explorations. In this study, we use data from the Survey of Professional Forecasters (SPF). First, we examine the covariance between changes in long-run forecasts and changes in short-run cyclical forecasts at the forecaster level. Specifically, we consider three-year-ahead forecasts for macroeconomic variables, such as the real GDP growth rate and the unemployment rate, as long-run forecasts. The difference between the h quarters ahead forecast of a relevant macroeconomic variable and its three-year-ahead forecast is defined as the cyclical forecast, capturing short-run deviations from the long-run forecast.

We then construct 'across-period changes' in both long-run and cyclical forecasts for each forecaster. Changes in long-run forecasts are calculated as the difference between their three-year-ahead forecasts in quarters t and $t-1$. Similarly, we calculate changes in cyclical forecasts. By construction, changes in long-run forecasts reflect belief changes in both the trend and cyclical components, while changes in cyclical forecasts are proportional to belief changes in the cyclical component.

The observable-trend model predicts a positive covariance between changes in

long-run forecasts and cyclical forecasts, as the same cyclical component drives both. This covariance should decrease as h increases, converging to zero when h approaches three years, since the cyclical component plays a lesser role over longer horizons. However, our empirical findings contrast this theoretical prediction. For both real GDP growth and the unemployment rate, the covariance of interest is negative and increases as h increases in the SPF data. In other words, not only is the sign of the covariance opposite to what is predicted, but its pattern over the horizon h is also reversed.

Second, we examine how the cross-sectional dispersion of forecasts varies over the forecast horizon. The observable-trend model predicts that forecast dispersion across forecasters should monotonically decrease as the forecast horizon increases, whether the horizon is short-run or long-run. This is because disagreement among forecasters, caused by heterogeneous information about cyclical components, would diminish as the forecast horizon extends.[1]

Using the SPF data, we observe that for most macroeconomic variables (after being transformed into growth rates), except for inflation, forecast dispersion increases as the forecast horizon extends from zero to four quarters ahead. This contradicts the observable-trend model, which predicts that dispersion should decrease over the horizon, even within a year. Additionally, we examine year-level forecast dispersion for real GDP growth and the unemployment rate over a longer forecast horizon and show that it increases as the horizon expands from one to three years. This evidence also contradicts the predictions of the observable-trend model.

Motivated by those findings, we propose an otherwise standard forecasting model that explicitly incorporates a non-stationary, unobservable trend component in the data generation process. Specifically, in this model, the state variable consists of a non-stationary random walk trend component and a cyclical component that follows the standard AR(1) process. The goal of forecasters is to minimize the squared error of their forecasts. The actual value of the state, which is the sum of these two components, is publicly announced and observed by forecasters at the end of each period.

The key assumption is that forecasters cannot directly observe the actual realizations of the trend and cyclical components. Instead, in each period, they receive two private noisy signals on the trend and cyclical components, respectively. This means that they are unable to differentiate the two components perfectly and have to make inferences about them.

In such a setting, forecasters will need to update their beliefs about the trend and cyclical components *twice* in each period. At the beginning of each period, forecasters

[1]For example, if the forecasted variable is assumed to follow a stationary data generation process (e.g., an AR(1) process with a constant long-run mean), when the forecast horizon is long enough, all the forecasts should converge to that long-run mean, and the forecast dispersion would go to zero.

receive private signals regarding the trend and cyclical components and then revise their beliefs on each component. Forecasters use this set of posterior beliefs to make forecasts that minimize the expected forecasting errors. At the end of each period, the actual state value is disclosed, which is informative about the trend and cyclical components as well. Therefore, forecasters will have to update their beliefs again, making revisions to their beliefs about the two components. That is the key difference from the situation where forecasters could differentiate trends and cycles perfectly. In that case, upon observing the actual state value, forecasters know the state perfectly, rendering their beliefs about the two components when they make forecasts redundant.

In this model, forecasters do not update their beliefs about the trend and cyclical components independently. In other words, they are rationally confused about distinguishing between the trend and cyclical components. For instance, when they perceive the trend component to be stronger than it actually is, they simultaneously perceive the cyclical component to be weaker than it actually is. In the following, we show that the confusion regarding the trend and cyclical components helps account for the documented empirical patterns.

Specifically, in the presence of this confusion mechanism, a positive trend signal plays a dual role. First, it provides information about the trend, indicating a strong trend component in the current period. Consequently, forecasters revise their posterior beliefs regarding the trend component upwards, from the prior beliefs inherited from the previous period. Second, the positive trend signal is useful for updating beliefs on the cyclical component. Forecasters rationally interpret the positive trend signal as indicating three possibilities: a positive state innovation in the trend, a positive noise in the signal, as well as an underestimation of the trend component in the previous period. Recognizing the likelihood of having underestimated the trend component previously, forecasters would conclude that they had likely overestimated the cyclical component previously. Consequently, they would revise their current beliefs regarding the cyclical component downward.[2]

In summary, the confusion between trend and cyclical components leads forecasters to rationally update their beliefs about these components in opposite directions. This mechanism gives rise to a negative covariance between the two beliefs. In the data, the constructed covariance between changes in long-term forecasts and changes in cyclical forecasts is proportional to the sum of the negative covariance of beliefs and the dispersion of beliefs about the cyclical component. When the confusion mechanism dominates, the covariance between changes in long-term and cyclical forecasts could be negative. Furthermore, as the forecast horizon h, which is used to construct

[2]Likewise, upon receiving a positive signal about the cyclical component, forecasters would revise their posterior beliefs about the cyclical component upwards from the prior beliefs inherited from the previous period. Additionally, they would revise their belief about the trend component downwards.

the cyclical forecasts, increases, the constructed change in cyclical forecasts reflects a smaller proportion of the changes in cyclical components. Therefore, the covariance of changes in forecasts should also diminish in magnitude as h increases.

This mechanism can also account for the observed increase in forecast dispersion over horizons. In this model, for any forecast horizon, the dispersion of forecasts can be broken down into three parts: the dispersion caused by heterogeneous beliefs about the cyclical and trend components, as well as their covariance. Similar to the predictions of the observable-trend model, the dispersion caused by heterogeneous beliefs about the cyclical component decreases over the forecast horizon, as the cyclical component becomes less influential for longer-term forecasts. Further, the dispersion caused by heterogeneous beliefs about the trend component is constant over the forecast horizon, as the trend component is equally important for all horizons.

The third part, characterized by the *negative covariance* of cross-forecaster mean beliefs regarding the two components, is a novel aspect of the model. It stems from forecasters' inability to perfectly distinguish between trends and cycles, and its importance diminishes over the forecast horizon as the cyclical component itself becomes less influential in forecasting. Therefore, the overall dispersion could either increase or decrease over horizon. We show that forecast dispersion would increases, under the condition that the trend is neither too volatile nor stable.

Application I: Explicit Inflation Targeting. Our framework not only helps organize the documented empirical findings but also offers insights into various policy-relevant issues related to expectation formation. To illustrate this, we examine the impact of implementing inflation targeting policy on forecasting behaviors. In 2012, the United States introduced an explicit inflation target of 2 percent for the first time (Shapiro and Wilson 2019). Through the lens of our framework, this policy can be interpreted as a shift in the data-generating process for inflation.

To uncover the corresponding change, we conduct structural estimation using the simulated method of moments (SMM) for both pre-2012 and post-2012 periods. We find that in the post-2012 period, the variance of the trend innovation becomes smaller, and the persistence of the cyclical component is also lower. These observed changes are intuitive, suggesting that after the policy shift, the central bank has a specific long-run target and would respond more to short-term deviations from the long-term target. As a result, forecasters would perceive that the trend component becomes more stable, and the cyclical fluctuation becomes less persistent.

What would be the consequences of this policy shift for forecasting behaviors? We have documented a set of changes in the pattern of inflation expectations across the two periods. First, using the inflation expectation data from the pre-2012 subsample, we find a statistically significant negative covariance between changes in forecasters'

long-run forecasts and those of the cyclical forecasts. However, after 2012, this covariance becomes positive and statistically insignificant. Second, we observe a steeper decline in forecast dispersion over the horizon in the post-2012 subsample compared to the preceding period.

We further demonstrate that the observed changes in forecasting behaviors following the policy shift are consistent with the predictions of our model, provided there is a decrease in the variance of trend innovations and a reduction in the persistence of cyclical components.

Application II: Optimal Policy. To illustrate that the new information friction we document and characterize is policy relevant, we consider the role of confusion in a monetary policy game, following Barro and Gordon (1983) and Huo et al. (2024). Central banks often possess superior ability to separate trend and cyclical components of desired inflation compared to the public. However, when designing monetary policy, central banks may overlook or misjudge this asymmetrical degree of confusion.

Our analysis demonstrates that such misperception leads to sub-optimal policies and additional welfare losses. These losses occur because the central bank's policy, based on an inaccurate assessment of the public's information set, creates a discrepancy between intended and actual economic outcomes. Specifically, when the central bank overestimates the public's ability to distinguish between inflation components, it fails to account for the full extent of uncertainty in private sector expectations. This misjudgment becomes more consequential as greater weight is assigned to unemployment relative to inflation targeting.

Discussion. We extend the model to allow forecasters access to a full range of multi-horizon forecasts from other forecasters at each period's end. These forecasts provide information about aggregate beliefs on trend and cyclical components, enriching the forecasters' information set. Despite this additional information, we show that forecasters still cannot perfectly differentiate between trend and cyclical components. While they can derive consensus forecasts for both components, these consensus forecasts retain time-varying errors. Importantly, our key qualitative results remain robust in this extended scenario.

We also examine an alternative scenario where confusion arises from forecasters misinterpreting signals. In such a model, forecasters observe trend and cyclical components at period-end but infer these components for the next period based on signals. Some forecasters may mistake trend signals for cyclical ones, and vice versa. This model can predict increasing forecast dispersion over horizons when the fraction of misinterpreting forecasters is moderate. However, it always predicts a non-negative covariance between changes in trend and cyclical forecasts, contradicting our findings.

Furthermore, we revisit the seminal work by Coibion and Gorodnichenko (2015) within our framework. They proposed using the coefficient from regressing forecast errors on forecast revisions at the consensus level to quantify information frictions. We demonstrate that in our model, this coefficient also captures the confusion between trends and cycles, providing a lower bound on the extent of information frictions in the data.

Literature Review. This paper complements recent studies that use survey data to investigate expectation formation. Studies within the noisy information paradigm have found that forecasters tend to under-react to new information at the aggregate level (Coibion and Gorodnichenko 2015), but exhibit overreactions at the individual level (Bordalo et al. 2020; Broer and Kohlhas 2022). New contributions to this literature further expand its scope. For instance, Kohlhas and Walther (2021) explore why individual forecast errors are negatively correlated with current realizations, while Rozsypal and Schlafmann (2023) examine how forecaster characteristics influence individual forecasts errors.

A common feature of these studies is that they assume the data-generating process for the state is stationary, often an AR(1) process. Our work examines a scenario in which the data generation process of the forecasted state incorporates a non-stationary trend component. This exploration is not only realistic but also empirically relevant, as prior research has established the presence of non-stationary trends in various macroeconomic variables, such as GDP growth rate (Stock and Watson 1998) and the unemployment rate (Blanchard and Summers 1986).[3] Our work emphasizes that the unobservability of trends to forecasters is crucial for understanding the patterns of forecasting behaviors. This framework, even in its simplest form, yields several predictions that align with a set of empirical facts concerning how forecast behaviors vary over the forecast horizon.

Farmer et al. (2024) presents a Bayesian learning model within a trend-cycle framework, focusing on model uncertainty about the data generation process as a key friction rather than noisy information. Their model addresses several anomalies in consensus forecasts. In contrast, our work, grounded in the paradigm of noisy information, examines heterogeneity in individual forecasting behaviors and uses variations in forecasting patterns across different forecast horizons to inform the process of expectation formation.

Fisher et al. (2024) present a behavioral model within a trend-cycle framework to address two important anomalies in long run inflation expectation data: the persistent

[3]Early studies such as Nelson and Plosser (1982) and Harvey (1985) have demonstrated the presence of a non-stationary trend component in GDP growth. Similar findings have also been observed in studies analyzing inflation data, such as Cogley and Sargent (2005) and Cogley and Sbordone (2008).

deviations of average expectations from actual trend inflation, and large and persistent disagreement regarding long-run inflation. They show that these misspecifications can be corrected by assuming forecasters misperceive the persistence and precision of their own private information. Our work, however, has a different focus: the pattern of covariance between changes in long-term forecasts and cyclical forecasts over the forecast horizon for macroeconomic variables in general. Moreover, our key confusion mechanism is fully rational.[4]

Our work contributes to a line of research examining forecasting behaviors across different forecast horizons. Afrouzi et al. (2023) who show that forecasting behaviors could vary over the forecast horizon within a lab setting. We document how forecasting behaviors vary over the forecast horizon in the survey data and find that they can be informative about how forecasters update beliefs and form expectations.

Furthermore, a number of studies have documented that forecast dispersion tend to be larger in the long run. Lahiri and Sheng (2008) and Patton and Timmermann (2010) assume that forecasters possess a diverse set of prior beliefs. As the forecast horizon extends, forecasters assign less weight to new information and instead rely more on their prior beliefs. Our model differs in that the confusion mechanism is rational rather than behavioral. Andrade et al. (2016) consider a case where forecasters can only occasionally observe the state value (i.e., the sticky information assumption) and the current trend shock has a more pronounced effect on the future state compared to its impact on the current state. Our model features noisy information and the trend component holds equal importance across all horizons. In addition, our model predicts that the changes in trend forecasts and changes in cyclical forecasts can be negatively correlated.

2 Evidence

This section presents two key empirical findings from the U.S. Survey of Professional Forecasters (SPF). First, we document a negative covariance between changes in forecasters' long-term and cyclical forecasts. Second, we show that forecast dispersion among forecasters tends to increase with the forecast horizon for most macroeconomic variables.

[4]Our model is fully rational and therefore differs from theoretical explorations that incorporate behaviorial biases, such as diagnostic expectations (Bordalo et al. 2018, Bianchi et al. 2021), overconfidence (Broer and Kohlhas 2022), ambiguity aversion (Chen et al. 2024, Huo et al. 2024), cognitive discounting (Gabaix 2020), level-K thinking (García-Schmidt and Woodford 2019, Farhi and Werning 2019), narrow thinking (Lian 2021), adaptive learning (Adam et al. 2012, Kuang and Mitra 2016), autocorrelation averaging (Wang 2021) and loss aversion (Elliott and Timmermann 2008, Capistrán and Timmermann 2009).

2.1 Survey of Professional Forecasters Data

The Survey of Professional Forecasters (SPF) of the U.S. is a source of predictions made by professional forecasters regarding a broad range of macroeconomic variables. The data is collected quarterly and goes back to 1968Q4. The Fed of Philadelphia surveys approximately 35 professional forecasters each quarter, assigning a unique ID number to each forecaster to track their forecast history.

For each variable, a forecaster provides six predictions, including one back-cast toward the previous period, a now-cast (forecast for the current quarter), and forecasts for the subsequent four quarters. In addition, they are asked to provide The annual projection of this variable for the current year, and the next year. Since 1991Q4, the survey has included an extra question regarding the Consumer Price Index (CPI) for a ten-year forecast. Since 1992Q1, the first quarter survey has included an additional question about the GDP for a ten-year forecast, while since 1996Q3, the third quarter survey has incorporated an additional question regarding the natural unemployment rate. Starting from 2009, SPF has expanded to encompass year-level forecasts of the unemployment rate and real GDP for two- and three-year periods. Table A1 provides a summary of the starting dates and frequency for each data series.

The survey is conducted before the end of each quarter, following the Bureau of Economic Analysis' (BEA) advance report of the national income and product accounts (NIPA) release. The BEA reports macroeconomic variables (e.g., GDP estimates) for the preceding quarter. At the beginning of the questionnaire, forecasters will be provided with the BEA reported value of the macro variable for the previous quarter. Therefore, when giving their predictions for current and future quarters, forecasters have access to information about the values of forecasted variables up to the last quarter.

2.2 Covariance: Changes in Long Term Forecasts and Cyclical Forecasts

Building on this dataset, the following section presents a novel empirical test that examines the covariance between changes in forecasters' long-term and cyclical forecasts across time. We will show that the covariance of these changes is informative about the process of expectation formation.

We start our investigation by constructing forecasters' long-run forecasts and cyclical forecasts. As discussed earlier, since 2009, the Survey of Professional Forecasters (SPF) has asked forecasters each quarter to report their long term forecasts for the unemployment rate and real GDP, precisely three years ahead. We employ forecaster i's three-year ahead forecast at quarter t, denoted as $F_{i,t}y_{t+3Y}$, to represent her long-run forecasts.[5] Furthermore, we utilize the deviation of forecaster i's forecast h period

[5]A possible concern is that three-year-ahead forecasts may not adequately represent long-run forecasts. To address this, we utilize two forecast series with longer horizons: ten-year forecasts for real

ahead at quarter t, denoted as $F_{i,t}y_{t+h}$, from the three-year ahead forecast as her cyclical forecasts. Specifically, forecaster i's cyclical forecasts is constructed as follows:

$$Cyc^h_{i,t} = F_{i,t}y_{t+h} - F_{i,t}y_{t+3Y}.$$

Then, we examine the covariance between the changes in the long-run forecasts and the cyclical forecasts:

$$COV^h_F = cov(F_{i,t}y_{t+3Y} - F_{i,t-1}y_{t-1+3Y}, Cyc^h_{i,t} - Cyc^h_{i,t-1}). \quad (1)$$

The first term on the right-hand side of Equation (1) represents the difference between three-year ahead forecasts for periods t and $t-1$. The second term corresponds to the change in cyclical forecasts between these two periods. The horizon $h = 0, 1, 2, 3, 4$ represents the forecast horizon for the short-term forecast, which is utilized to construct the forecasts on cyclical components.

The observable-trend model predicts that this covariance will be positive. This is because changes in cyclical forecasts reflect changes in the cyclical components from quarter t to quarter $t-1$. Similarly, changes in long-term forecasts represent shifts in both the trend and cyclical components between these quarters. The covariance must be positive, provided that the innovations in trend and cyclical components are uncorrelated. Furthermore, the covariance should decrease as h (i.e., the forecast horizon for the short-term forecast used to construct cyclical forecast) increases, since the changes in cyclical forecasts would be less proportional to changes in cyclical innovations when h is longer. This set of predictions is characterized in section 4.1.

Figure 1 illustrates the covariance between changes in long-run forecasts and cyclical forecasts for both the unemployment rate and real GDP growth. The x-axis represents the forecast horizons set at $h = 0, 1, 2, 3, 4$. Figure 1(a) shows the COV^h_F for the unemployment rate, while Figure 1(b) depicts the COV^h_F for real GDP growth. We observe a negative and significant COV^h_F for both variables, with the covariance increasing as the horizon h expands. Details of this estimation are shown in Table A2.

These findings suggest that when a forecaster updates her long-run forecast upward, she tends to simultaneously revise her cyclical forecast downward. The empirical results reveal a pattern contrary to the predictions of the observable-trend model: not only is the covariance negative instead of positive, but it also increases over the

GDP (available every first quarter since 1992Q1) and forecasts of the natural unemployment rate (available every third quarter since 1996Q3). In Appendix A.2, we demonstrate that three-year-ahead forecasts are highly correlated with those for longer horizons, making them reasonable representations of long-run forecasts. We do not use the ten-year forecasts for GDP and the natural unemployment rate in our analysis due to the coarse frequency of observations at the yearly level. Instead, we focus on three-year-ahead forecasts, which are available at the quarterly level.

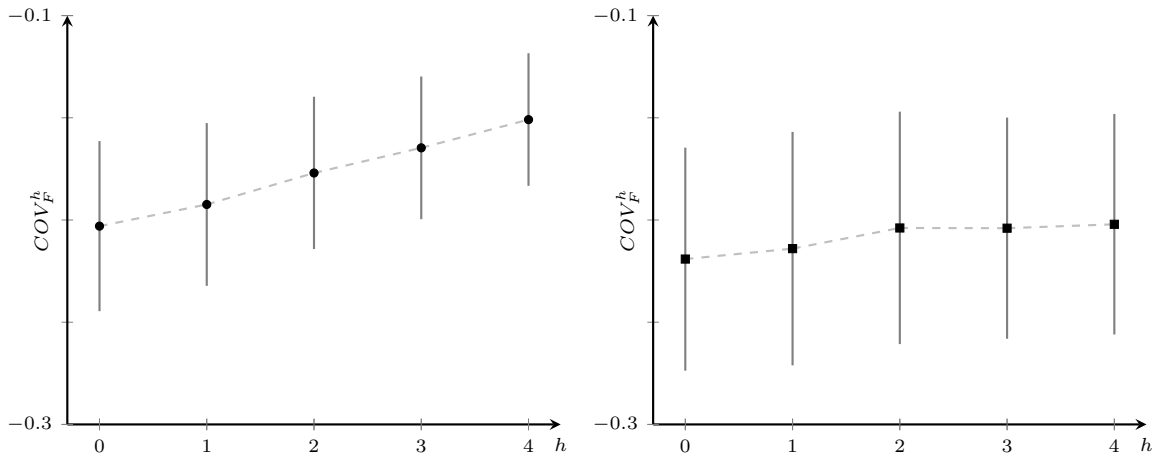

(a) Unemployment (b) Real GDP growth

Figure 1. *Covariance between the changes in long-run forecasts and cyclical forecasts across forecast horizon h. Note: This figure illustrates the covariance COV_F^h for the unemployment rate and real GDP growth across various forecast horizons h. The left panel shows the COV_F^h for the unemployment rate, while the right panel depicts the COV_F^h for real GDP growth. In both cases, the covariance is negative and statistically significant, increasing as the forecast horizon extends. The black dots represent the estimates, and the gray solid lines denote the 95% confidence intervals.*

horizon h rather than decreases.

2.3 Forecast Dispersion over Forecast Horizon

In this section, we explore whether the dispersion in forecasts among forecasters varies as the forecast horizon extends. This analysis is informative for understanding the role of beliefs concerning trends and cycles. The observable-trend model predicts that forecast dispersion should decrease monotonically as the forecast horizon increases, whether for short-term forecasts (forecasts within a year) or longer-term forecasts. This set of predictions will be characterized in section 4.1.

First, we investigate the short-term forecasts, for which we have forecast data for most macroeconomic variables. Using SPF data, we estimate the following equation:

$$\text{Forecast dispersion}_{th} = \alpha + \beta_1 h + \epsilon_{th}, \tag{2}$$

where Forecast dispersion$_{th}$ represents the cross-forecaster dispersion in forecasts $F_{i,t}y_{t+h}$ provided by forecaster i at period t for h quarters ahead and the forecast horizon is defined as $h = 0, 1, 2, 3, 4$. The standard error is clustered at the year-quarter level.

We consider two measures of forecast dispersion: the variance of forecasts across forecasters and the difference between the 75th percentile and the 25th percentile. We estimate Equation (2) using all available macroeconomic variables. The estimated coefficient β_2 is of particular interest and is presented in Table 1.

Column (1) of Table 1 presents the results using forecast variance as the measure of

Table 1. *Forecast dispersion over forecast horizon*

	Dependent Variable: Forecast Dispersion				
	Variance of forecasts		50 percentile difference		
	β_1	SE	β_1	SE	Obs
Forecast Variable	(1)	(2)	(3)	(4)	
Nominal GDP	0.337***	0.026	0.204***	0.008	1,025
Real GDP	0.242***	0.022	0.162***	0.007	1,025
GDP price index inflation	0.118***	0.008	0.119***	0.004	1,025
Real consumption	0.125***	0.013	0.127***	0.006	770
Industrial production	0.860***	0.062	0.320***	0.014	1,025
Real nonresidential investment	1.647***	0.127	0.497***	0.018	770
Real residential investment	6.021***	0.547	0.932***	0.039	770
Real federal government consumption	1.284***	0.102	0.393***	0.019	770
Real state and local government consumption	0.317***	0.028	0.210***	0.009	770
Housing start	0.004***	0.000	0.020***	0.001	1,024
Unemployment	0.034***	0.002	0.081***	0.003	1,014
Inflation (CPI)	-0.066***	0.021	-0.073***	0.012	770
Three-month Treasury rate	0.091***	0.010	0.132***	0.007	770
Ten-year Treasury rate	0.045***	0.001	0.094***	0.003	560

Note: This table shows results from estimating Equation (2). The sample period is from 1968Q4 to 2019Q4. In column (1), the dependent variable is the variance of forecasts across forecasters. In column (3), we use the difference between the 25% percentile and 50% percentile. Standard errors are clustered at the year-quarter level.

forecast dispersion. The coefficient for the forecast horizon h is positive ($\beta_2 > 0$) and statistically significant for most variables, indicating that forecasts among forecasters become more dispersed as the forecast horizon increases. The only exception is inflation. We will revisit the analysis of inflation expectations in section 5.1. In column (3), we repeat our estimations using the difference between the 75th and 25th percentiles as the measure of forecast dispersion. The results are rather similar. To confirm that the pattern is robust to the inclusion of time fixed effect, we report the estimation results with year-quarter fixed effect in Table A3. In addition, using the coefficient of variation as the measure of forecast dispersion, the results would be very similar.

Second, we investigate the longer-term forecasts, for which we have forecast data for fewer variables. Specifically, we focus on a subset of variables with annual forecast data that spans an extended horizon. Starting from 2009Q1, the U.S. Survey of Professional Forecasters (SPF) includes forecasts for real GDP and the unemployment rate one year, two years, and three years into the future. We utilize this dataset to estimate the following specification:

$$\text{Forecast dispersion}_{tH} = \alpha_2 + \sum_{H=1}^{3} \beta_H \, \text{horizon}_H + \epsilon_t, \tag{3}$$

where $\text{Forecast dispersion}_{tH}$ is the dispersion of forecasts of horizon H across all forecasters and horizon_H is a dummy variable for horizon H, taking the value 1 if the forecast horizon is $H = 1$ year, 2 years, or 3 years ahead; and 0 otherwise. The co-

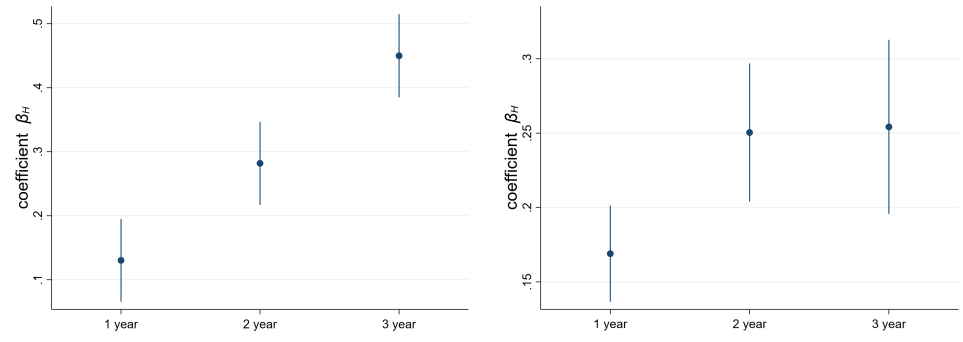

(a) Unemployment rate (b) Real GDP growth

Figure 2. *Dispersion of the year-level forecasts. Note: The figure presents the estimation results from Equation (3). The panel on the left displays the estimated coefficients for the unemployment rate, while the panel on the right shows those for real GDP growth. The sample period spans from 2009Q1 to 2019Q4. In both cases, β_H is greater than zero and increases as H increases, indicating larger dispersion as the forecast horizon expands.*

efficient β_H captures the difference in forecast dispersion between forecasts H years ahead and current year predictions ($H = 0$).

Figure 2 presents the estimation results. Figure 2(b) shows results for real GDP, while Figure 2(a) displays results for the unemployment rate. In both cases, the coefficients β_H are positive and increase with the forecast horizon. These findings also contradict the predictions of the observable-trend model, which states that dispersion should decrease monotonically.

In the literature, several studies have investigated this particular pattern, which offer similar findings that are inconsistent with the observable-trend model. Lahiri and Sheng (2008) use the *Consensus Forecasts* data and show that the forecast dispersion of real GDP growth is larger in a longer forecast horizon for all the G7 countries. Patton and Timmermann (2010) utilize the same data and find that both the forecast dispersion regarding the U.S. GDP growth and inflation is higher at longer horizons. Andrade et al. (2016) study the data from Blue Chip Survey and find a steady increase in the dispersion of Federal Fund rate forecasts as the forecast horizon extends.

3 Forecasting Model with Trend-cycle Confusion

3.1 Setup

Utility function. In this model, there exists a continuum of forecasters, indexed by $i \in [0, 1]$, who make forecasts about a stochastic state variable y_t. The objective of the forecasters is to minimize forecasting errors. We consider a standard quadratic utility function, which is given by:

$$U(F_{i,t}y_{t+h}) = -(F_{i,t}y_{t+h} - y_{t+h})^2, \tag{4}$$

where y_{t+h} is the actual value of the state in period $t+h$ and $F_{i,t}y_{t+h}$ denotes the forecast made by forecaster i at period t for the state h periods in the future.

Data generation process. We assume that the state variable y_t is composed of two components: a trend component, μ_t, representing long-term trend, and a cyclical component, x_t, capturing short-term fluctuations. In particular, the trend follows a random walk process, while the cycle is modeled as an AR(1) process. Specifically, the data generation process for the state can be described as follows:

$$\begin{aligned} y_t &= \mu_t + x_t, \\ \mu_t &= \mu_{t-1} + \gamma_t^{\mu}, \\ x_t &= \rho x_{t-1} + \gamma_t^{x}, \end{aligned} \tag{5}$$

where ρ is the persistence for the AR(1) process and γ_t^{μ} and γ_t^{x} are the innovations of the trend and cyclical components, both of which are normally distributed with zero mean and variances of σ_{μ}^2 and σ_x^2, respectively, i.e.,$\gamma_t^{\mu} \sim N(0, \sigma_{\mu}^2)$ and $\gamma_t^{x} \sim N(0, \sigma_x^2)$. We use $\boldsymbol{\theta_t} = (\mu_t, x_t)'$ to denote the state components in period t. Consistent with the previous literature, we assume that the data generating process (DGP) is common knowledge for all forecasters.[6]

In each period, forecasters receive private noisy signals for each component, that is, $\boldsymbol{s_{i,t}} = (s_{i,t}^{\mu}, s_{i,t}^{x})'$, where

$$s_{i,t}^{\mu} = \mu_t + \epsilon_{i,t}; \quad \text{and} \quad s_{i,t}^{x} = x_t + e_{i,t}. \tag{6}$$

We assume that the error terms of the signals are independent and normally distributed. The variance-covariance matrix of i's private signals is given by:

$$\boldsymbol{\Sigma_s} = \begin{pmatrix} \sigma_{\epsilon}^2 & 0 \\ 0 & \sigma_e^2 \end{pmatrix}.$$

At the end of each period t, we allow forecasters to observe the actual state variable y_t but not the trend and cyclical components. Therefore, upon the announcement of the actual state value, forecasters revise their beliefs regarding the trend and cyclical components. The updated beliefs about the two components become the prior beliefs for the next period.

Throughout the paper, we use $\boldsymbol{\theta}_{1,t}^{i}$ to represent forecaster i's posterior belief after forecaster i receive signals about the trend and cyclical components in period t (i.e., the first update). We use $\boldsymbol{\theta}_{2,t}^{i}$ to represent forecaster i's posterior belief after they observe

[6] In Appendix C.1, we discuss the scenario in which a common shock affects both the trend and cyclical components. This specification resembles that in Delle Monache et al. (2024). We demonstrate that this setting cannot produce the observed empirical patterns if the trend component is observable.

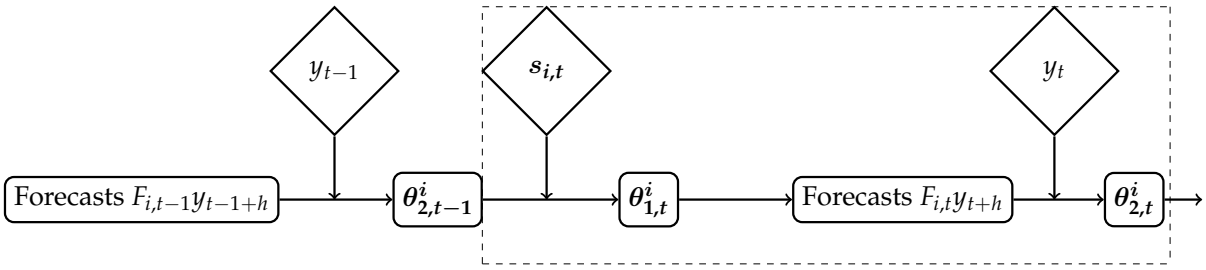

Figure 3. *Timeline. In each period t, forecaster i will update her beliefs twice. First, based on the observed private signals, forecaster i adjusts her beliefs and provides forecasts for the current and future periods, i.e., $F_{i,t}y_{t+h}$. Second, forecaster i revises her beliefs regarding the trend and cycle upon observing the actual realization of the state variable. The diamond boxes represent exogenous information flow. The squared boxes stands for the forecaster i's beliefs.*

the actual realization of the state in period t (i.e., the second update). The subscript 1 and 2 stand for the first and second updating in period t, respectively. We summarize the timeline of our setting in Figure 3:

- At the beginning of period t, forecaster i is endowed with the prior belief $\boldsymbol{\theta}^i_{2,t-1}$, which is the posterior of the second updating from the period $t-1$.
- Forecaster i observes the private signal $\boldsymbol{s_{i,t}}$ and then update her belief accordingly (the first updating).
- Given the updated beliefs $\boldsymbol{\theta}^i_{1,t}$, forecasters choose their optimal forecasts of the current and future period $F_{i,t}y_{t+h}$.
- At the end of period t, y_t is revealed.
- Forecasters revise their beliefs again, forming beliefs $\boldsymbol{\theta}^i_{2,t}$ (the second updating).

3.2 Equilibrium Characterization

In this section, we turn to the characterization of forecasters' optimal forecasts. We start our analysis by considering the posterior belief obtained from the second update in period $t-1$, which is the prior belief of forecaster i at the beginning of period t:

$$\boldsymbol{\theta^i_{2,t-1}} = (\mu^i_{2,t-1}, \rho x^i_{2,t-1})',$$

where $\mu^i_{2,t-1}$ and $x^i_{2,t-1}$ are forecaster i's beliefs about trend and cyclical components at the end of period $t-1$, respectively. Let $z_{i,t-1}$ be forecaster i's error in her belief regarding the trend in period $t-1$.

Lemma 1. Suppose the error term $z_{i,t-1}$ in period $t-1$ is normally distributed, then $z_{i,t}$ must also be normally distributed. The set of beliefs $\mu^i_{2,t-1}$ and $x^i_{2,t-1}$ can always

be written in the form:

$$\mu^i_{2,t-1} \equiv \mu_{t-1} + z_{i,t-1} \quad and \quad x^i_{2,t-1} \equiv x_{t-1} - z_{i,t-1}, \tag{7}$$

which implies:

$$\mu^i_{2,t-1} + x^i_{2,t-1} = y_{t-1}.$$

The proof and subsequent proofs are collected in Appendix B. In the following, we call $z_{i,t-1}$ the *separation error*. First, if the separation error follows a normal distribution in one particular period, it will continue to be normally distributed indefinitely, given that both the state innovations and signals are also normally distributed. Second, given the actual y_{t-1} is observed at the end of $t-1$, the normality assumption and the Bayes' rule requires that beliefs regarding the two components $\mu^i_{2,t-1}$ and $x^i_{2,t-1}$ must sum up to y_{t-1}. That is, the error terms in the two beliefs are of the same magnitude but opposite in sign.

Denote the variance of $z_{i,t-1}$ as $\sigma^2_{z,t-1}$, then the variance-covariance matrix of $\boldsymbol{\theta^i_{2,t-1}}$ follows:

$$\boldsymbol{\Sigma}_{\boldsymbol{\theta^i_{2,t-1}}} = \begin{pmatrix} \sigma^2_{z,t-1} + \sigma^2_\mu & -\rho\sigma^2_{z,t-1} \\ -\rho\sigma^2_{z,t-1} & \rho^2\sigma^2_{z,t-1} + \sigma^2_x \end{pmatrix}.$$

The sub-diagonal term $-\rho\sigma^2_{z,t-1}$ in the covariance matrix is negative. Intuitively, if a forecaster believes that the trend is stronger than it actually is (i.e., forecasting error on the trend component is positive), she will tend to believe that the cyclical component is weaker than it actually is, and vice versa. Note that when forecasters can perfectly distinguish between the trend and cyclical components, the corresponding sub-diagonal term will be zero. We will refer to $\sigma^2_{z,t}$ as the extent of confusion in distinguishing between the trend and cyclical components.

Lemma 2. There exists a unique steady state σ^2_z for the variance $\sigma^2_{z,t}$.

The variance $\sigma^2_{z,t}$ always converges to a steady-state value, σ^2_z. To understand why the variance of the error term, or the extent of confusion, converges, we observe two opposing forces resulting from the observation of actual data y_t. On the one hand, the change in state provides information about the cyclical component in the last period, given by $y_t - y_{t-1} = -(1-\rho)x_{t-1} + \gamma^x_t + \gamma^\mu_t$. This assists forecasters in separating the cyclical component from the trend, reducing their confusion. On the other hand, because y_t comprises both components, forecasters use the observation of the state and their beliefs about trends (i.e., $y_t - \mu^i_{1,t}$) to revise their beliefs regarding the cyclical component x_t, thereby increasing their confusion.

When $\sigma^2_{z,t-1}$ is large, it implies lower-quality prior beliefs and therefore a lower quality of $\mu^i_{1,t}$. Consequently, the second force becomes less important, and the first

force dominates, leading to a smaller $\sigma^2_{z,t}$. Conversely, when $\sigma^2_{z,t-1}$ is small, the second force dominates, resulting in an increase in the extent of confusion. Therefore, the steady-state value of σ^2_z always exists. Throughout the paper, we assume that the separation error z_i has converged to the steady state, given the results are qualitatively similar when the error term has not converged.

In the following, we present how forecasters update their beliefs and make forecasts by following the timeline of events. The first step involves characterizing the process of belief updating after forecasters receive their private signals regarding trends and cycles. In period t, after acquiring the private signals $\boldsymbol{s}_{i,t}$, forecaster i updates her beliefs on the trend and cyclical components and form her beliefs $\boldsymbol{\theta}^i_{1,t}$, which is joint-normally distributed. The expectations of these beliefs are given by:

$$\boldsymbol{\theta}^i_{1,t} = \boldsymbol{\theta}^i_{2,t-1} + \boldsymbol{\kappa} \times (\boldsymbol{s}_{i,t} - \boldsymbol{\theta}^i_{2,t-1}), \tag{8}$$

where $\boldsymbol{\kappa}$ is the Kalman gain and $(\boldsymbol{s}_{i,t} - \boldsymbol{\theta}^i_{2,t-1})$ is the surprise from signals:

$$\boldsymbol{\kappa} = \begin{pmatrix} \frac{V+\sigma^2_e(\sigma^2_z+\sigma^2_\mu)}{\Omega} & -\frac{\rho\sigma^2_e\sigma^2_z}{\Omega} \\ -\frac{\rho\sigma^2_e\sigma^2_z}{\Omega} & \frac{V+\sigma^2_\epsilon(\sigma^2_x+\rho^2\sigma^2_z)}{\Omega} \end{pmatrix} \quad \text{and} \quad \boldsymbol{s}_{i,t} - \boldsymbol{\theta}^i_{2,t-1} = \begin{pmatrix} s^\mu_{i,t} - \mu^i_{2,t-1} \\ s^x_{i,t} - \rho x^i_{2,t-1} \end{pmatrix}.$$

The variance-covariance matrix of $\boldsymbol{\theta}^i_{1,t}$ is given by:

$$(\boldsymbol{\Sigma}_{\boldsymbol{s}}^{-1} + \boldsymbol{\Sigma}^{-1}_{\boldsymbol{\theta}^i_{2,t-1}})^{-1} = \begin{pmatrix} \text{Var}^T & \widetilde{COV} \\ \widetilde{COV} & \text{Var}^C \end{pmatrix} = \begin{pmatrix} \frac{\sigma^2_\epsilon[\Omega-\sigma^2_\epsilon(\sigma^2_x+\sigma^2_e+\rho^2\sigma^2_z)]}{\Omega} & -\frac{\rho\sigma^2_e\sigma^2_\epsilon\sigma^2_z}{\Omega} \\ -\frac{\rho\sigma^2_e\sigma^2_\epsilon\sigma^2_z}{\Omega} & \frac{\sigma^2_e[\Omega-\sigma^2_e(\sigma^2_\epsilon+\sigma^2_\mu+\sigma^2_z)]}{\Omega} \end{pmatrix}, \tag{9}$$

where Ω and V are positive constants:

$$\Omega = (\sigma^2_z + \sigma^2_\mu + \sigma^2_\epsilon)(\sigma^2_x + \sigma^2_e + \rho^2\sigma^2_z) - \rho^2\sigma^4_z \quad \text{and} \quad V = (\sigma^2_z + \sigma^2_\mu)(\sigma^2_x + \rho^2\sigma^2_z) - \rho^2\sigma^4_z.$$

The Kalman gain matrix $\boldsymbol{\kappa}$ has two parts. The elements on the main diagonal resemble those in the standard belief updating. That is, forecasters use signals about the trend (cycle) to update their beliefs on the trend (cycle).

When there is no confusion (i.e., σ^2_z goes to zero), the model reduces to the standard Bayesian case. In this scenario, the Kalman gain for the trend component reduces to $\sigma^2_\mu/(\sigma^2_\mu + \sigma^2_\epsilon)$, and for the cyclical component, it reduces to $\sigma^2_x/(\sigma^2_x + \sigma^2_e)$. When there is confusion (i.e., $\sigma^2_z > 0$), the Kalman gain becomes larger than the Bayesian case without confusion. In other words, the confusion mechanism leads to less precise prior beliefs, and forecasters rely more on the signals, which provide new information. A similar argument holds true for the Kalman gain for the cyclical component.

Crucially, the non-zero elements on the sub-diagonal of the Kalman gain matrix, distinguish our model from the observable-trends model, where the counterpart terms are zero. This indicates that in our framework, forecasters incorporate information about the trend (cycle) component when updating their beliefs about the cyclical (trend) component. Consider a scenario where the private signal indicates that the cyclical component is stronger than the forecaster's prior belief. This situation could arise from three possibilities: Firstly, it might reflect a substantial positive innovation in the cyclical component itself. Secondly, it could be due to positive noise in the signal. Thirdly, it might suggest that the actual value of the cyclical component in the previous period was larger than what the forecaster believed. As forecasters cannot know the true value of each component with certainty, they will adjust their prior beliefs by increasing their estimate of the cyclical component from the last period and correspondingly decreasing their estimates of the trend component for both the last and current periods.

The variance-covariance matrix in Equation (9) warrants further discussion. Firstly, the elements on the main diagonal correspond to the perceived variance of the trend and cyclical components, which are influenced by the confusion mechanism. These variances are larger compared to the case where there is no confusion (i.e., the components can be perfectly observed). We denote them as Var^T and Var^C, respectively.

Secondly, the elements on the sub-diagonal components are non-zero and negative. That is, forecasters cannot perfectly distinguish between the trend and cycle, which gives rise to a negative covariance between the beliefs of these two components. Intuitively, when there are strong positive signals about the cyclical component, forecasters will simultaneously revise the cyclical component upward and the trend component downward. We denote this covariance of beliefs as $\widetilde{\text{COV}}$.

The second step is the stage of making forecasts. Forecaster i makes a series of forecasts about the state in h periods ahead. Under a quadratic utility function, her optimal prediction is the expected value of the state variable.

Lemma 3. The optimal forecast of forecaster i over horizon h is determined by their beliefs of trend and cyclical components, i.e.,

$$F_{i,t}y_{t+h} = E_{i,t}[\mu_t + \rho^h x_t] = \mu^i_{1,t} + \rho^h x^i_{1,t}.$$

This lemma says that the trend and cyclical beliefs play different roles over forecast horizons: the trend belief consistently influences predictions across all horizons, while the influence of the cyclical belief diminishes as the forecast horizon extends.

The final step involves forecasters revising their beliefs again upon observing the actual value of the current state (y_t). This set of posterior beliefs becomes the prior beliefs for the next period. The forecasting error present in this set of posterior beliefs

is the separation error ($z_{i,t}$). Lemma 4 characterizes its construction.

Lemma 4. Upon observing the actual state value y_t, the separation error $z_{i,t}$ present in the posterior beliefs is given by:

$$z_{i,t} = \frac{(\text{Var}^T + \widetilde{\text{COV}})(x_t - x^i_{1,t}) - (\text{Var}^C + \widetilde{\text{COV}})(\mu_t - \mu^i_{1,t})}{(\text{Var}^T + \widetilde{\text{COV}}) + (\text{Var}^C + \widetilde{\text{COV}})}. \tag{10}$$

The extent of confusion σ_z^2 increases as σ_μ^2, σ_x^2, σ_e^2, and σ_ϵ^2 increase, converges to zero if any of these parameters goes to zero and is also bounded:

$$0 \leq \sigma_z^2 \leq \min\{\text{Var}^C, \text{Var}^T\}. \tag{11}$$

Recall that Var^T and Var^C represent the variances of forecasters' posterior beliefs regarding the trend and cyclical components, respectively, while $\widetilde{\text{COV}}$ denotes the corresponding covariance between the two components, as shown in Equation (9).

Lemma 4 states that the separation error after forecasters observe the actual state, is a weighted combination of the error terms in forecasters' beliefs regarding the trend and cyclical components *before* they observe the actual state. If they over-predict the trend component (i.e., $\mu_t - \mu^i_{1,t} < 0$), then $z_{i,t}$ tends to be positive. Conversely, if they over-predict the cyclical component (i.e., $x_t - x^i_{1,t} < 0$), then $z_{i,t}$ tends to be negative.[7]

Note that after observing the actual state value, the covariance between beliefs regarding the trend and cyclical components is represented as $-\sigma_z^2$. The extent of confusion, denoted by σ_z^2, is influenced by two primary factors: the quality of signals (i.e., σ_e^2 and σ_ϵ^2) and the volatility of the state variables (i.e., σ_μ^2 and σ_x^2). First, forecasters receive private signals about each component in every period, which help them differentiate between the two. Consequently, more accurate signals decrease the level of confusion. Second, when the state innovations in the trend or cyclical component are more volatile, it becomes more difficult to identify each component, resulting in a higher level of confusion. Intuitively, the confusion is upper bounded by the uncertainty in either the trend or cyclical beliefs.

4 Forecasts over Horizon: Main Results

4.1 Special Case: Observable Trends

Before presenting our model predictions regarding forecasting behaviors over the forecast horizon, we examine a special case where trends are stochastic, but forecasters can

[7] Consider a special case nested in Equation (10). When the trend is stable (i.e., $\sigma_\mu^2 = 0$), forecasters can predict the trend component perfectly. Therefore, the error term in their beliefs regarding the trend component is zero. In this scenario, both the variance of the belief regarding the trend component (Var^T) and the covariance ($\widetilde{\text{COV}}$) would also be zero. As a result, the separation error in this case would be zero.

observe the actual trend component at the end of each period. This allows forecasters to perfectly distinguish between the trend and cyclical components. In this scenario, the key information friction in our model is absent, while all other assumptions remain unchanged. Contrasting this special case and our benchmark model helps illustrate the importance of the information friction arising from trends and cycles not being separable.

In this case, forecasters can perfectly separate the two components, which implies that the separation error becomes zero (i.e., $z_{i,t} = 0$) and the variance of the separation error also reduces to zero (i.e., $\sigma_z^2 = 0$). Consequently, both the Kalman gain matrix in Equation (8) and the variance-covariance matrix in Equation (9) become standard:

$$\boldsymbol{\kappa} = \begin{pmatrix} \frac{\sigma_\mu^2}{\sigma_\mu^2+\sigma_\epsilon^2} & 0 \\ 0 & \frac{\sigma_x^2}{\sigma_x^2+\sigma_e^2} \end{pmatrix} \quad \text{and} \quad \begin{pmatrix} \text{Var}_s^T & \widetilde{\text{COV}}_s \\ \widetilde{\text{COV}}_s & \text{Var}_s^C \end{pmatrix} = \begin{pmatrix} \frac{\sigma_\epsilon^2\sigma_\mu^2}{\sigma_\epsilon^2+\sigma_\mu^2} & 0 \\ 0 & \frac{\sigma_e^2\sigma_x^2}{\sigma_x^2+\sigma_e^2} \end{pmatrix}.$$

In this scenario, the sub-diagonal elements of the Kalman gain matrix are zero, indicating that forecasters do not use information from the trend or cyclical component to update their beliefs about the other. That is, they treat these components as independent, resulting in zero covariance (i.e., $\widetilde{COV}_s = 0$).

In the following, we investigate whether this model could help address the two empirical patterns documented in section 2. We first examine the covariance between changes in long-run forecasts and cyclical forecasts. Keep in mind that in the empirical analysis, we take three-year-ahead forecasts (i.e., $h = 3Y$) as forecasters' long-run forecasts. We calculate the difference between h-quarter-ahead forecasts and three-year-ahead forecasts to obtain the cyclical forecasts. We construct the exact model counterparts as follows:

$$F_{i,t}y_{t+3Y} - F_{i,t-1}y_{t-1+3Y} = (E_{i,t}[\mu_t] - E_{i,t-1}[\mu_{t-1}]) + \rho^{3Y}(E_{i,t}[x_t] - E_{i,t-1}[x_{t-1}]),$$

and

$$Cyc_{i,t}^h - Cyc_{i,t-1}^h = (\rho^h - \rho^{3Y})(E_{i,t}[x_t] - E_{i,t-1}[x_{t-1}]).$$

Therefore, the model predicts a positive covariance between changes in the long-run forecasts and cyclical forecasts:

$$COV_F^h = \rho^{3Y}(\rho^h - \rho^{3Y})Var(E_{i,t}[x_t] - E_{i,t-1}[x_{t-1}]) > 0.$$

It holds because the belief updating of trend and cyclical components is independent (i.e., $\widetilde{COV}_s = 0$) and the covariance between the changes in trend beliefs and cyclical beliefs is zero, i.e., $cov(E_{i,t}[\mu_t] - E_{i,t-1}[\mu_{t-1}], E_{i,t}[x_t] - E_{i,t-1}[x_{t-1}]) = 0$. In addition, as the forecast horizon h increases, the model predicts that COV_F^h decreases with h, since

ρ is less than one.

Furthermore, in this special case, the forecast variance across forecasters can be decomposed into two components:

$$\text{Forecast dispersion}_{th} = E[(F_{i,t}y_{t+h} - \overline{E}[F_{i,t}y_{t+h}])^2] \quad = \rho^{2h}\phi_s^C \text{Var}_s^C + \phi_s^T \text{Var}_s^T, \quad (12)$$

where $\phi_s^C = \sigma_x^2/(\sigma_x^2 + \sigma_e^2) < 1$, $\phi_s^T = \sigma_\mu^2/(\sigma_\mu^2 + \sigma_\epsilon^2) < 1$ and $\overline{E}[\cdot]$ is the mean forecast across all forecasters. Note the dispersion of forecasts across forecasters is smaller than the variance of individual forecasters' beliefs because their information sets are correlated. This explains why both ϕ_s^C and ϕ_s^T are less than one.

When the forecast horizon h increases, the dispersion across forecasters caused by their noisy information on the cyclical component becomes less significant, i.e., ρ^{2h} decreases in h. However, the dispersion caused by their noisy information on the trend component remains stable over the horizon. As a result, the total dispersion decreases monotonically over the forecast horizon.

In summary, when trends and cycles are separable, the model fails to generate either of the two empirical patterns documented. In fact, its predictions are exactly opposite to the observed patterns in the data. We further extend this special case by allowing the data generation process to be a general ARMA model instead of an AR(1). However, this does not alter the model predictions. Further discussion of this result is provided in Appendix B. Moving forward, we will elaborate on the scenario where the two components are not perfectly separable. We will then explore the conditions under which the model predictions can be reversed.

4.2 Covariance of Beliefs

The key difference between our benchmark model and the special case is that forecasters cannot perfectly observe trends and cycles. As a result, their beliefs about these two components are correlated, even when they are, in fact, independent. In this section, we analyze the covariance between forecasters' beliefs regarding trends and cycles after they have observed their private signals.

The covariance between forecasters' beliefs about the trend and cyclical components, captured by $\widetilde{\text{COV}}$ in Equation (9), is a crucial element of our model. This covariance depends on the volatility of the two components as well as the persistence of the cyclical component. Proposition 1 provides a detailed characterization of how these factors determine the sign and magnitude of the covariance of beliefs.

Proposition 1. *(i) The magnitude of the covariance between the trend and cyclical beliefs $|\widetilde{COV}|$ first increases and then decreases in the variance of trend innovations σ_μ^2; and it is zero when $\sigma_\mu^2 = 0$ and converges to zero when σ_μ^2 goes to ∞. (ii) The magnitude of the covariance increases with the persistence of the cyclical component (ρ).*

To understand part (i), recall the covariance is characterized by $\widetilde{\text{COV}} = -\rho\sigma_\epsilon^2\sigma_e^2\sigma_z^2/\Omega$. As the variance of trend innovations (σ_μ^2) increases, two effects emerge. Firstly, Lemma 4 has shown that forecaster i's confusion, represented by σ_z^2, increases. Secondly, forecaster i's uncertainty about the state, represented by Ω, also increases. When the variance of trend innovations remains relatively small, the increase in confusion (σ_z^2) dominates. Conversely, when it is relatively large, the increase in overall variance (Ω) dominates.

Consider the following polar cases. When the trend is stable (i.e., $\sigma_\mu^2 = 0$), there is no confusion (i.e., $\sigma_z^2 = 0$). Therefore, the covariance is zero. When the trend innovation is very large (i.e., $\sigma_\mu^2 \to \infty$), forecaster i's uncertainty about the state is also very large (i.e., $\Omega \to \infty$), the confusion mechanism becomes irrelevant, and the covariance converges to zero too.

To understand part (ii), we first examine an extreme case where the persistence of the cyclical component is zero (i.e., $\rho = 0$). That is, the cyclical component becomes independent over time. Consequently, signals regarding the cyclical components offer information solely about the cyclical components, which are uninformative for the trend components. Therefore, the covariance of beliefs regarding the two components is rendered to be zero. As the persistence of the cyclical component increases, signals regarding the cyclical components become more valuable for revising trend beliefs, giving rise to a larger covariance in magnitude.

4.3 Covariance between changes of long-run forecasts and cyclical forecasts

In this section, we examine the model's prediction for the covariance between changes in long-run and cyclical forecasts, which can be constructed from the data. Interestingly, we can relate the observable covariance in the data to the unobservable covariance between trend and cyclical beliefs in the model. We show the necessary and sufficient conditions under which our model can produce either a positive or negative covariance between changes in long-run and cyclical forecasts, and that the magnitude of the covariance decreases as the horizon h increases.

We begin our analysis by decomposing both the changes in the long-run forecasts and the cyclical forecasts. The changes in long-run forecasts is captured by changes in the forecasts for $h = 3Y$ periods ahead, which can be rewritten by:

$$F_{i,t}y_{t+3Y} - F_{i,t-1}y_{t-1+3Y} = (\mu_{1,t}^i - \mu_{1,t-1}^i) + \rho^{3Y}(x_{1,t}^i - x_{1,t-1}^i).$$

The changes in the long-run forecasts therefore reflect one's belief updates both in trend component (i.e., $\mu_{1,t}^i - \mu_{1,t-1}^i$) and cyclical component (i.e., $x_{1,t}^i - x_{1,t-1}^i$). On the other hand, the changes in the cyclical forecasts consist only the belief changes

regarding the cyclical component:

$$Cyc^h_{i,t} - Cyc^h_{i,t-1} = (\rho^h - \rho^{3Y})(x^i_{1,t} - x^i_{1,t-1}). \tag{13}$$

The covariance between the changes in the long-run forecasts and cyclical forecasts can be written as follows:

$$\begin{aligned} &cov(F_{i,t}y_{t+3Y} - F_{i,t-1}y_{t-1+3Y}, Cyc^h_{i,t} - Cyc^h_{i,t-1}) \\ &= \underbrace{(\rho^h - \rho^{3Y})}_{(+)} \underbrace{\left\{\widetilde{\text{COV}} + \rho^{3Y}\text{Var}^C\right\}}_{(+)\ or\ (-)}. \end{aligned} \tag{14}$$

The covariance COV^h_F can be positive or negative. For example, when a forecaster receives a signal indicating a stronger-than-expected cyclical component in the current period, she tends to revise the cyclical forecasts upwards. That is, $Cyc^h_{i,t} - Cyc^h_{i,t-1} > 0$. However, she can revise the long-term forecast either upwards ($F_{i,t}y_{t+3Y} - F_{i,t-1}y_{t-1+3Y} > 0$) or downwards ($F_{i,t}y_{t+3Y} - F_{i,t-1}y_{t-1+3Y} < 0$).

On the one hand, since the long-term forecast is partially driven by cyclical components, she may revise it upwards too. On the other hand, because the cyclical component is persistent, she revises her belief about the previous period's cyclical component upwards. This revision leads her to adjust her belief about the previous period's trend component downwards. This mechanism is shown in Section 3.2 (see Equation 9). It would suppress the estimate of trend component of the current period, causing a downward adjustment of the long-term forecasts.

The covariance term can be further decomposed into two parts, as shown in the second line of Equation (14). The first term, $(\rho^h - \rho^{3Y})$, is always positive and its magnitude depends on the forecast horizon h used to construct the cyclical forecasts. It decreases as the horizon h increases. When the cyclical forecast is constructed using the nowcast (i.e., $h = 0$), the first term reaches its largest value. As h approaches three years (i.e., $h = 3Y$), the first term goes to zero.

The second term can be either positive or negative. It consists of the covariance between trend and cyclical beliefs (i.e., $\widetilde{\text{COV}}$), and the variance of the cyclical belief (i.e., Var^C), each corresponding to one of the two mechanisms discussed earlier. Proposition 2 presents the necessary and sufficient conditions for the sum of the two terms to be negative.

Proposition 2. *There exists a threshold $\overline{\sigma}^2_\mu$ for the variance of the trend component innovation, such that:*
(i) for any $\sigma^2_\mu \in [\overline{\sigma}^2_\mu, +\infty)$, COV^h_F is positive;
(ii) for any $\sigma^2_\mu \in (0, \overline{\sigma}^2_\mu)$, there exists a threshold $\overline{\sigma}^2_x$ such that COV^h_F is negative if and only if

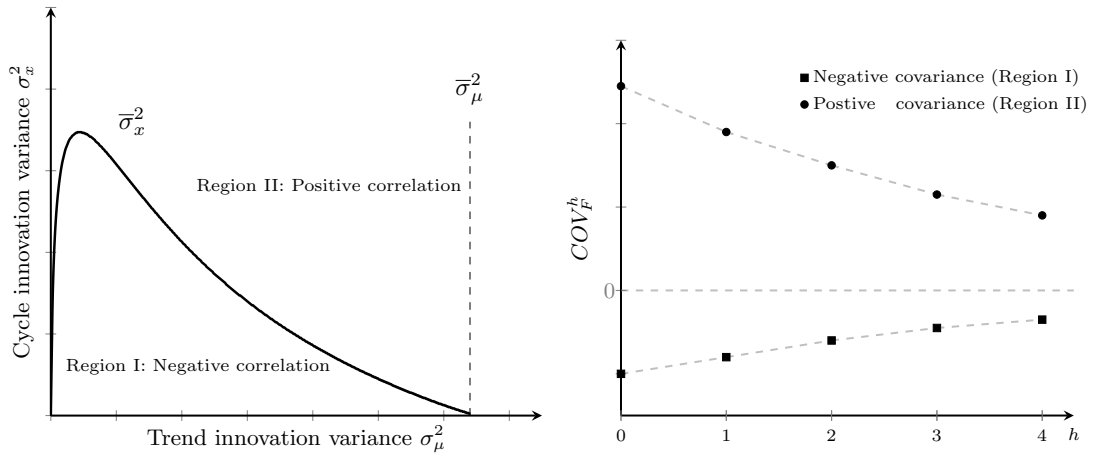

Figure 4. *The sign and the magnitude of the covariance between changes in the long-run forecasts and cyclical forecasts. Figure 4(a) demonstrates the sign of the COV_F^h. For a pair of state innovation $(\sigma_\mu^2, \sigma_x^2)$, the model predicts a negative covariance, if it lies inside Region I and a positive covariance if it lies in Region II. Figure 4(b) plots the COV_F^h at horizon $h = 0, 1, 2, 3, 4$. The figure shows that the magnitude of COV_F^h is always decreasing in h.*

$\sigma_x^2 < \overline{\sigma}_x^2$; and it is positive, otherwise;
(iii) and the magnitude of COV_F^h is decreasing as the horizon h increases.

Figure 4 illustrates how the sign and the magnitude of COV_F^h change, which is characterized by Proposition 2. Figure 4(a) demonstrates the sign of COV_F^h as the variance of the trend and cyclical innovation varies. For a pair of signal quality (captured by σ_ϵ^2 and σ_e^2), the model predicts a negative covariance when the trend component is moderately volatile, and the cyclical component is not excessively volatile.

As shown in Equation (14), the changes in long-run forecasts and cyclical forecasts exhibit a negative covariance when $\widetilde{\text{COV}}$ dominates. As shown in Proposition 1, this scenario occurs when the trend component is neither too stable nor too volatile. That explains item (i) in this proposition.

In addition, as the variance of the cyclical innovation (i.e., σ_x^2) increases, the variance of belief changes concerning the cyclical component (represented by the second term on the right-hand side of Equation (14)) also increases. If the cyclical component is too volatile, the confusion mechanism becomes less relevant. We show the existence of a threshold, $\overline{\sigma}_x^2$, for the volatility of cyclical components, such that changes in trend forecasts and cyclical forecasts exhibit a negative covariance when σ_x^2 is lower than this threshold. This explains item (ii) in this proposition.

Figure 4(b) shows that the magnitude of COV_F^h decreases as the forecast horizon increases. As Equation (13) shows, as h increases, changes in cyclical forecasts correspond to a smaller proportion of cyclical updates. That is, $(\rho^h - \rho^{3Y})$ decreases in h. Therefore, the magnitude of the covariance decreases and converges to zero as the

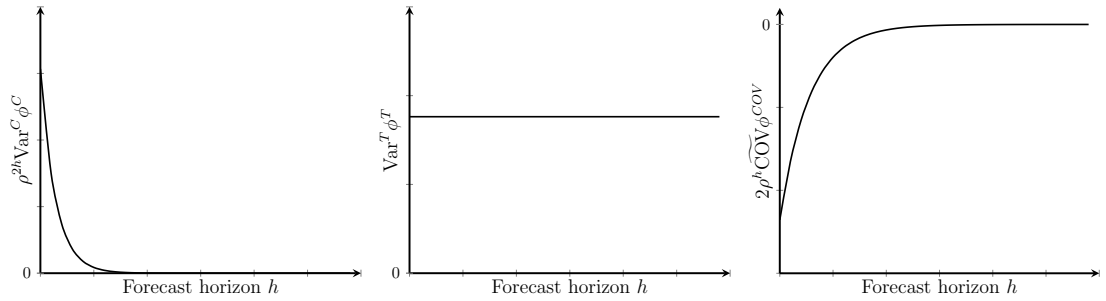

(a) Cycle beliefs (b) Trend beliefs (c) Covariance term

Figure 5. *Dispersion decomposition as the horizon extends. Note: This figure shows how each part of the dispersion changes as the forecast horizon extends.*

forecast horizon h increases. That explains item (iii) in this proposition.

4.4 Forecast dispersion

We proceed to examine the prediction of our model regarding the relationship between the forecast dispersion and the forecast horizon. In our model, the forecast dispersion can either increase or decrease as the forecast horizon becomes longer. Proposition 3 characterizes the necessary and sufficient conditions for the forecast dispersion to increase or decrease over the forecast horizon.

To expound the mechanism, we decompose the dispersion of forecasts across forecasters for any horizon into three components: the variance arising from heterogeneous beliefs about the trend component, the cyclical component, and their covariance. To be specific, the forecast dispersion is given by:

$$E[(F_{i,t}y_{t+h} - \overline{E}[F_{i,t}y_{t+h}])^2] = \rho^{2h}\mathrm{Var}^C\phi^C + \mathrm{Var}^T\phi^T + 2\rho^h\widetilde{\mathrm{COV}}\phi^{COV}, \tag{15}$$

where $0 < \phi^C < 1$, $0 < \phi^T < 1$ and $0 < \phi^{COV} < 1$ are positive scalars, whose expressions are collected in the proof of Proposition 3. Note that $\overline{E}[\cdot]$ is the mean forecast across all forecasters.

Figure 5 illustrates how each part changes as the forecast horizon extends. Figure 5(a) shows that the variance from heterogeneous beliefs about the cyclical component decreases when the forecast horizon extends. This reduction occurs because the cyclical component's influence diminishes in longer-term forecasts. Figure 5(b) demonstrates that the variance due to heterogeneous beliefs about the trend component remains constant across all horizons. This is expected, as the trend component's influence is consistent regardless of the forecast horizon. The behavior of these two components over different horizons aligns with what is observed in the special case (see section 4.1).

Figure 5(c) depicts the covariance term. Its magnitude decreases as the forecast

horizon extends, due to the diminished importance of the cyclical component over longer horizons. This feature, though intuitive, is crucial for understanding our model's predictions. On the one hand, the covariance term is negative, reducing overall forecast dispersion across forecasters for any horizon. On the other hand, as the forecast horizon extends, the impact of the covariance term diminishes, leading to a force that drives up the forecast dispersion.

The change in forecast dispersion over a longer horizon is determined by the relative strength of two forces: the diminishing force from dispersion due to heterogeneous beliefs about the cyclical component, and the increasing force from the covariance term. Interestingly, in this model, forecast dispersion must increase with the forecast horizon when h is large enough. The dispersion of cyclical beliefs converges to zero more rapidly as the forecast horizon extends than the covariance between trend and cyclical beliefs. This is evident from Equation (15): ρ^{2h} converges to zero more quickly than ρ^h. Therefore, when the forecast horizon is sufficiently long, the increasing force of the covariance becomes dominant, leading to greater dispersion. Proposition 3 fully characterizes this property.

Proposition 3. *The dispersion of forecasts across forecasters is strictly increasing in the forecast horizon h, if and only if:*

$$h > \underline{h} = \underbrace{\frac{1}{\ln \rho}}_{-} \underbrace{\ln \frac{-\widetilde{COV}}{Var^C} \frac{\phi^{COV}}{\phi^C} W}_{-\ \ or\ \ +}; \tag{16}$$

where $W < 1$ is a positive scalar given by $E[(z_{i,t} - E[z_{i,t}])^2]/\sigma_z^2$ and $\ln \rho < 0$.

When the threshold is negative ($\underline{h} \leq 0$), forecast dispersion always increases over the forecast horizon. This scenario occurs when the variance of the trend innovation is moderate. As shown in Proposition 1, in such cases, the impact of the covariance between trend and cyclical beliefs (i.e., $\widetilde{COV}$) is greatest.

Conversely, when the threshold value on the right-hand side of Equation (16) approaches infinity ($\underline{h} \to \infty$), forecast dispersion always decreases over the forecast horizon. This scenario occurs in the special case described in section 4.1, where forecasters can perfectly differentiate between trend and cyclical components, resulting in a covariance term of zero.

5 Applications

In the preceding sections, we presented a model of expectation formation where forecasters cannot perfectly separate cyclical and trend components. This model accounts for empirical regularities observed in SPF data. We now provide two applications of this framework. First, in Section 5.1, we explore its use in analyzing policy-relevant

issues. Second, in Section 5.2, we study the role of this friction in a policy game, highlighting its relevance in policy design.

5.1 Application: Explicit Inflation Targeting and Forecasting Behaviors

In this section, we examine the effects of a significant policy change in the United States in 2012 - the introduction of explicit inflation targeting. This new approach to monetary policy implementation began with an announcement on January 25th by Ben Bernanke, the Chairman of the U.S. Federal Reserve, who set a specific inflation target of 2%. Prior to this policy change, the United States did not have an explicit inflation target, relying instead on regularly announced desired target ranges for inflation.[8]

Through the lens of our model, the implication of this policy for forecasters is that the underlying data generation process for inflation could undergo changes which would necessitate changes in forecasting behaviors. To quantify the underlying changes caused by the policy implementation, we begin by dividing the sample into two subsamples: the period before 2012 and the period after. We then structurally estimate the model using moments obtained from both the pre- and post-2012 sub-samples. We then assess the estimated changes in the data generation process and examine how they impact the empirical patterns of forecasts quantitatively. While all the details of the estimation are provided in Appendix A.5, we summarize the estimation procedures below. Note that we use the ten-year-ahead forecasts of the inflation rate in the SPF as the long-term forecasts because the SPF does not provide three-year-ahead forecasts for inflation. The ten-year-ahead forecast data have been available since 1991Q4.

Our model can be fully specified by five parameters: $\{\rho, \sigma_\mu^2, \sigma_x^2, \sigma_\epsilon^2, \sigma_e^2\}$. The first three parameters are related to the data generating process, while the last two capture the precision of the signals. To structurally estimate the values of these parameters, we follow the approach of Chernozhukov and Hong (2003) and compute Laplace-type estimators (LTE) using a Markov Chain Monte Carlo method. To identify changes in the underlying parameters, we estimate them for each subsample period.

We estimated the model parameters by targeting the forecast variance across different horizons in each subsample period. We then used the estimated model to simulate data and examine the covariance patterns, which were not targeted in the estimation. This approach allowed us to assess the model's quantitative predictions about the effects of the policy shift in 2012.

To be concrete, we compute the across quarters average variances of forecasts for

[8]Before the era of the Greenspan Fed, the Federal Reserve operated under a stop-and-go policy without a specific inflation target. Starting in 1992, the Greenspan Fed aimed to maintain low long-term inflation rates (see Goodfriend 2004 for a comprehensive review). From the 1990s until the Great Recession, there was a consensus among market participants and FOMC members that the optimal inflation target would fall between 1% and 2%. However, there was no explicit inflation target (Shapiro and Wilson 2019). In January 2012, the FOMC announced a target of 2% for the inflation rate, marking the first time in its history that it adopted an explicit inflation-targeting approach.

Table 2. *Estimated Model Parameters*

	Parameter Estimation					
	Pre-2012			Post-2012		
	Mean	90 HPDI	95 HPDI	Mean	90 HPDI	95 HPDI
σ_μ^2	1.14	(0.96,1.38)	(0.91,1.38)	0.84	(0.66,1.08)	(0.61,1.08)
σ_x^2	2.57	(2.41,2.67)	(2.43,2.75)	2.60	(2.37,2.76)	(2.40,2.88)
σ_ϵ^2	0.78	(0.62,0.89)	(0.61,0.95)	0.72	(0.48,0.89)	(0.47,0.97)
σ_e^2	1.62	(1.47,1.76)	(1.47,1.77)	1.54	(1.31,1.74)	(1.30,1.76)
ρ	0.84	(0.73,0.94)	(0.74,0.97)	0.64	(0.53,0.76)	(0.53,0.79)

Note: This table presents the estimated parameter values for the pre-2012 and post-2012 periods. We provide the mean values, as well as the 90% and 95% Highest Posterior Density Intervals (HPDI).

different horizons, specifically for $h = 0, 1, 2, 3, 4$, using the subsamples before and after 2012. These variances will be treated as the target moments in our estimation and denoted as $\hat{m}$. Furthermore, we construct the model counterpart of $\hat{m}$ and define the distance between the two as follows:

$$\Lambda(\Theta) = [m(\Theta) - \hat{m}]' \hat{W} [m(\Theta) - \hat{m}], \tag{17}$$

where $\hat{W}$ is the weighting matrix, where the diagonal elements represent the precision of the moments $\hat{m}$. We solve for the parameter values (Θ) to minimize the constructed distance, that is, finding the set of parameter values that best matches the forecast variance at each forecast horizon.

The estimated parameters for each subsample are reported in Table 2 together with the 90% and 95% high posterior density interval (HPDI). A comparison of the two sets of estimated parameters reveals that there are minimal changes in the innovations in cycles variance (i.e., σ_x^2) and the precision of signals on trends and cycles (i.e., σ_ϵ^2 and σ_e^2) following the policy change in 2012. This indicates that this set of parameters remain relatively stable before and after the policy change.

There are two noteworthy changes. First, there is a sizable decrease in the variance of trend innovation (i.e., σ_μ^2). Before the policy change, the estimated variance was 1.14. After the policy change, it dropped to 0.84. This suggests that the trend is more stable after the policy implementation, consistent with the policy goal of providing a specific long-run target. Second, the persistence of the cyclical component (i.e., ρ) decreases. Before the policy change, the estimated persistence of the cyclical component was 0.84, aligning with previous literature. For instance, Carvalho et al. (2023) estimated a value of $\rho = 0.87$. After the policy change, the estimated persistence dropped to 0.64, indicating that short-term fluctuations have become less persistent.

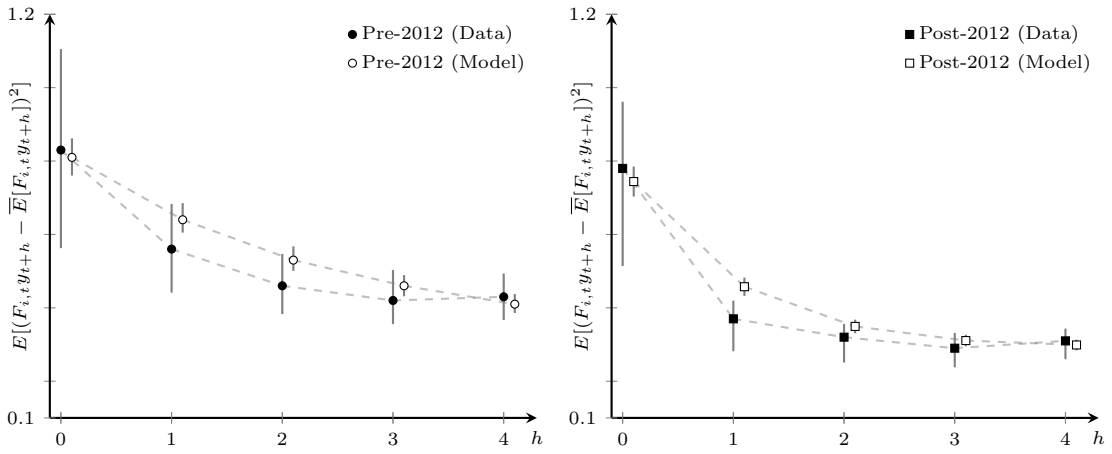

(a) Forecast variance before 2012 (b) Forecast variance after 2012

Figure 6. *Forecast variance over horizon for the subsamples before and after 2012. Black dots represent results from SPF data, while white dots depict simulated data. Figure 6(a) shows forecast variance before 2012, and Figure 6(b) illustrates it after 2012. The gray solid line marks the 95% confidence interval using the bootstrap method. Our model fits the data closely in both sub-samples. The pre-2012 period spans from 1990Q1 to 2011Q4, and the post-2012 period from 2012Q1 to 2019Q4.*

The observed change in the estimated persistence of the cyclical component is intuitive. Following the policy change, the central bank would respond more aggressively to short-term deviations from the long-term target. Consequently, the persistence of the cyclical component would decrease.

Next, we investigate whether the estimated model can reproduce the set of findings documented in Section 2 concerning inflation forecasts before and after 2012. First, we examine the forecast variance across various forecast horizons, which were targeted moments in the estimation. Figure 6 displays the forecast variance of the SPF data and the simulated data before and after 2012. The black dots represent results obtained using the SPF data, while the white dots represent the simulated data. The gray solid line corresponds to the 95% confidence interval using the bootstrap method. In both sub-samples, the simulated models closely fit the empirical data.

In the SPF data, a notable difference between the two sample periods is observed: the forecast variance declines more rapidly as the forecast horizon extends in the post-2012 sub-sample compared to the pre-2012 period. Specifically, in the pre-2012 subsample, the forecast variance decreases by 32.5%, from 0.833 at the now-cast ($h = 0$) to 0.562 for forecasts one quarter ahead. In contrast, the post-2012 subsample exhibits a much sharper decline of 52.5%, with the variance dropping from 0.737 at the now-cast to 0.350 for one-quarter-ahead forecasts.

The change in empirical patterns across the two periods aligns qualitatively with our model's predictions. According to Proposition 1, when the trend component becomes more stable (i.e., σ_μ^2 decreases) and the cyclical component becomes less persis-

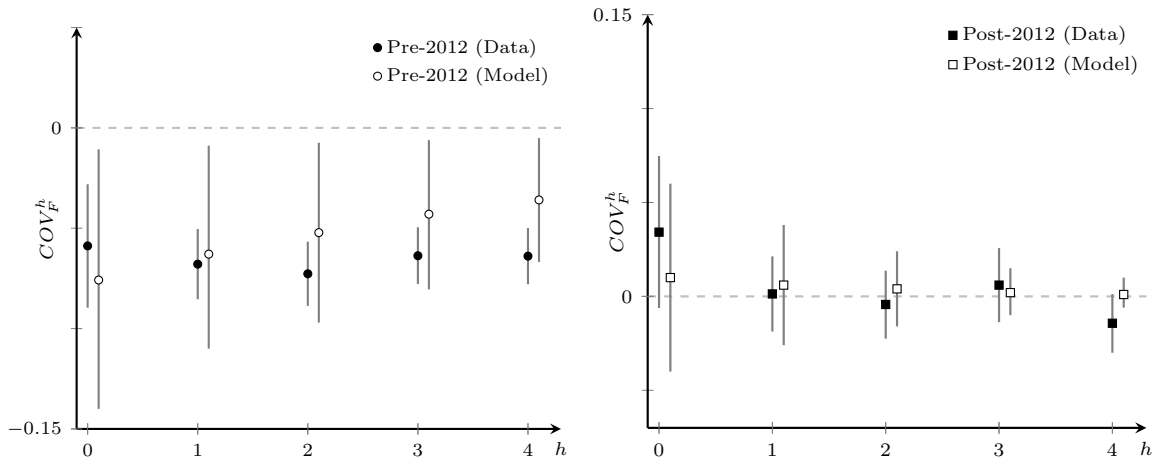

(a) COV_F^h before 2012 (b) COV_F^h after 2012

Figure 7. *The estimated COV_F^h for the subsamples before and after 2012. Black dots represent the results obtained using SPF data, while white dots represent the simulated data. In Figures 7(a) and 7(b), we observe that the covariance is negative before 2012 and positive or close to zero after 2012. The sample period for the pre-2012 sub-sample ranges from 1990Q1 to 2011Q4, while the post-2012 sub-sample spans from 2012Q1 to 2019Q4.*

tent (i.e., ρ decreases), the magnitude of the negative covariance between trend and cyclical beliefs decreases. This is because, as the trend component becomes more stable, forecasters can better separate the trend from the cycle; and as the persistence of the cyclical component decreases, new information about the cyclical component becomes less relevant for updating the trend component. As a result, the force from the confusion mechanism plays a less important role, and the overall forecast dispersion decreases at a faster rate.

Second, we examine the covariance between changes in the long-run forecasts and cyclical forecasts in both sub-samples. It is important to stress that this covariance was not a targeted moment in the estimation.

The empirical results from the SPF data reveal an intriguing shift in forecasting behavior. Figure 7(a) shows a significant negative covariance between changes in long-run forecasts and cyclical forecasts in the pre-2012 sub-sample. In constrast, Figure 7(b) illustrates that this covariance becomes positive and insignificant in the post-2012 sub-sample.

This reversal in sign following the implementation of inflation targeting aligns with our model's prediction. As previously discussed, when the trend component becomes more stable and the cyclical component less persistent, the confusion mechanism's effect weakens. Consequently, the empirical covariance patterns should more closely match those predicted by the observable-trend model in section 4.1, where the confusion mechanism is absent. Our model predicts that after the policy change, the co-

variance between changes in trend forecasts and changes in cyclical forecasts is more likely to be non-negative.

Qualitatively, the estimated results from the simulated data closely align with the empirical results using the SPF data in both subsamples. Figure 7 contrasts the results in the SPF data with those from the simulation data. Despite its simplicity and limited number of parameters, our model effectively captures the shift in forecasting patterns following the policy change and quantitatively reproduces the changes observed in the actual data.

5.2 Application: Optimal Monetary Policy and Information Friction

In this section, we investigate the policy implications of the new information friction we introduced. Policy makers may possess a superior ability to distinguish between trends and cycles compared to private sector agents, owing to their access to more information sources and better research capabilities. There may exist a disparity in the degree of confusion between policy makers and the public. Crucially, if policy makers overlook this discrepancy in information friction when designing policies, the resulting policies may be sub-optimal, potentially leading to social welfare losses. To illustrate, we introduce this friction into a simple policy game following Barro and Gordon (1983) and build upon Huo et al. (2024), a new contribution in expectation formation.

Central Bank's Objective In this model, there is a central bank that designs monetary policy and agents in the private sector. The central bank selects the inflation rate π_t to minimize the total social loss given by:

$$\mathcal{L} = E[\mathrm{U}_t^2 + \omega(\pi_t - \pi_t^*)^2],$$

where U_t represents the unemployment rate and ω captures the central bank's preference for targeting the optimal inflation rate over reducing the unemployment rate. π_t denotes the inflation rate in period t, determined by the central bank. π_t^* is the optimal inflation rate in period t, following a stochastic process.

The unemployment rate U_t is determined by the average inflation surprise according to:

$$\mathrm{U}_t = \mathrm{U}^N - \beta(\pi_t - \overline{E}[\pi_t]),$$

where U^N represents the natural unemployment rate, β is the slope of the Phillips curve, and $\overline{E}[\pi_t]$ denotes the average forecast of the inflation rate for the current period. To simplify notation, we assume that U^N is zero.

Trend, Cycle and Information Structure We assume that π_t^* comprises a trend com-

ponent and a cyclical component:

$$\pi_t^* = \mu_t^\pi + x_t^\pi,$$

$$\mu_t^\pi = \mu_{t-1}^\pi + \gamma_t^\mu \quad \text{and} \quad x_t^\pi = \rho x_{t-1}^\pi + \gamma_t^x,$$

where γ_t^μ and γ_t^x represent the state innovations of the trend and cyclical components. We assume that γ_t^μ and γ_t^x follow normal distributions with zero mean and variances σ_μ^2 and σ_x^2, respectively. That is, we assume the state variable π_t^* follows the same data-generating process that we discussed in the benchmark model (section 3.1).

To model the information advantage of the central bank, we assume that the central bank can observe the trend and cyclical components of optimal inflation at the end of each period, but agents cannot. That is, the central bank could observe both μ_{t-1}^π and x_{t-1}^π while agents can only observe π_{t-1}^*. This represents a situation where the central bank can perfectly separate trend and cycle, but agents cannot.

Upon deciding on the inflation rate for the current period, the central bank cannot observe the actual value of each component. Instead, the central bank observes signals regarding the trend and cyclical components:

$$s_{c,t}^\mu = \mu_t^\pi + \epsilon_{c,t} \quad \text{and} \quad s_{c,t}^x = x_t^\pi + e_{c,t},$$

where $\epsilon_{c,t}$ and $e_{c,t}$ are the noise in the signal. The noise terms are assumed to be normally distributed with zero mean and variance $\sigma_{\epsilon,c}^2$ and $\sigma_{e,c}^2$ respectively.

Three comments about this model are noteworthy. First, we assume that the central bank lacks perfect information about trends and cycles when designing policy at the beginning of each period, only obtaining this knowledge at the period's end. Consequently, the central bank's belief updating process regarding these two components is independent, while the agents' process is not. Second, our assumption about the difference in information friction is stark and made to simplify our analysis, as the key focus of our model is to examine how differences in the degree of separability could affect optimal policy design. We could extend this model to allow imperfect observation of trends and cycles by the central bank. The insights would still hold as long as the central bank is better at separating trend and cycle than the agents. Third, our results do not rely on the fact that π_{t-1}^* is revealed to agents. The same qualitative pattern could emerge if agents can only observe π_{t-1}.

Setting Inflation Following Barro and Gordon (1983), we consider a scenario in which the central bank employs a time-consistent policy:

$$\pi_t = (1-\alpha)E_{CB}[\pi_t^*] + \alpha E_{CB}[\overline{E}[\pi_t]], \quad \alpha = \frac{\beta^2}{\beta^2 + \omega},$$

where $E_{CB}[\cdot]$ represents the belief of the central bank.

In essence, the central bank needs to decide between targeting the optimal inflation rate or targeting the average forecasts. The parameter α captures the central bank's intention to reduce the unemployment rate compared to targeting the optimal inflation rate. When α is zero, the central bank only targets the optimal inflation rate, resulting in $\pi_t = E_{CB}[\pi_t^*]$. Conversely, when $\alpha = 1$, the central bank only cares about the unemployment rate, leading to $\pi_t = E_{CB}[\overline{E}[\pi_t]]$.

Agents The agent i's utility is determined by the difference between their prediction and the actual inflation rate:

$$U(F_{i,t}\pi_t, \pi_t) = -(F_{i,t}\pi_t - \pi_t)^2.$$

Agents cannot directly observe the optimal inflation target π_t^*; instead, they observe private signals regarding the trend and cyclical components:

$$s_{i,t}^{\mu} = \mu_t^{\pi} + \epsilon_{i,t} \quad \text{and} \quad s_{i,t}^{x} = x_t^{\pi} + e_{i,t},$$

where $\epsilon_{i,t}$ and $e_{i,t}$ represent the noise present in the private signals. These noise terms are assumed to follow a normal distribution with zero mean and variances σ_ϵ^2 and σ_e^2 respectively.

In equilibrium, the optimal policy is contingent on the optimal inflation target (π_t^*) and the central bank's perception of the average expectation ($E_{CB}[\overline{E}[\pi_t]]$). We explore two scenarios: in the first case, the central bank knows that agents in the private sector cannot observe the actual values of the trend and cyclical components when setting inflation. In the second case, the central bank mistakenly believes the public knows the actual values of the trend and cyclical components as the central bank itself does. Lemma 5 characterizes the average forecast when the public can or cannot observe the value of the two components.

Lemma 5. (i) If the public can observe the actual values of the trend and cyclical components at the end of each period, the average forecast of the current inflation is:

$$\overline{E}_{ob}[\pi_t] = \boldsymbol{I}[(\boldsymbol{I} - \boldsymbol{\kappa^{ob}})\boldsymbol{\theta_{t-1}} + \boldsymbol{\kappa^{ob}}\boldsymbol{\theta_t}], \tag{18}$$

where $\boldsymbol{\kappa^{ob}}$ is the Kalman gain matrix:

$$\boldsymbol{\kappa^{ob}} = \begin{pmatrix} \frac{\sigma_\mu^2}{\sigma_\mu^2 + (1-\alpha)^{-1}\sigma_\epsilon^2} & 0 \\ 0 & \frac{\sigma_x^2}{\sigma_x^2 + (1-\alpha)^{-1}\sigma_e^2} \end{pmatrix}.$$

(ii) If the public cannot observe the actual values of the trend and cyclical components,

the average forecast of the current inflation is:

$$\overline{E}_{un}[\pi_t] = \boldsymbol{I}[(\boldsymbol{I} - \boldsymbol{\kappa^{un}})\overline{\boldsymbol{\theta}}_{\boldsymbol{t-1}} + \boldsymbol{\kappa^{un}}\boldsymbol{\theta_t}], \tag{19}$$

where $\overline{\boldsymbol{\theta}}_{\boldsymbol{t-1}}$ is the average belief of the trend and cyclical component at the end of period $t-1$, and $\boldsymbol{\kappa^{un}}$ is the Kalman gain matrix:

$$\boldsymbol{\kappa^{un}} = \boldsymbol{\kappa}\begin{pmatrix} C^{\mu} & 0 \\ 0 & C^{x} \end{pmatrix} = \begin{pmatrix} \frac{V+\sigma_{\epsilon}^2(\sigma_z^2+\sigma_{\mu}^2)}{\Omega} & -\frac{\rho\sigma_{\epsilon}^2\sigma_z^2}{\Omega} \\ -\frac{\rho\sigma_{\epsilon}^2\sigma_z^2}{\Omega} & \frac{V+\sigma_{\epsilon}^2(\sigma_x^2+\rho^2\sigma_z^2)}{\Omega} \end{pmatrix}\begin{pmatrix} C^{\mu} & 0 \\ 0 & C^{x} \end{pmatrix}.$$

Note that $\boldsymbol{\kappa}$ is specified in Equation (8). The constants $0 \leq C^{\mu} \leq 1$ and $0 \leq C^{x} \leq 1$ depend on α; when $\alpha = 0$, $C^{\mu} = C^{x} = 1$, and when $\alpha = 1$, $C^{\mu} = C^{x} = 0$.

Since the actual inflation depends on the average forecast, there is an additional coordination motive for the public compared to the benchmark model. This coordination motive leads individuals to place less weight on private signals, which is captured by $(1-\alpha)^{-1}$ in the first case and C^{μ} and C^{x} in the second case, shown by the theorem provided by Huo and Pedroni (2020).

Building on this set of characterization, we investigate the optimal policy and the corresponding social welfare loss in two scenarios.

Proposition 4. *Suppose agents cannot observe the actual values of the trend and cyclical components. (i) If the central bank knows that the public does not know the value of each component, the total social welfare loss is given by:*

$$\mathcal{L}1 = [\beta^2(1-\alpha)]E\left[(\overline{E}_{un}[\pi_t] - \pi_t^*)^2\right] + E\left[[(1-\alpha)(E_{CB}[\pi_t^*] - \pi_t^*) + \alpha(E_{CB}^{un}[\pi_t] - \overline{E}_{un}[\pi_t])]^2\right]. \tag{20}$$

(ii) If the central bank mistakenly perceives that the public knows the value of each component, the total social welfare loss is given by:

$$\begin{aligned}\mathcal{L}2 = {} & [\beta^2(1-\alpha)]E\left[(\overline{E}_{un}[\pi_t] - \pi_t^*)^2\right] + E\left[[(1-\alpha)(E_{CB}[\pi_t^*] - \pi_t^*) + \alpha(E_{CB}^{un}[\pi_t] - \overline{E}_{un}[\pi_t])]^2\right] \\ & + \alpha\beta^2 E\left[(E_{CB}^{ob}[\pi_t] - E_{CB}^{un}[\pi_t])^2\right],\end{aligned} \tag{21}$$

where $E_{CB}^{ob}[\pi_t] = E_{CB}[\overline{E}_{ob}[\pi_t]]$, $E_{CB}^{un}[\pi_t] = E_{CB}[\overline{E}_{un}[\pi_t]]$ are the central bank's perceptions regarding the average belief.

(iii) The total social welfare loss is always larger when the central bank believes that the public could separate the trend and cyclical components perfectly, i.e., $\mathcal{L}1 < \mathcal{L}2$.

Proposition 4 characterizes the total social welfare loss in both cases and shows that the welfare loss is always larger when the central bank mistakenly perceives the public's ability to separate the two components. Equation (20) demonstrates that when

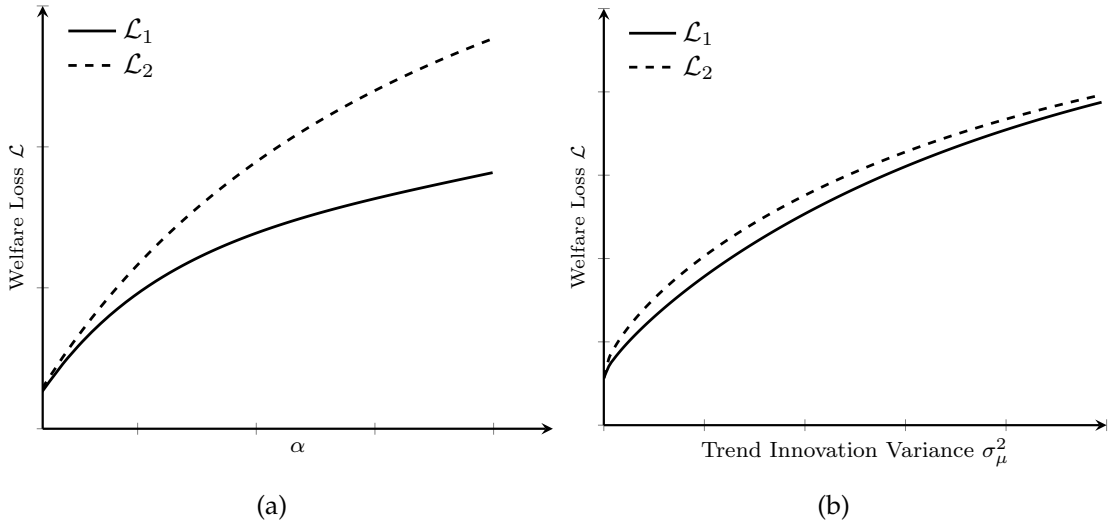

(a) (b)

Figure 8. *The figure plots the total social welfare loss for the two cases over different α and σ_μ^2. The solid line shows the total loss when the public cannot observe the actual values of the trend and cyclical components, and the central bank acknowledges this. The dashed line shows the total social welfare loss when the public cannot observe the actual values of the trend and cyclical components, but the central bank mistakenly believes the public can observe these values. The total loss of the latter is always higher than that in the first case.*

the central bank accurately assesses the public's ability to separate components, the welfare loss arises from two sources: (1) the deviation of the average forecast from the optimal inflation rate, and (2) a weighted average of two forecasting errors - the central bank's error in predicting the optimal inflation rate and its error in estimating the public's average forecast.

Contrasting with Equation (20), we observe from Equation (21) that when the central bank mistakenly believes the public knows the actual values of the trend and cyclical components, it results in an additional welfare loss, captured by the third term in Equation (21). This additional loss term depends on the disparity between the central bank's perceived average beliefs under two scenarios: when the public can perfectly separate the two components and when they cannot (i.e., $E_{CB}^{ob}[\pi_t] - E_{CB}^{un}[\pi_t]$).

Figure 8(a) illustrates how social welfare loss ($\mathcal{L}_1$ and $\mathcal{L}_2$) varies with α for the two cases. When α is small, social welfare primarily depends on the deviation from the optimal inflation rate. This results in similar welfare losses for both cases, as $\alpha^2\beta^2$ is also small. As α increases, the welfare loss becomes more sensitive to the unemployment rate and average forecast. Thus, when the central bank misperceives the public's ability, it leads to a larger additional loss for higher values of α.

Figure 8(b) shows how social welfare loss varies with σ_μ^2. When $\sigma_\mu^2 = 0$, the public perfectly separates trend and cyclical components, resulting in identical losses for both cases. For $\sigma_\mu^2 > 0$, misperceiving public ability always induces additional welfare loss due to forecast discrepancies between the central bank's perception and reality.

6 Extensions and Discussions

6.1 Forecasts of Other Forecasters

In this section, we explore a scenario where forecasters have access to a richer set of information. Specifically, we examine the case where forecasters not only observe the actual state value but also the forecasts made by their peers across various horizons. That is, we assume that at the end of period t, forecaster i observes both the current period's actual state value and the distribution of $F_{i,t}y_{t+h}$ across all forecasters. We will show that this additional information enhances the forecasters' estimates regarding both trend and cyclical components. However, despite this expanded information set, forecasters still cannot perfectly distinguish between the trend and cyclical components.

While Appendix C.2 provides a complete characterization, we discuss the key intuitions in the following. In our model, the individual forecast error comprises both the individual-specific forecast error and the common forecast error. The individual-specific forecast error arises from the noise term in the private signals (i.e., $\epsilon_{i,t}$ and $e_{i,t}$), while the common forecast error arises from the state innovations (i.e., γ_t^μ and γ_t^x). The observation of forecasts from others helps to eliminate the individual-specific error and reduce the separation error. Consequently, forecaster i would anchor to the consensus beliefs after observing the entire distribution, as it includes only the common forecast error.

After observing the forecasts of others, the separation error, $z_{i,t}$, becomes common across all forecasters (i.e., $z_{i,t} = z_{j,t}$ for any i, j). We denote this common separation error as z_t. Importantly, we show that z_t remains non-zero, even when forecasters can observe all the forecasts from others. This implies that they still cannot perfectly separate the trend and cyclical components, and the key results from our benchmark model continue to hold.

To understand why the common forecast error is non-zero in the steady state, in Appendix C.2, we show that the common separation error z_t is a weighted average of the consensus forecast errors regarding the two components and only includes the state innovations. The common separation error is still non-zero given that the consensus forecast error is non-zero.

In summary, these findings demonstrate that our benchmark model's key results remain robust even when forecasters have access to richer information sets, as the key friction of separating trend and cyclical components persists.

6.2 Misinterpretation of Signals

The previous sections characterized our benchmark model and examined its application in analyzing various issues related to patterns of expectation formation. In this

section, we will explore an alternative approach to modeling trend-cycle confusion and compare its implications with those of our model.

Specifically, we consider the source of confusion arises from misinterpreting signals. In this model, forecasters can observe both components at the end of each period. However, they may misinterpret the signals before making forecasts, mistaking a trend signal for a cyclical one or vice versa. Appendix C.3 provides all the details of the model, including assumptions, characterizations, and results. We summarize the findings and intuitions below.

In this model, forecasters can perfectly separate the two components at the end of each period (i.e., $\sigma_z^2 = 0$). Therefore, forecasters would update their beliefs regarding the trend and cyclical components independently, a key difference from our model. As a result, in this alternative model, the covariance between an individual's trend beliefs and cyclical beliefs is zero ($\widetilde{COV} = 0$); therefore, the covariance between changes in long-term and cyclical forecasts is always positive ($COV_F^h \geq 0$), which contradicts our empirical findings.

However, in this model, forecast dispersion may increase as the forecast horizon extends under certain conditions. The confusion between trends and cycles arises from only a fraction of forecasters misinterpreting the signals, which leads to a negative covariance between the cross-forecaster mean trend and cyclical beliefs at the aggregate level. For instance, when a positive trend signal is given, a group of forecasters misinterprets it as a cyclical signal. This misinterpretation results in lower mean trend beliefs across all forecasters than would be the case without misinterpretation, and higher mean cyclical beliefs across all forecasters. This mechanism weakens over the forecast horizon, constituting a force that drives up forecast dispersion.

6.3 Revisiting CG Regression

In this section, we revisit the seminal work by Coibion and Gorodnichenko (2015) and examine the empirical approach they propose within our framework. In that study, they propose a new specification to quantify the degree of information rigidity or the extent of information frictions using forecast data. They consider the following consensus level regression:

$$\underbrace{y_t - F_t y_t}_{Forecast\ Error} = c + \beta_{CG}(\underbrace{F_t y_t - F_{t-1} y_t}_{Forecast\ Revision}) + v_t, \tag{22}$$

where $F_t y_t$ is the consensus or mean forecast of y_t across forecasters, i.e., $F_t y_t \equiv \overline{E}[F_{i,t} y_t]$. The main finding of Coibion and Gorodnichenko (2015) is that the coefficient β_{CG} is positive for many macroeconomic variables. This indicates a positive correlation between the consensus forecast error (FE) and the consensus forecast revision (FR). That is, the ex post mean forecast error across forecasters is systematically predictable using

ex ante mean forecast revisions. The documented predictability can be interpreted as the gradual adjustment of beliefs by all forecasters to noisy information.

In a setting where the macroeconomic variable follows an AR(1) process (or an even more general stationary process), Coibion and Gorodnichenko (2015) show that the estimated "CG coefficient"(i.e., β_{CG} in specification (22)) corresponds to the extent of information friction within the framework of noisy information.

In our framework, the data generation process includes non-stationary trend components, which forecasters cannot perfectly distinguish from cyclical components. Proposition 5 re-examines this approach and investigates how the CG coefficient relates to the extent of underlying information frictions in this environment.

Proposition 5. *When y_t consists of both trend and cyclical components described by Equation (5), the CG coefficient β_{CG}^{Trend}, estimated using Equation (22), can be decomposed by:*

$$\begin{aligned}\beta_{CG}^{Trend} = & \underbrace{\frac{1-\boldsymbol{\kappa}_{11}}{\boldsymbol{\kappa}_{11}} + \frac{1-\boldsymbol{\kappa}_{22}}{\boldsymbol{\kappa}_{22}}}_{(+)\ Effect\ of\ noisy\ information} + \underbrace{\frac{\boldsymbol{\kappa}_{11}\boldsymbol{\kappa}_{12}(\boldsymbol{\kappa}_{21}-\boldsymbol{\kappa}_{22}) + \boldsymbol{\kappa}_{22}\boldsymbol{\kappa}_{21}(\boldsymbol{\kappa}_{12}-\boldsymbol{\kappa}_{11})}{\boldsymbol{\kappa}_{11}\boldsymbol{\kappa}_{22}(\boldsymbol{\kappa}_{11}\boldsymbol{\kappa}_{22}-\boldsymbol{\kappa}_{12}\boldsymbol{\kappa}_{21})}}_{(+)\ Effect\ of\ confusing\ trends\ and\ cycles} \\ & \underbrace{- \boldsymbol{I}\boldsymbol{\kappa}^{-1}(\boldsymbol{I}-\boldsymbol{\kappa})\boldsymbol{I}' \frac{cov(F_t y_t - F_{t-1}y_t,\ F_{2,t-1}y_t - F_{t-1}y_t)}{var(F_t y_t - F_{t-1}y_t)}}_{(+)\ Effect\ of\ the\ second\ updating} \\ & > 0,\end{aligned} \tag{23}$$

where $\boldsymbol{I}$ is the identity matrix, $\boldsymbol{\kappa}$ is the Kalman gain matrix specified in Equation (8), and $\boldsymbol{\kappa}_{ij}$ represents the element at row i and column j of the Kalman gain matrix.

Proposition (5) implies that the estimated β_{CG}^{Trend} in this environment provides a lower bound for the extent of information friction. To understand, we start by characterizing the consensus forecast error as follows:

$$\underbrace{y_t - F_t y_t}_{Forecast\ Error} = \boldsymbol{I}\boldsymbol{\kappa}^{-1}(\boldsymbol{I}-\boldsymbol{\kappa})\boldsymbol{I}' \underbrace{(F_t y_t - F_{t-1}y_t)}_{Forecast\ Revision} - \boldsymbol{I}\boldsymbol{\kappa}^{-1}(\boldsymbol{I}-\boldsymbol{\kappa})\boldsymbol{I}' \underbrace{(F_{2,t-1}y_t - F_{t-1}y_t)}_{Effect\ of\ the\ second\ updating}, \tag{24}$$

where $F_{2,t-1}y_t$ is the mean forecast across forecasters after observing the actual state value y_{t-1}, i.e., $F_{2,t-1}y_t \equiv \overline{E}[\mu^i_{2,t-1} + \rho x^i_{2,t-1}]$. Note that in our model, forecasters update their beliefs twice each period. As a result, the prior belief of period t is $F_{2,t-1}y_t$, which is the posterior belief after observing y_{t-1} at the end of period $t-1$.

The information friction in this model comes from two sources: noisy information and confusion, which are embedded in the term $\boldsymbol{I}\boldsymbol{\kappa}^{-1}(\boldsymbol{I}-\boldsymbol{\kappa})\boldsymbol{I}'$ of Equation (24). The first term on the right-hand side of Equation (23) captures the former, representing a weighted average of the extent of information friction in the two components. Note

that when the trends are stable (i.e., $\kappa_{11} = 1$), this term reduces to $(1 - \kappa_{22})/\kappa_{22}$, which is the CG coefficient β_{CG} characterized in Coibion and Gorodnichenko (2015).

The second term on the right-hand side of Equation (23) captures the impact of confusion. In our model, forecasters utilize the trend (cyclical) signal to update their beliefs about the cyclical (trend) component. For example, when forecasters observe a positive surprise from the trend signal (i.e., $s^{\mu}_{i,t} - \mu^{i}_{2,t-1} > 0$), they may interpret it partly as an indication of a strong trend innovation and partly as a lower trend component in the previous period. This leads to a situation that is observationally equivalent to forecasters having noisier signals. This mechanism drives up the correlation between forecast revisions and forecast errors, explaining why the second term on the right-hand side of Equation (23) is positive. Note that if trends and cycles are perfectly observable (i.e., $\kappa_{12} = \kappa_{21} = 0$), this term reduces to zero.

The third term on the right-hand side of Equation (23) characterizes the effect of the second belief updating at the of period $t-1$ after forecasters observe the statistics y_{t-1}, which is embedded in the term $(F_{2,t-1}y_t - F_{t-1}y_t)$ in Equation (24). When y_{t-1} is observable, it is used to update the belief about y_t, and the posterior belief becomes $F_{2,t-1}y_t$. The observation of y_{t-1} affects both forecast revisions and forecast errors. For example, when y_{t-1} is larger, the updated forecast for y_t next period $(F_t y_t)$ tends to be larger, resulting in a larger forecast revision $(F_t y_t - F_{t-1}y_t)$ and a smaller forecast error $(y_t - F_t y_t)$. This mechanism biases the coefficient downwards, explaining why the third term is negative.

Interestingly, when y_{t-1} is not observable, the posterior belief about y_t in period $t-1$ would be $F_{t-1}y_t$. There would be no second updating and the term $(F_{2,t-1}y_t - F_{t-1}y_t)$ in Equation (24) would be zero. In this case, forecasters would update their beliefs about trend and cyclical components independently, leading to no confusion between the two. That is, $\kappa_{12} = \kappa_{21} = 0$. Therefore, the second term on the right-hand side of Equation (23) reduces to zero too. Consequently, the CG coefficient would correspond exactly to the extent of noisy information.

Because the third term on the right-hand side of Equation (23) is negative, the actual extent of information friction can be even larger than the coefficient β^{Trend}_{CG} suggests. In other words, the CG coefficient provides a lower bound on the level of information friction. This finding suggests that the CG specification remains a robust measure for uncovering information friction stemming from noisy information, even within our framework.

6.4 Effects of the Pandemic

Our main results, presented in Section 2, focus on the pre-COVID period. However, examining forecaster behavior during the distinct circumstances of the pandemic can be both important and intriguing. This section presents empirical findings from the

pandemic period, comparing them to those of the pre-COVID period. We then discuss potential explanations for the observed shifts in forecaster behavior.

To begin with, we analyze how the empirical patterns of forecast variance and covariance between changes in long-term and cyclical forecasts, using the data from the COVID-19 period. Appendix A.6 plots the forecast variance and COV_F^h over forecast horizon for both unemployment rate and real GDP growth using data from the pandemic period.

The empirical patterns observed during the COVID-19 pandemic period differ from the pre-COVID findings in two key ways. First, the covariance between changes in long-run and cyclical unemployment rate forecasts becomes positive, while remaining negative for real GDP growth. Second, the forecast variance exhibits a substantial increase, rising from 0.019 to 0.737 for unemployment and from 0.152 to 0.900 for real GDP growth.

The positive COV_F^h observed for the unemployment rate during the COVID-19 pandemic could be caused by the fact that forecasters perceived greater variance in state innovations. Consequently, this heightened uncertainty dominated the negative covariance (i.e., $\widetilde{\text{COV}}$) between trend and cyclical beliefs. As Proposition 1 shows, the magnitude of $\widetilde{\text{COV}}$ diminishes when forecasters perceive significant variance in state innovations.

Furthermore, the substantial increase in forecast variance observed during the pandemic implies greater disagreement among forecasters. This heightened disagreement could stem from two potential sources. First, forecasters may have perceived an increase in the variance of state innovations, leading them to place greater weight on their own private signals. Second, the rise in forecast dispersion could indicate that the private signals themselves became noisier during this period, resulting in increased disagreement.

In our benchmark model, we assume forecasters possess perfect knowledge of the data generation process, which does not evolve over time. However, the pandemic associated with COVID-19 is "once in a lifetime" shock to the macroeconomy. To account for changes during the pandemic period using our model, it would be realistic to incorporate dynamics that allows for learning about changes in the state generating process. This would also allow for a more nuanced understanding of the observed shifts in forecasting behavior during the pandemic period. We leave this extension for future research.

7 Conclusion

This paper presents a framework where forecasters cannot perfectly distinguish between trend and cyclical components of the state variable. We demonstrate that this key feature qualitatively accounts for a set of observed empirical patterns at both in-

dividual and aggregate levels. Quantitatively, we apply this framework to examine the impact of the 2012 explicit inflation targeting policy on forecasting behaviors. The policy relevance of this friction is illustrated through a simple policy game.

This work suggests two promising avenues for future research. First, our model can incorporate various behavioral biases explored in the literature. Investigating their interaction with the confusion mechanism will offer valuable insights into the process of expectation formation. Second, this framework has applications beyond forecasting models. For example, it could be applied to understand investors who cannot separate sectoral and firm-specific components of firms' earnings, or voters who grapple with disentangling candidates' quality from luck. We defer the exploration of these research questions to future developments of this framework.

References

Adam, K., P. Kuang, and A. Marcet (2012). House price booms and the current account. *NBER Macroeconomics Annual 26*(1), 77–122.

Afrouzi, H., S. Y. Kwon, A. Landier, Y. Ma, and D. Thesmar (2023). Overreaction in expectations: Evidence and theory. *The Quarterly Journal of Economics 138*(3), 1713–1764.

Almeida, H., M. Campello, and M. S. Weisbach (2004). The cash flow sensitivity of cash. *The journal of finance 59*(4), 1777–1804.

Andrade, P., R. K. Crump, S. Eusepi, and E. Moench (2016). Fundamental disagreement. *Journal of Monetary Economics 83*, 106–128.

Antolin-Diaz, J., T. Drechsel, and I. Petrella (2017). Tracking the slowdown in long-run gdp growth. *Review of Economics and Statistics 99*(2), 343–356.

Barro, R. J. and D. B. Gordon (1983). Rules, discretion and reputation in a model of monetary policy. *Journal of monetary economics 12*(1), 101–121.

Bianchi, F., C. L. Ilut, and H. Saijo (2021). Diagnostic business cycles. Technical report, National Bureau of Economic Research.

Blanchard, O. J. and L. H. Summers (1986). Hysteresis and the european unemployment problem. *NBER macroeconomics annual 1*, 15–78.

Bordalo, P., N. Gennaioli, Y. Ma, and A. Shleifer (2020). Overreaction in macroeconomic expectations. *American Economic Review 110*(9), 2748–2782.

Bordalo, P., N. Gennaioli, and A. Shleifer (2018). Diagnostic expectations and credit cycles. *The Journal of Finance 73*(1), 199–227.

Broer, T. and A. N. Kohlhas (2022). Forecaster (mis-) behavior. *Review of Economics and Statistics*, 1–45.

Capistrán, C. and A. Timmermann (2009). Disagreement and biases in inflation expectations. *Journal of Money, Credit and Banking 41*(2-3), 365–396.

Carvalho, C., S. Eusepi, E. Moench, and B. Preston (2023). Anchored inflation expectations. *American Economic Journal: Macroeconomics 15*(1), 1–47.

Chen, H., G. Pei, Q. Xin, and X. Li (2024). Heterogeneous overreaction in expectation formation: Evidence and theory. *Journal of Economic Theory, Forthcoming*.

Chernozhukov, V. and H. Hong (2003). An mcmc approach to classical estimation. *Journal of econometrics 115*(2), 293–346.

Cogley, T. and T. J. Sargent (2005). Drifts and volatilities: monetary policies and outcomes in the post wwii us. *Review of Economic dynamics 8*(2), 262–302.

Cogley, T. and A. M. Sbordone (2008). Trend inflation, indexation, and inflation persistence in the new keynesian phillips curve. *American Economic Review 98*(5), 2101–2126.

Coibion, O. and Y. Gorodnichenko (2015). Information rigidity and the expectations formation process: A simple framework and new facts. *American Economic Review 105*(8), 2644–2678.

Delle Monache, D., A. De Polis, and I. Petrella (2024). Modeling and forecasting macroeconomic downside risk. *Journal of Business & Economic Statistics 42*(3), 1010–1025.

Elliott, G. and A. Timmermann (2008). Economic forecasting. *Journal of Economic Literature 46*(1), 3–56.

Farhi, E. and I. Werning (2019). Monetary policy, bounded rationality, and incomplete markets. *American Economic Review 109*(11), 3887–3928.

Farmer, L., E. Nakamura, and J. Steinsson (2024). Learning about the long run. *Journal of Political Economy, forthcoming.*.

Fisher, J. D. M., L. Melosi, and S. Rast (2024). Long-run inflation expectations.

Folland, G. B. (2009). *Fourier analysis and its applications*, Volume 4. American Mathematical Soc.

FOMC, S. (2012). Statement on longer-run goals and monetary policy strategy.

Furlanetto, F., A. Lepetit, Ø. Robstad, J. Rubio Ramírez, and P. Ulvedal (2021). Estimating hysteresis effects.

Gabaix, X. (2020). A behavioral new keynesian model. *American Economic Review 110*(8), 2271–2327.

García-Schmidt, M. and M. Woodford (2019). Are low interest rates deflationary? a paradox of perfect-foresight analysis. *American Economic Review 109*(1), 86–120.

Goldstein, N. and Y. Gorodnichenko (2022). Expectations formation and forward information. Technical report, National Bureau of Economic Research.

Goodfriend, M. (2004). Inflation targeting in the united states? In *The inflation-targeting debate*, pp. 311–352. University of Chicago Press.

Harvey, A. C. (1985). Trends and cycles in macroeconomic time series. *Journal of Business & Economic Statistics*, 216–227.

Huo, Z. and M. Pedroni (2020). A single-judge solution to beauty contests. *American Economic Review 110*(2), 526–568.

Huo, Z., M. Pedroni, and G. Pei (2024). Bias and sensitivity under ambiguity. *American Economic Review, Forthcoming*.

Kohlhas, A. N. and A. Walther (2021). Asymmetric attention. *American Economic Review 111*(9), 2879–2925.

Kuang, P. and K. Mitra (2016). Long-run growth uncertainty. *Journal of Monetary Economics 79*, 67–80.

Lahiri, K. and X. Sheng (2008). Evolution of forecast disagreement in a bayesian learning model. *Journal of Econometrics 144*(2), 325–340.

Lian, C. (2021). A theory of narrow thinking. *The Review of Economic Studies 88*(5), 2344–2374.

Morris, S. and H. S. Shin (2002). Social value of public information. *american economic review 92*(5), 1521–1534.

Nelson, C. R. and C. R. Plosser (1982). Trends and random walks in macroeconmic time series: some evidence and implications. *Journal of monetary economics 10*(2), 139–162.

Patton, A. J. and A. Timmermann (2010). Why do forecasters disagree? lessons from the term structure of cross-sectional dispersion. *Journal of Monetary Economics 57*(7), 803–820.

Rozsypal, F. and K. Schlafmann (2023). Overpersistence bias in individual income expectations and its aggregate implications. *American Economic Journal: Macroeconomics 15*(4), 331–371.

Shapiro, A. and D. J. Wilson (2019). The evolution of the fomc's explicit inflation target. *Evolution 2019*, 12.

Srinivasan, N. and P. Mitra (2012). Hysteresis in unemployment: Fact or fiction? *Economics Letters 115*(3), 419–422.

Stock, J. H. and M. W. Watson (1998). Median unbiased estimation of coefficient variance in a time-varying parameter model. *Journal of the American Statistical Association 93*(441), 349–358.

Wang, C. (2021). Under-and overreaction in yield curve expectations. *Available at SSRN 3487602*.

Appendix

A Data and Robustness Tests

A.1 Sample periods and variable definition

The data used in this paper are from the Survey of Professional Forecasters (SPF). Table A1 provides a list of the periods for which each forecast variable is available.

Table A1. *Summary of sample periods*

Summary of sample periods	
Forecast Variable	Sample periods
Panel A. Short-term Forecasts.	
Nominal GDP	1968Q4 - 2019Q4
Real GDP	1968Q4 - 2019Q4
GDP price index inflation	1968Q4 - 2019Q4
Real consumption	1981Q3 - 2019Q4
Industrial production	1968Q4 - 2019Q4
Real nonresidential investment	1981Q3 - 2019Q4
Real residential investment	1981Q3 - 2019Q4
Real federal government consumption	1981Q3 - 2019Q4
Real state and local government consumption	1981Q3 - 2019Q4
Housing start	1968Q4 - 2019Q4
Unemployment	1968Q4 - 2019Q4
Inflation (CPI)	1981Q3 - 2019Q4
Three-month Treasury rate	1981Q3 - 2019Q4
Ten-year Treasury rate	1992Q1 - 2019Q4
Panel B. Long-term Forecasts.	
Three-year ahead Real GDP	2009Q2-2019Q4
Three-year ahead unemployment	2009Q2-2019Q4
Ten-year ahead inflation (CPI)	1991Q3-2019Q4
Ten-year ahead Real GDP	1992Q1-2019Q1; first quarter only
Natural rate of unemployment	1996Q3-2019Q3; third quarter only

Following Bordalo et al. (2020), we convert macroeconomic variables to annual growth rates. For variables that are already presented as rates, we use the original data directly.

Variables changed to the annual growth rate include nominal GDP (NGDP), real GDP (RGDP), GDP price index inflation (PGDP), real consumption (RCONSUM), Industrial production (INDPROD), real nonresidential investment (RNRESIN), real residential investment (RRESINV), real federal government consumption (RGF), real state and local government consumption (RGSL). Forecast of h period ahead: $F_{i,t}y_{t+h} = (\frac{F_{i,t}\widetilde{y}_{t+h}}{\widetilde{y}_{t+h-4}} - 1) \times 100$, where $F_{i,t}\widetilde{y}_{t+h}$ is the original survey forecast from the forecaster i provided in period t regarding the state variable $\widetilde{y}$ in h period ahead. $\widetilde{y}_{t+h-4}$ is the actual state value of period $t+h-4$ already released. The procedures are a replication of Bordalo et al. (2020).

Variables that are taken directly from the survey data include unemployment rate

(UNEMP), housing start (HOUSING), CPI, Three-month Treasury rate (Tbills), Ten-year Treasury rate (Tbonds).

A.2 Three years ahead forecast and forecasts of longer horizon

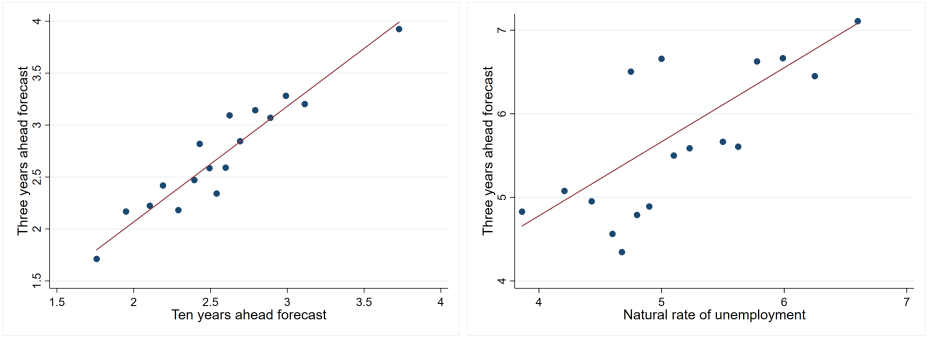

(a) Real GDP (b) Unemployment

Figure A1. *Three-year-ahead forecasts and forecasts for longer horizons. Note: The sample period is from 2009 to 2019, based on data availability. Forecasts of the natural unemployment rate are only available in the third quarter survey, while forecasts of ten-year-ahead real GDP are only available in the first quarter survey. Figure 1(a) illustrates the real GDP forecasts for three years ahead and ten years ahead. Figure 1(b) shows unemployment forecasts for three years ahead and the natural rate of unemployment. The correlation between the three-year horizon forecasts and longer-horizon forecasts, as depicted in the upper two figures, is 0.903 for real GDP growth and 0.886 for unemployment.*

A.3 Eestimation Results: Covaraince between changes in long-term forecasts and cyclical forecasts

Table A2. *Covariance between changes in long term forecasts and cyclical forecasts*

Covariance between changes in long term forecasts and cyclical forecasts			
	COV_F^h	95% bootstrap CI	Obs
Panel A. Unemployment rate			
$h = 0$	-0.203	(-0.244, -0.161)	794
$h = 1$	-0.192	(-0.232, -0.152)	815
$h = 2$	-0.177	(-0.214, -0.139)	819
$h = 3$	-0.164	(-0.199, -0.129)	817
$h = 4$	-0.151	(-0.183, -0.118)	818
Panel B. Real GDP growth			
$h = 0$	-0.219	(-0.273, -0.164)	783
$h = 1$	-0.214	(-0.271, -0.156)	781
$h = 2$	-0.204	(-0.260, -0.147)	785
$h = 3$	-0.204	(-0.258, -0.149)	785
$h = 4$	-0.202	(-0.256, -0.148)	785

Note: This table shows the covariance between the changes in long-term forecasts and cyclical forecasts. The sample period is from 2009Q2 to 2019Q4. Panel A shows the results of the unemployment rate, while Panel B shows the results of the Real GDP growth.

A.4 Robustness: Forecast dispersion over forecast horizon with time fixed effect

Table A3. *Forecast dispersion over forecast horizon with time FE*

	Dependent Variable: Forecast Dispersion					
	Variance of forecasts		50 percentile difference			
	β_1	SE	β_1	SE	Time FE	Obs
Forecast Variable	(1)	(2)	(3)	(4)		
Nominal GDP	0.337***	0.014	0.204***	0.005	Yes	1,025
Real GDP	0.242***	0.013	0.162***	0.004	Yes	1,025
GDP price index inflation	0.118***	0.005	0.119***	0.003	Yes	1,025
Real consumption	0.125***	0.008	0.127***	0.004	Yes	770
Industrial production	0.860***	0.034	0.320***	0.009	Yes	1,025
Real nonresidential investment	1.647***	0.068	0.497***	0.012	Yes	770
Real residential investment	6.021***	0.299	0.932***	0.026	Yes	770
Real federal government consumption	1.284***	0.065	0.393***	0.013	Yes	770
Real state and local government consumption	0.317***	0.016	0.210***	0.006	Yes	770
Housing start	0.004***	0.000	0.020***	0.001	Yes	1,024
Unemployment	0.034***	0.001	0.082***	0.002	Yes	1,014
Inflation rate (CPI)	-0.066***	0.013	-0.073***	0.008	Yes	770
Three-month Treasury rate	0.053***	0.002	0.106***	(0.003	Yes	770
Ten-year Treasury rate	0.045***	0.001	0.094***	0.002	Yes	560

Note: This table shows the coefficients from estimating Equation (2) with year-quarter fixed effect. The sample period is from 1968Q4 to 2019Q4. In column (1), the dependent variable is the variance of forecasts. In column (3), the dependent variable is the difference between the 25% percentile and 50% percentile. Standard errors are clustered at the year-quarter level.

A.5 Estimation procedures: Inflation

To estimate the set of parameters $\Theta = \{\rho, \sigma_\mu^2, \sigma_x^2, \sigma_e^2, \sigma_\epsilon^2\}$ before and after 2012, we begin by dividing the entire dataset into two subsets: one before 2012 and one after 2012. For each subset, we compute the average forecast variance for different forecast horizons ($h = 0, 1, 2, 3, 4$). These sets of forecast variances serve as the targets for estimation denoted as $\hat{m}$.

Since we want to capture the forecast variance across all the horizons, we give equal weights to all the targeted moments. Table A4 provides the summary statistic of the estimation moments.

Table A4. *Estimation Moments*

	Estimation Moments			
	Pre-2012		Post-2012	
	Target	SE	Target	SE
h=0	0.833	1.276	0.737	0.693
h=1	0.562	0.568	0.350	0.182
h=2	0.464	0.370	0.303	0.123
h=3	0.429	0.324	0.284	0.103
h=4	0.430	0.282	0.301	0.071

The distance is defined in Equation (17) as the weighted squared difference between the target moments $\hat{m}$ and the model prediction $m(\Theta)$, which represents the moments implied by the model for the given parameter set (Θ). Using MCMC with the Metropolis-Hastings algorithm, we choose the set of model parameters that minimize the distance $\Lambda(\Theta)$. The estimation of the parameter set before and after 2012

follows the exact same procedures, with different estimation targets derived from the respective subsets of the data.

A.6 The empirical patterns for the COVID period

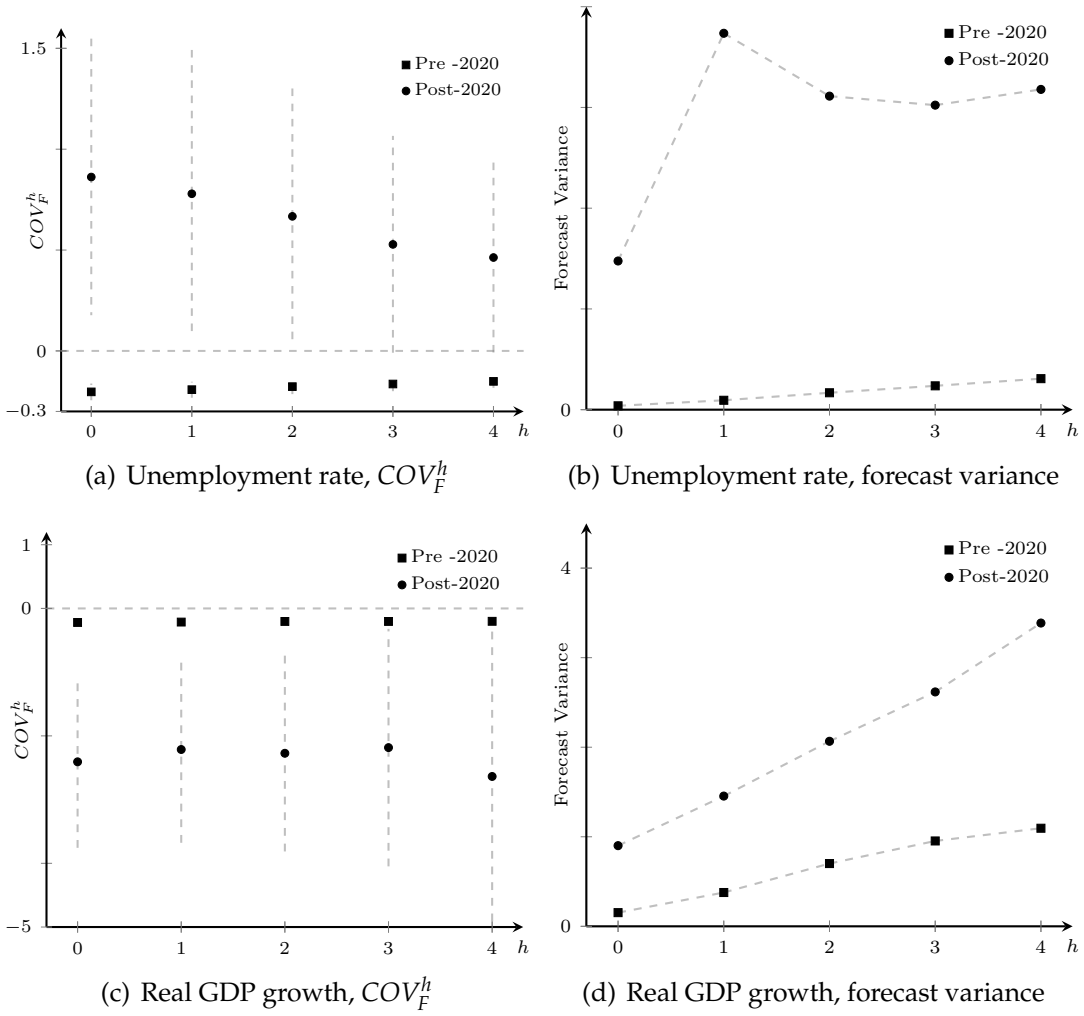

(a) Unemployment rate, COV_F^h

(b) Unemployment rate, forecast variance

(c) Real GDP growth, COV_F^h

(d) Real GDP growth, forecast variance

Figure A2. *Forecast patterns during the COVID-19 pandemic crisis. Note: This figure displays the COV_F^h and forecast variance of the unemployment rate and real GDP growth for different subsamples. The pre-2020 sample covers the period from 1968Q4 to 2019Q4, while the post-2020 sample covers the period from 2020Q1 to 2022Q4. The results for the pre-2020 period are plotted as square dots, while the post-2020 results are plotted as circle dots.*

B Proofs

Characterization of special case when the trend is observable in section 4.1.

Consider a special case where both the state and trend components are observable at the end of each period. Without loss of generality, we assume the cyclical component follows an AR(N) process:

$$x_t = \sum_{h=0}^{N} \rho^h L^h x_t + \gamma_t^x,$$

where L is the lag operator.

The private signal of forecaster i is given by:

$$s_{i,t}^{\mu} = \mu_t + \epsilon_{i,t} \quad \text{and} \quad s_{i,t}^{x} = x_t + e_{i,t}.$$

Given the trend component is observable at the end of each period, one's prior belief before observing the signals is:

$$\boldsymbol{\theta}_{2,t-1}^{i} = \begin{pmatrix} \mu_{t-1} \\ \sum_{h=0}^{N} \rho^h L^h x_t \end{pmatrix}.$$

The posterior beliefs regarding the two components upon observing the signals is given by:

$$\boldsymbol{\theta}_{1,t}^{i} = \boldsymbol{\theta}_{2,t-1}^{i} + \boldsymbol{\kappa} \times (\boldsymbol{s}_{i,t} - \boldsymbol{\theta}_{2,t-1}^{i}),$$

where the Kalman gain matrix and the variance-covariance matrix is same as the ones in the main text:

$$\boldsymbol{\kappa} = \begin{pmatrix} \frac{\sigma_\mu^2}{\sigma_\mu^2+\sigma_\epsilon^2} & 0 \\ 0 & \frac{\sigma_x^2}{\sigma_x^2+\sigma_e^2} \end{pmatrix}, \quad \text{and} \quad \begin{pmatrix} \text{Var}_s^T & \widetilde{\text{COV}}_s \\ \widetilde{\text{COV}}_s & \text{Var}_s^C \end{pmatrix} = \begin{pmatrix} \frac{\sigma_\epsilon^2\sigma_\mu^2}{\sigma_\epsilon^2+\sigma_\mu^2} & 0 \\ 0 & \frac{\sigma_e^2\sigma_x^2}{\sigma_x^2+\sigma_e^2} \end{pmatrix}.$$

The forecast variance across forecasters is given by:

$$\begin{aligned} E[(F_{i,t}y_{t+h} - \overline{E}[F_{i,t}y_{t+h}])^2] &= \rho^{2h} \underbrace{\frac{\sigma_x^2}{\sigma_x^2+\sigma_e^2}}_{\phi_s^C} \text{Var}_s^C + \underbrace{\frac{\sigma_\mu^2}{\sigma_\mu^2+\sigma_\epsilon^2}}_{\phi_s^T} \text{Var}_s^T \\ &= \rho^{2h}(\frac{\sigma_x^2}{\sigma_x^2+\sigma_e^2})^2\sigma_e^2 + (\frac{\sigma_\mu^2}{\sigma_\mu^2+\sigma_\epsilon^2})^2\sigma_\epsilon^2. \end{aligned}$$

It is evidence that the forecast variance across forecasters is decreasing, as the forecast horizon extends.

In addition, changes in trend forecasts and changes cyclical forecasts can be written as follows:

$$F_{i,t}y_{t+3Y} - F_{i,t-1}y_{t-1+3Y} = (\mu^i_{1,t} - E_{i,t-1}[\mu_{t-1}]) + \rho^{3Y}(E_{i,t}[\sum_{h=0}^{N}\rho^h L^h x_{t+3Y}] - E_{i,t-1}[\sum_{h=0}^{N}\rho^h L^h x_{t+3Y-1}]),$$

and

$$Cyc_{i,t} - Cyc_{i,t-1} = (1-\rho^{3Y})(E_{i,t}[\sum_{h=0}^{N}\rho^h L^h x_{t+3Y}] - E_{i,t-1}[\sum_{h=0}^{N}\rho^h L^h x_{t+3Y-1}]).$$

Following the same logic as the main text, the covariance between changes in the beliefs about the trend component and changes in beliefs about the cyclical component at any horizon should be non-negative. That is,

$$\begin{aligned}&COV^h_F(F_{i,t}y_{t+3Y} - F_{i,t-1}y_{t-1+3Y}, Cyc_{i,t} - Cyc_{i,t-1})\\ &= \rho^{3Y}(1-\rho^{3Y})Var(E_{i,t}[\sum_{h=0}^{N}\rho^h L^h x_{t+3Y}] - E_{i,t-1}[\sum_{h=0}^{N}\rho^h L^h x_{t+3Y-1}]) \geq 0.\end{aligned}$$

In this special case, where trends and cycles are observable at the end of each period, the model fails to replicate either of the two empirical patterns documented, even when we allow the data generation process for the cyclical component to follow an AR(N) process.

Proof of Lemma 1. To begin, we assume that the error term in the last period ($z_{i,t-1}$) is normally distributed with the variance $\sigma^2_{z,t-1}$. With the prior belief and the signal structures given by Equation (6) and (7), the posterior belief of forecaster i after receiving signals is given by:

$$\begin{aligned}p(\boldsymbol{\theta}|\boldsymbol{s}_{i,t}) &\propto p(\boldsymbol{\theta}^i_{2,t-1})p(\boldsymbol{s}_{i,t}|\boldsymbol{\theta}^i_{2,t-1})\\ &\propto \exp\left\{-\frac{1}{2}[\boldsymbol{\theta}^T(\boldsymbol{\Sigma}_{\boldsymbol{s}}^{-1} + \boldsymbol{\Sigma}^{-1}_{\boldsymbol{\theta}^i_{2,t-1}})\boldsymbol{\theta} - 2(\boldsymbol{\Sigma}_{\boldsymbol{s}}^{-1} + \boldsymbol{\Sigma}^{-1}_{\boldsymbol{\theta}^i_{2,t-1}})^{-1}(\boldsymbol{\Sigma}_{\boldsymbol{s}}^{-1} + \boldsymbol{\Sigma}^{-1}_{\boldsymbol{\theta}^i_{2,t-1}})(\boldsymbol{s}^T_{i,t}\boldsymbol{\Sigma}_{\boldsymbol{s}}^{-1} + \boldsymbol{\theta}^{i,T}_{2,t-1}\boldsymbol{\Sigma}^{-1}_{\boldsymbol{\theta}^i_{2,t-1}})\boldsymbol{\theta}]\right\}\\ &\propto \exp[-\frac{1}{2}(\boldsymbol{\theta} - \boldsymbol{\theta}^i_{1,t})^T(\boldsymbol{\Sigma}_{\boldsymbol{s}}^{-1} + \boldsymbol{\Sigma}^{-1}_{\boldsymbol{\theta}^i_{2,t-1}})(\boldsymbol{\theta} - \boldsymbol{\theta}^i_{1,t})],\end{aligned}$$

where

$$\boldsymbol{\theta}^i_{1,t} = (\boldsymbol{\Sigma}_{\boldsymbol{s}}^{-1} + \boldsymbol{\Sigma}^{-1}_{\boldsymbol{\theta}^i_{2,t-1}})^{-1}(\boldsymbol{s}^T_{i,t}\boldsymbol{\Sigma}_{\boldsymbol{s}}^{-1} + \boldsymbol{\theta}^{i,T}_{2,t-1}\boldsymbol{\Sigma}^{-1}_{\boldsymbol{\theta}^i_{2,t-1}})^T.$$

Therefore, $\mu^i_{1,t}$ and $x^i_{1,t}$ are joint normally distributed. To be specific, $\boldsymbol{\theta}^i_{1,t} = (\mu^i_{1,t}, x^i_{1,t})'$

is given by:

$$\mu^i_{1,t} = \underbrace{\frac{\sigma^2_\epsilon(\rho^2\sigma^2_{z,t-1}+\sigma^2_x+\sigma^2_e)}{\Omega_t}}_{prior\ weight}\mu^i_{2,t-1} + \underbrace{\frac{V_t+\sigma^2_\epsilon(\sigma^2_{z,t-1}+\sigma^2_\mu)}{\Omega_t}}_{signal\ weight} s^\mu_{i,t} - \frac{\rho\sigma^2_\epsilon\sigma^2_{z,t-1}}{\Omega_t}\underbrace{(s^x_{i,t}-\rho x^i_{2,t-1})}_{surprise\ from\ cycle}, \tag{A1}$$

$$x^i_{1,t} = \underbrace{\frac{\sigma^2_e(\sigma^2_{z,t-1}+\sigma^2_\mu+\sigma^2_\epsilon)}{\Omega_t}}_{prior\ weight}\rho x^i_{2,t-1} + \underbrace{\frac{V_t+\sigma^2_\epsilon(\sigma^2_x+\rho^2\sigma^2_{z,t-1})}{\Omega_t}}_{signal\ weight} s^x_{i,t} - \frac{\rho\sigma^2_e\sigma^2_{z,t-1}}{\Omega_t}\underbrace{(s^\mu_{i,t}-\mu^i_{2,t-1})}_{surprise\ from\ trend}. \tag{A2}$$

where Ω_t and V_t are constants:

$$\Omega_t = (\sigma^2_{z,t-1}+\sigma^2_\mu+\sigma^2_\epsilon)(\sigma^2_x+\sigma^2_e+\rho^2\sigma^2_{z,t-1}) - \rho^2\sigma^4_{z,t-1},\ V_t = (\sigma^2_{z,t-1}+\sigma^2_\mu)(\sigma^2_x+\rho^2\sigma^2_{z,t-1}) - \rho^2\sigma^4_{z,t-1}.$$

And the variance-covariance matrix of $\mu^i_{1,t}$ and $x^i_{1,t}$ is:

$$(\mathbf{\Sigma_s^{-1}} + \mathbf{\Sigma^{-1}_{\theta^i_{2,t-1}}})^{-1} = \begin{pmatrix} \mathrm{Var}^T_t & \widetilde{\mathrm{COV}}_t \\ \widetilde{\mathrm{COV}}_t & \mathrm{Var}^C_t \end{pmatrix} = \begin{pmatrix} \frac{\sigma^2_\epsilon[\Omega_t-\sigma^2_\epsilon(\sigma^2_x+\sigma^2_e+\rho^2\sigma^2_{z,t-1})]}{\Omega_t} & -\frac{\rho\sigma^2_e\sigma^2_\epsilon\sigma^2_{z,t-1}}{\Omega_t} \\ -\frac{\rho\sigma^2_e\sigma^2_\epsilon\sigma^2_{z,t-1}}{\Omega_t} & \frac{\sigma^2_e[\Omega_t-\sigma^2_e(\sigma^2_\epsilon+\sigma^2_\mu+\sigma^2_{z,t-1})]}{\Omega_t} \end{pmatrix}, \tag{A3}$$

The observation of y_t provides new information and forecasters would update their beliefs accordingly:

$$\begin{aligned} f^i(\mu_t|y_t) &\propto \exp\left\{-\frac{1}{2(1-r_t^2)}[\frac{(\mu_t-\mu^i_{1,t})^2}{\mathrm{Var}^T_t} - \frac{2r_t(\mu_t-\mu^i_{1,t})(y_t-\mu_t-x^i_{1,t})}{\sqrt{\mathrm{Var}^T_t\mathrm{Var}^C_t}} + \frac{(y_t-\mu_t-x^i_{1,t})^2}{\mathrm{Var}^C_t}]\right\} \\ &\propto \exp\{-\frac{1}{2(1-r_t^2)}[\frac{(\mathrm{Var}^T_t + 2r_t\sqrt{\mathrm{Var}^T_t\mathrm{Var}^C_t} + \mathrm{Var}^C_t)\mu_t^2}{\mathrm{Var}^T_t\mathrm{Var}^C_t} \\ &\quad - 2\mu_t\frac{\mathrm{Var}^C_t\mu^i_{1,t} + r_t\sqrt{\mathrm{Var}^T_t\mathrm{Var}^C_t}(\mu^i_{1,t}+y_t-x^i_{1,t}) + \mathrm{Var}^T_t(y_t-x^i_{1,t})}{\mathrm{Var}^T_t\mathrm{Var}^C_t}]\}, \end{aligned} \tag{A4}$$

and

$$f^i(x_t|y_t) \propto \exp\left\{-\frac{1}{2(1-r_t^2)}[\frac{(y_t-x_t-\mu_{1,t}^i)^2}{\text{Var}_t^T} - \frac{2r_t(y_t-x_t-\mu_{1,t}^i)(x_t-x_{1,t}^i)}{\sqrt{\text{Var}_t^T\text{Var}_t^C}} + \frac{(x_t-x_{1,t}^i)^2}{\text{Var}_t^C}]\right\}$$

$$\propto \exp\{-\frac{1}{2(1-r_t^2)}(\frac{\text{Var}_t^T + 2r_t\sqrt{\text{Var}_t^T\text{Var}_t^C} + \text{Var}_t^T)x_t^2}{\text{Var}_t^T\text{Var}_t^C})$$

$$-2x_t\frac{\text{Var}_t^C(y_t-\mu_{1,t}^i) + r_t\sqrt{\text{Var}_t^T\text{Var}_t^C}(y_t-\mu_{1,t}^i+x_{1,t}^i) + \text{Var}_t^T x_{1,t}^i}{\text{Var}_t^T\text{Var}_t^C}\}, \tag{A5}$$

where r_t is given by:

$$r_t = \frac{\widetilde{\text{COV}}_t}{\sqrt{\text{Var}_t^T\text{Var}_t^C}}. \tag{A6}$$

According to Equations (A4) and (A5), the posterior beliefs $f^i(\mu_t|y_t)$ and $f^i(x_t|y_t)$ are normal distributions. Therefore, $\mu_{2,t}^i$ and $x_{2,t}^i$ are normally distributed. As a result, $z_{i,t}$ will also be normally distributed. That shows first part of the lemma.

Furthermore, the means of the posterior beliefs are given by:

$$\begin{aligned}\mu_{2,t}^i &= \frac{\text{Var}_t^C\mu_{1,t}^i + \text{Var}_t^T(y_t-x_{1,t}^i) + r_t\sqrt{\text{Var}_t^T\text{Var}_t^C}(\mu_{1,t}^i+y_t-x_{1,t}^i)}{\text{Var}_t^T + 2r_t\sqrt{\text{Var}_t^T\text{Var}_t^C} + \text{Var}_t^C} \\ &= \frac{(\text{Var}_t^C + \widetilde{\text{COV}}_t)\mu_{1,t}^i + (\text{Var}_t^T + \widetilde{\text{COV}}_t)(y_t-x_{1,t}^i)}{\text{Var}_t^T + \text{Var}_t^C + 2\widetilde{\text{COV}}_t}.\end{aligned} \tag{A7}$$

and

$$\begin{aligned}x_{2,t}^i &= \frac{\text{Var}_t^C(y_t-\mu_{1,t}^i) + r_t\sqrt{\text{Var}_t^T\text{Var}_t^C}(y_t-\mu_{1,t}^i+x_{1,t}^i) + \text{Var}_t^T x_{1,t}^i}{\text{Var}_t^T + 2r_t\sqrt{\text{Var}_t^T\text{Var}_t^C} + \text{Var}_t^C} \\ &= \frac{(\text{Var}_t^C + \widetilde{\text{COV}}_t)(y_t-\mu_{1,t}^i) + (\text{Var}_t^T + \widetilde{\text{COV}}_t)x_{1,t}^i}{\text{Var}_t^T + \text{Var}_t^C + 2\widetilde{\text{COV}}_t}.\end{aligned}$$

We show that

$$\begin{aligned}\mu_{2,t}^i + x_{2,t}^i &= \frac{(\text{Var}_t^C + \widetilde{\text{COV}}_t)\mu_{1,t}^i + (\text{Var}_t^T + \widetilde{\text{COV}}_t)(y_t-x_{1,t}^i)}{\text{Var}_t^T + \text{Var}_t^C + 2\widetilde{\text{COV}}_t} \\ &\quad + \frac{(\text{Var}_t^C + \widetilde{\text{COV}}_t)(y_t-\mu_{1,t}^i) + (\text{Var}_t^T + \widetilde{\text{COV}}_t)x_{1,t}^i}{\text{Var}_t^T + \text{Var}_t^C + 2\widetilde{\text{COV}}_t} \\ &= y_t.\end{aligned}$$

The second part of the lemma is shown.

Proof of Lemma 2. We first establish the existence of the steady state and then show that the steady state is unique. According to Equations (A4) and (A5), after observing y_t, the variance of the separation error is given by:

$$\sigma_{z_t}^2 = \frac{(1-r_t^2)\text{Var}_t^T\text{Var}_t^C}{\text{Var}_t^T + 2r_t\sqrt{\text{Var}_t^T\text{Var}_t^C} + \text{Var}_t^C}. \tag{A8}$$

Recall the definitions of Var_t^T, Var_t^C and r_t in Equations (A3) and (A6), we notice that the right-hand-side of Equation (A8) is a function of $\sigma_{z,t-1}^2$. Therefore, the steady state value σ_z^2 is a fixed point of the condition characterized by Equation (A8). Solving for the fixed point of Equation (A8) gives:

$$\sigma_z^2 = \frac{-\sigma_\mu^2[\Lambda + 2\rho(1-\rho)\sigma_e^2\sigma_\epsilon^2] + \sqrt{\sigma_\mu^2\Lambda[\sigma_\mu^2(\Lambda + 4\rho\sigma_e^2\sigma_\epsilon^2) + 4\sigma_e^2\sigma_\epsilon^2\sigma_x^2]}}{2[\Lambda + \rho^2\sigma_\mu^2(\sigma_e^2+\sigma_\epsilon^2)]}, \tag{A9}$$

where $\Lambda = (1-\rho)^2\sigma_e^2\sigma_\epsilon^2 + \sigma_x^2(\sigma_e^2+\sigma_\epsilon^2)$.

In the next step, we demonstrate that regardless of the initial variance of the separation error, denoted as $\sigma_{z_0}^2$, it always converges to a unique steady state value σ_z^2. We first simplify Equation (A8) to:

$$\sigma_{z,t}^2 = \frac{g_1(\sigma_{z,t-1}^2)}{g_2(\sigma_{z,t-1}^2)}, \tag{A10}$$

where

$$g_1(\sigma_{z,t-1}^2) = w_1\sigma_{z,t-1}^2 + \eta_1 \quad \text{and} \quad g_2(\sigma_{z,t-1}^2) = w_2\sigma_{z,t-1}^2 + \eta_2,$$

$$w_1 = \sigma_e^2\sigma_\epsilon^2(\rho^2\sigma_\mu^2 + \sigma_x^2);\ \eta_1 = \sigma_e^2\sigma_\epsilon^2\sigma_\mu^2\sigma_x^2;$$

$$w_2 = \rho^2(\sigma_e^2\sigma_\epsilon^2 + \sigma_e^2\sigma_\mu^2 + \sigma_\mu^2\sigma_\epsilon^2) + \sigma_e^2\sigma_\epsilon^2 + \sigma_e^2\sigma_x^2 + \sigma_\epsilon^2\sigma_x^2 - 2\rho\sigma_e^2\sigma_\epsilon^2;\ \eta_2 = \sigma_e^2\sigma_\epsilon^2(\sigma_\mu^2+\sigma_x^2) + \sigma_\mu^2\sigma_x^2(\sigma_e^2+\sigma_\epsilon^2).$$

Define the difference between $\sigma_{z,t}^2$ and $\sigma_{z,t-1}^2$ as:

$$D(\sigma_{z,t-1}^2) = \sigma_{z,t}^2 - \sigma_{z,t-1}^2 = \frac{g_1(\sigma_{z,t-1}^2)}{g_2(\sigma_{z,t-1}^2)} - \sigma_{z,t-1}^2.$$

To show the steady state is unique, it is sufficient to show that $D(\sigma_{z,t-1}^2)$ is monotonically decreasing. We first show that evaluated at $\sigma_{z,t-1}^2 = 0$, the derivative is negative.

$$\frac{\partial D(\sigma_{z,t-1}^2)}{\partial\sigma_{z,t-1}^2}\Big|_{\sigma_{z,t-1}^2=0} = \left[\frac{\sigma_e^2\sigma_\epsilon^2(\rho\sigma_\mu^2+\sigma_x^2)}{\sigma_e^2\sigma_\epsilon^2(\rho\sigma_\mu^2+\sigma_x^2) + \sigma_\mu^2\sigma_x^2(\sigma_e^2+\sigma_\epsilon^2)}\right]^2 - 1 < 0.$$

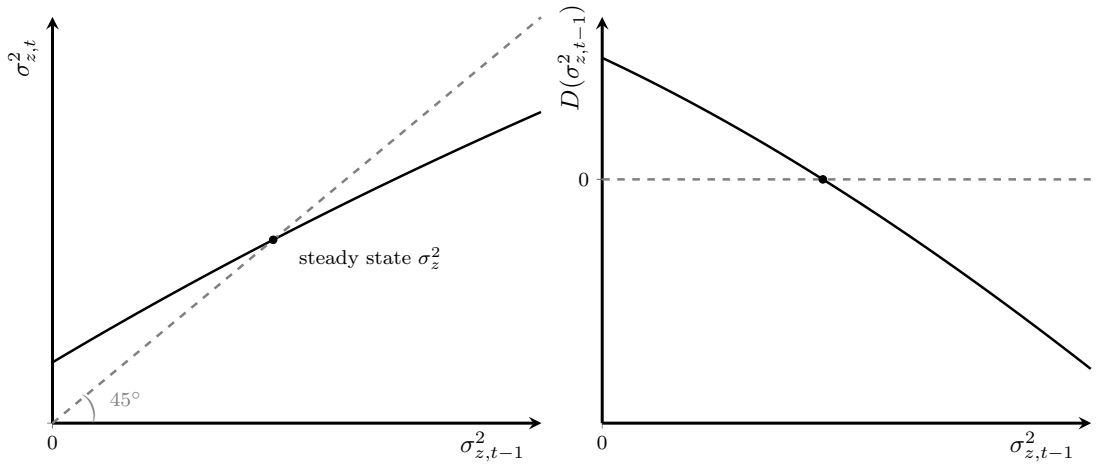

(a) $\sigma^2_{z,t-1}$ and $\sigma^2_{z,t}$ (b) $D(\sigma^2_{z,t-1})$ and $\sigma^2_{z,t-1}$

Figure A3. *The relationship between $\sigma^2_{z,t-1}$ and $\sigma^2_{z,t}$.*

Then we show that the first-order derivative of $D(\sigma^2_{z,t-1})$ is negative. The derivative is given by:

$$\frac{\partial D(\sigma^2_{z,t-1})}{\partial \sigma^2_{z,t-1}} = \frac{w_1\eta_2 - w_2\eta_1}{(w_2\sigma^2_{z,t} + \eta_2)^2} - 1 = \left[\frac{\sigma^2_e\sigma^2_\epsilon(\rho\sigma^2_\mu + \sigma^2_x)}{(w_2\sigma^2_{z,t} + \eta_2)}\right]^2 - 1. \tag{A11}$$

It is always decreasing, because we show that the second-order derivative is negative:

$$\frac{\partial^2 D(\sigma^2_{z,t-1})}{\partial(\sigma^2_{z,t-1})^2} = -2w_2\frac{[\sigma^2_e\sigma^2_\epsilon(\rho\sigma^2_\mu + \sigma^2_x)]^2}{(w_2\sigma^2_{z,t} + \eta_2)^3} < 0.$$

Since $D(\sigma^2_{z,t})$ is monotonously decreasing and concave and the steady state exists, it is unique. Figure 3(a) illustrates the relationship between $\sigma^2_{z,t-1}$ and $\sigma^2_{z,t}$, while Figure 3(b) further illustrates how the difference between the two variances (i.e., $\sigma^2_{z,t} - \sigma^2_{z,t-1}$) responds to $\sigma^2_{z,t-1}$, highlighting the convergence property.

Proof of Lemma 3. Given the quadratic utility function, the forecaster's optimal forecasts are given by the following:

$$\begin{aligned} F_{i,t}y_{t+h} &= E_{i,t}[y_{t+h}] \\ &= E_{i,t}[\mu_t + \rho^h x_t] \\ &= \mu^i_{1,t} + \rho^h x^i_{1,t}. \end{aligned}$$

The first equality is derived from the first order condition of the standard quadratic utility function. With a quadratic utility function, forecasters would minimize the expected squared error, and the first-order condition is given by:

$$E_{i,t}[F_{i,t}y_{t+h} - y_{t+h}] = 0.$$

The second equality follows given the data generation process is known to forecasters. The third equality states that the expected value of the sum of μ_t and $\rho^h x_t$ is the sum of the expected values of the two components, a well known property using Fourier transform (Folland 2009).

Proof of Lemma 4. From Equation (A7) in the proof of Lemma 2, we obtain:

$$\begin{aligned} z_{i,t-1} &= \mu^i_{2,t-1} - \mu_{t-1} \\ &= \frac{(\text{Var}^T + \widetilde{\text{COV}})(x_{t-1} - x^i_{1,t-1}) - (\text{Var}^C + \widetilde{\text{COV}})(\mu_{t-1} - \mu^i_{1,t-1})}{\text{Var}^T + \widetilde{\text{COV}} + \text{Var}^C + \widetilde{\text{COV}}}, \end{aligned}$$

which is the first part of Lemma 4.

For the second part of Lemma 4, we show the steady state value of σ_z^2 increases in σ_μ^2. Our idea is to show that the solid line in Figure 3(a) shifts upwards when σ_μ^2 is larger. Towards this end, we prove the following claim.

Claim 1. For any given $\sigma^2_{z,t-1}$, the induced $\sigma^2_{z,t}$ is increasing in σ_μ^2.

Using Equation (A10), we obtain the derivative:

$$\frac{\partial \sigma^2_{z,t}}{\partial \sigma_\mu^2} = \frac{\partial [g_1(\sigma^2_{z,t-1})/g_2(\sigma^2_{z,t-1})]}{\partial \sigma_\mu^2} = \frac{\sigma_e^4 \sigma_\epsilon^4 [\sigma_x^2 - \rho(1-\rho)\sigma^2_{z,t-1}]^2}{g_2(\sigma^2_{z,t-1})^2} > 0. \tag{A12}$$

The claim is shown. Consequently, given the properties of $D(\sigma^2_{z,t-1})$ shown earlier, a larger steady state value for σ_z^2 is implied. The comparative statics with respect to σ_x^2, σ_ϵ^2, and σ_e^2 are analogous.

It is worth noting that $z_{i,t}$ is obtained via Bayesian updating, using the prior belief $\mu^i_{1,t}$ and $y_t - x^i_{1,t}$ shown in Equation (A9). As the variance of the posterior belief is always smaller than the variance of both prior beliefs, we can obtain:

$$0 \leq \sigma_z^2 \leq \min\{\text{Var}^C, \text{Var}^T\}.$$

In a special case when the variance of private signals go to infinity (i.e., $\sigma_e^2 \to +\infty$, $\sigma_\epsilon^2 \to +\infty$), the steady state σ_z^2 is:

$$\sigma_z^2 = \frac{-(1-\rho^2)\sigma_\mu^2 + \sqrt{\sigma_\mu^2(1-\rho)^2[(1+\rho)^2\sigma_\mu^2 + 4\sigma_x^2]}}{2(1-\rho)^2}$$

Similarly, considering the case that when the persistence of the cyclical component ρ changes:

$$\frac{\partial \sigma_{z,t}^2}{\partial \rho} = \frac{\sigma_{z,t-1}^2}{g_2(\sigma_{z,t-1}^2)^2} \left\{ 2\sigma_e^4 \sigma_\epsilon^4 [\rho \sigma_\mu^2 + \sigma_x^2][\sigma_\mu^2 + (1-\rho)\sigma_{z,t-1}^2] \right\} > 0.$$

Therefore, the steady state value of σ_z^2 is increasing in ρ. The logic underlying this statement is analogous.

Proof of Proposition 1. To show the first item, we note the following. When $\sigma_\mu^2 = 0$, according to Lemma 4, σ_z^2 goes to zero, and therefore $\widetilde{\text{COV}}$ becomes zero. When $\sigma_\mu^2 \to +\infty$, Lemma 4 states that $\sigma_z^2 \to \min\{\text{Var}^C, \text{Var}^T\}$, but $\Omega \to +\infty$ in this case. Therefore, $\widetilde{\text{COV}}$ goes to zero.

To show the second term, we first show that the second order derivative of σ_z^2 with respect to σ_μ^2 is negative. In Equation (A12), $g_2(\sigma_{z,t-1}^2)^2$ increases in σ_μ^2. Then the derivative $\partial \sigma_z^2 / \partial \sigma_\mu^2$ decreases when σ_μ^2 is larger. As σ_μ^2 approaches infinity, $\partial \sigma_z^2 / \partial \sigma_\mu^2$ approaches zero. That is,

$$Z'_\mu \equiv \frac{\partial \sigma_z^2}{\partial \sigma_\mu^2} > 0 \quad \text{and} \quad Z''_\mu \equiv \frac{\partial^2 \sigma_z^2}{(\partial \sigma_\mu^2)^2} < 0.$$

We then derive the derivative with respect to σ_μ^2:

$$\frac{\partial |\widetilde{\text{COV}}|}{\partial \sigma_\mu^2} \propto Z'_\mu (\sigma_e^2 + \sigma_x^2)(\sigma_\epsilon^2 + \sigma_\mu^2) - \sigma_z^2 (\rho^2 \sigma_z^2 + \sigma_e^2 + \sigma_x^2).$$

We show that evaluated at $\sigma_\mu^2 = 0$,

$$\frac{\partial |\widetilde{\text{COV}}|}{\partial \sigma_\mu^2}|_{\sigma_\mu^2 = 0} \propto Z'_\mu (\sigma_e^2 + \sigma_x^2)\sigma_\epsilon^2 > 0.$$

That is because $\sigma_z^2 = 0$ when $\sigma_\mu^2 = 0$. The second-order derivative is given by:

$$\frac{\partial^2 |\widetilde{\text{COV}}|}{(\partial \sigma_\mu^2)^2} \propto Z''_\mu (\sigma_\mu^2 + \sigma_\epsilon^2)(\sigma_e^2 + \sigma_x^2) - 2\rho^2 \sigma_z^2 Z'_\mu < 0.$$

To see the inequality we note that $Z'_\mu > 0$, and $Z''_\mu < 0$. Therefore, there exists a unique $\widetilde{\sigma}_\mu^2 > 0$, such that $\partial |\widetilde{\text{COV}}| / \partial \sigma_\mu^2 = 0$. For any $\sigma_\mu^2 < \widetilde{\sigma}_\mu^2$, $|\widetilde{\text{COV}}|$ is increasing in σ_μ^2; and for any $\sigma_\mu^2 > \widetilde{\sigma}_\mu^2$, $|\widetilde{\text{COV}}|$ is decreasing in σ_μ^2. The property that $|\widetilde{\text{COV}}|$ increases and then decrease is implied.

It is straightforward to show the second item that $|\widetilde{\text{COV}}|$ is always increasing in ρ,

because

$$\frac{\partial|\widetilde{\text{COV}}|}{\partial\rho} = \frac{\sigma_e^2\sigma_\epsilon^2}{\Omega^2}\left\{(\sigma_x^2+\sigma_e^2)[\sigma_z^4+\rho Z'_\rho(\sigma_\mu^2+\sigma_\epsilon^2)]+\sigma_z^2(\sigma_\mu^2+\sigma_\epsilon^2)[\sigma_x^2+\sigma_e^2-\rho^2\sigma_z^2]\right\} > 0,$$

where $Z'_\rho \equiv \partial\sigma_z^2/\partial\rho > 0$.

Proof of Proposition 2. The covariance between the changes in the long term forecasts and the cyclical forecasts is given by:

$$\begin{aligned} COV_F^h &= cov(F_{i,t}y_{t+3Y} - F_{i,t-1}y_{t-1+3Y}, Cyc_{i,t}^h - Cyc_{i,t-1}^h) \\ &= (\rho^h-\rho^{3Y})\left[cov(\mu_{1,t}^i-\mu_{1,t-1}^i, x_{1,t}^i-x_{1,t-1}^i)+\rho^{3Y}var(x_{1,t}^i-x_{1,t-1}^i)\right] \\ &= (\rho^h-\rho^{3Y})(\widetilde{\text{COV}}+\rho^{3Y}\text{Var}^C) \\ &= \frac{(\rho^h-\rho^{3Y})\sigma_e^2}{\Omega}\left\{\rho^{3Y}[\Omega-\sigma_e^2(\sigma_\epsilon^2+\sigma_\mu^2+\sigma_z^2)]-\rho\sigma_\epsilon^2\sigma_z^2\right\} \\ &\propto \rho^{3Y}[\Omega-\sigma_e^2(\sigma_\epsilon^2+\sigma_\mu^2+\sigma_z^2)]-\rho\sigma_\epsilon^2\sigma_z^2. \end{aligned} \tag{A13}$$

Define $K \equiv \rho^{3Y}[\Omega-\sigma_e^2(\sigma_\epsilon^2+\sigma_\mu^2+\sigma_z^2)]-\rho\sigma_\epsilon^2\sigma_z^2$. Then the sign of the covariance between changes in trend forecasts and changes in cyclical forecasts depends on the sign of K.

To prove the properties in the proposition, we first show that for any given σ_μ^2, there is a threshold $\overline{\sigma}_x^2$ such that if and only if $\sigma_x^2 < \overline{\sigma}_x^2$, then $K < 0$; and otherwise, $K \geq 0$. To see this, we derive the first-order derivative of K with respect to σ_x^2:

$$\begin{aligned} \frac{\partial K}{\partial\sigma_x^2} &= \rho^{3Y}[\sigma_z^2+\sigma_\mu^2+\sigma_\epsilon^2+\sigma_x^2Z'_x+\rho^2Z'_x(\sigma_\mu^2+\sigma_\epsilon^2)]-\rho\sigma_\epsilon^2Z'_x \\ &= Z'_x\left[\rho^{3Y}(\frac{\sigma_z^2+\sigma_\mu^2+\sigma_\epsilon^2}{Z'_x}+\sigma_x^2+\rho^2\sigma_\mu^2+\rho^2\sigma_\epsilon^2)-\rho\sigma_\epsilon^2\right]. \end{aligned} \tag{A14}$$

According to Lemma 4, $Z'_x > 0$ and $Z''_x < 0$. Therefore, the sum of first two terms in Equation (A14), $(\sigma_z^2+\sigma_\mu^2+\sigma_\epsilon^2)/Z'_x+\sigma_x^2$, increases in σ_x^2.

If $\partial K/\partial\sigma_x^2 \geq 0$ when evaluated at $\sigma_x^2 = 0$, then it always holds $\partial K/\partial\sigma_x^2 \geq 0$. If $\partial K/\partial\sigma_x^2 < 0$ when evaluated at $\sigma_x^2 = 0$, $\partial K/\partial\sigma_x^2$ crosses zero only once from below. Note that $\partial K/\partial\sigma_x^2$ must be positive when σ_x^2 is sufficiently large.

Furthermore, we characterize how K changes in σ_x^2. When $\sigma_x^2 = 0$, $K = 0$. That is because $\sigma_z^2 = 0$. When $\sigma_x^2 > 0$, K is either always positive, or K initially decreases and then crosses zero from below. This property implies that for any given value of σ_μ^2, there exists a threshold $\overline{\sigma}_x^2 \geq 0$, such that $K|_{\sigma_x^2=\overline{\sigma}_x^2} = 0$, and for any $\sigma_x^2 < \overline{\sigma}_x^2$, $K < 0$.

Given this property, we start proving the first item in this proposition. Towards this end, we show the following claim.

Claim: When $\sigma_x^2 = 0$, there exists a threshold $\overline{\sigma}_\mu^2$ for σ_μ^2, such that when $\sigma_\mu^2 \geq \overline{\sigma}_\mu^2$, $\overline{\sigma}_x^2 = 0$; when $0 < \sigma_\mu^2 < \overline{\sigma}_\mu^2$, $\overline{\sigma}_x^2 > 0$; and when $\sigma_\mu^2 = 0$, $\overline{\sigma}_x^2 = 0$.

To prove this claim, we first evaluate $\partial K/\partial \sigma_x^2$ at $\sigma_x^2 = 0$:

$$\frac{\partial K}{\partial \sigma_x^2}|_{\sigma_x^2=0} = Z'_{x=0}\left[\rho^{3Y}(\frac{\sigma_\mu^2+\sigma_\epsilon^2}{Z'_{x=0}} + \rho^2\sigma_\mu^2 + \rho^2\sigma_\epsilon^2) - \rho\sigma_\epsilon^2\right],$$

where $Z'_{x=0}$ is derivative of σ_z^2 evaluated at $\sigma_x^2 = 0$. It is given by:

$$Z'_{x=0} \equiv \frac{\partial \sigma_z^2}{\partial \sigma_x^2}|_{\sigma_x^2=0} = \begin{cases} \frac{2\rho(\sigma_e^2+\sigma_\epsilon^2)}{(1-\rho)(1+\rho)}\sigma_\mu^2 + \frac{2\sigma_e^2\sigma_\epsilon^2}{1+\rho}, & \text{if } \sigma_\mu^2 > 0. \\ 0, & \text{if } \sigma_\mu^2 = 0. \end{cases} \tag{A15}$$

There are only two cases. (i) When $\partial K/\partial \sigma_x^2|_{\sigma_x^2=0} \geq 0$, then K is always positive when $\sigma_x^2 > 0$ and $\overline{\sigma}_x^2 = 0$; and (ii) when $\partial K/\partial \sigma_x^2|_{\sigma_x^2=0} < 0$, K is negative and then crosses zero from below at $\sigma_x^2 = \overline{\sigma}_x^2 > 0$. Therefore, the necessary and sufficient condition for $\overline{\sigma}_x^2 > 0$ is given by $\partial K/\partial \sigma_x^2|_{\sigma_x^2=0} < 0$, which is equivalent to

$$\rho^{3Y}(\frac{\sigma_\mu^2+\sigma_\epsilon^2}{Z'_{x=0}} + \rho^2\sigma_\mu^2 + \rho^2\sigma_\epsilon^2) - \rho\sigma_\epsilon^2 < 0$$

or using the expression of $Z'_{x=0}$ in Equation (A15),

$$\frac{2\rho^4(\sigma_e^2+\sigma_\epsilon^2)}{1-\rho^2}(\sigma_\mu^2)^2 + \left[1 + \frac{2\rho^2\sigma_e^2\sigma_\epsilon^2}{1+\rho}(1+\rho^2-\rho^{1-3Y})\right]\sigma_\mu^2 - \left[\rho(\rho^{-h}-1)\frac{2\sigma_e^2\sigma_\epsilon^2}{1+\rho} + \rho^{1-3Y}\right]\sigma_\epsilon^2 < 0. \tag{A16}$$

The left-hand-side of Equation (A16) is quadratic in σ_μ^2, therefore there are two roots. Note that The left-hand-side of Equation (A16) is decreasing and then increasing in σ_μ^2 and it is negative when $\sigma_\mu^2 = 0$. Therefore, there must exist a unique positive root $\overline{\sigma}_\mu^2 > 0$.

Therefore, when $\sigma_\mu^2 \geq \overline{\sigma}_\mu^2$, $\overline{\sigma}_x^2 = 0$, which implies $K > 0$ on condition that $\sigma_x^2 > 0$. The first item in this proposition is shown. When $0 < \sigma_\mu^2 < \overline{\sigma}_\mu^2$, $\overline{\sigma}_x^2 > 0$, which implies $K > 0$ on condition that $\sigma_x^2 > \overline{\sigma}_x^2$. The second item is shown.

In addition, from the third equivalent of Equation (A13), as the forecast horizon h used to construct the cyclical forecast increases, the magnitude of COV_F^h is decreasing. The third item is shown.

Proof of Proposition 3. Given the optimal forecasts characterized by Lemma 3, the

forecast variance across all forecasters is given by:

$$Var(F_{i,t}y_{t+h}) = E[(\mu^i_{1,t} - \overline{E}[\mu_t])^2] + \rho^{2h}E[(x^i_{1,t} - \overline{E}[x_t])^2] + 2\rho^h E[(\mu^i_{1,t} - \overline{E}[\mu_t])]E[(x^i_{1,t} - \overline{E}[x_t])].$$

$\overline{E}[\cdot]$ stands for the mean forecast across all forecasters. To be specific:

$$E[(\mu^i_{1,t} - \overline{E}[\mu_t])^2] = \text{Var}^T - \frac{\sigma_\epsilon^4(\rho^2\sigma_z^2 + \sigma_x^2 + \sigma_e^2)^2}{\Omega^2} - \frac{\rho^2\sigma_\epsilon^4\sigma_z^4}{\Omega^2} - \frac{\sigma_\epsilon^4(\sigma_e^2 + \sigma_x^2)^2}{\Omega^2} = \text{Var}^T\phi^T,$$

where ϕ^T is given by:

$$\begin{aligned}\phi^T &= 1 - \frac{\sigma_\epsilon^4}{\text{Var}^T} \times \frac{\sigma_\mu^2(\rho^2\sigma_z^2 + \sigma_x^2 + \sigma_e^2)^2 + \rho^2\sigma_x^2\sigma_z^4 + (\sigma_e^2 + \sigma_x^2)^2 W\sigma_z^2}{\Omega^2} \\ &= \frac{[V + \sigma_\epsilon^2(\sigma_\mu^2 + \sigma_z^2)]^2 + \rho^2\sigma_e^2\sigma_\epsilon^2\sigma_z^4 + \sigma_\epsilon^2(\sigma_e^2 + \sigma_x^2)^2 W\sigma_z^2}{\Omega[\Omega - \sigma_\epsilon^2(\sigma_x^2 + \sigma_e^2 + \rho^2\sigma_z^2)]} < 1.\end{aligned}$$

Note that $W = E[(z_{i,t-1} - \overline{E}[z_{i,t-1}])^2]/\sigma_z^2$ is a positive scalar in steady state and invariant in t. To obtain the numerator term $E[(z_{i,t} - \overline{E}[z_{i,t}])^2]$, we rewrite Equation (10) and express $z_{i,t}$ as the follows:

$$\begin{aligned}z_{i,t} = &\frac{\sigma_e^2\sigma_\epsilon^2}{\Omega(\text{Var}^T + 2\widetilde{\text{COV}} + \text{Var}^C)}\{-[\sigma_x^2 + \rho(\rho-1)\sigma_z^2]\gamma_t^\mu + [\sigma_\mu^2 + (1-\rho)\sigma_z^2]\gamma_t^x \\ &+ \sigma_e^2 V\epsilon_{i,t} - \sigma_\epsilon^2 V e_{i,t} + (\rho\sigma_\mu^2 + \sigma_x^2)z_{i,t-1}\}.\end{aligned} \quad \text{(A17)}$$

This allows us to obtain:

$$z_{i,t} - \overline{E}[z_{i,t}] = \frac{\sigma_e^2\sigma_\epsilon^2}{\Omega(\text{Var}^T + 2\widetilde{\text{COV}} + \text{Var}^C)}\left[\sigma_e^2 V\epsilon_{i,t} - \sigma_\epsilon^2 V e_{i,t} + (\rho\sigma_\mu^2 + \sigma_x^2)(z_{i,t-1} - \overline{E}[z_{i,t-1}])\right].$$

and

$$E[(z_{i,t} - \overline{E}[z_{i,t}])^2] = \frac{(\sigma_e^2 + \sigma_\epsilon^2)\sigma_z^2 V^2}{(\sigma_e^2 + \sigma_\epsilon^2)V^2 + \sigma_e^2\sigma_\epsilon^2\{\sigma_\mu^2[\sigma_x^2 + \rho\sigma_z^2(\rho-1)]^2 + \sigma_x^2[\sigma_\mu^2 + (1-\rho)\sigma_z^2]^2\}}.$$

Therefore, W is given by:

$$W = \frac{(\sigma_e^2 + \sigma_\epsilon^2)V^2}{(\sigma_e^2 + \sigma_\epsilon^2)V^2 + \sigma_e^2\sigma_\epsilon^2\{\sigma_\mu^2[\sigma_x^2 + \rho\sigma_z^2(\rho-1)]^2 + \sigma_x^2[\sigma_\mu^2 + (1-\rho)\sigma_z^2]^2\}} < 1.$$

Similarly, $E[(x^i_{1,t} - \overline{E}[x_t])^2]$ and $E[(\mu^i_{1,t} - \overline{E}[\mu_t])]E[(x^i_{1,t} - \overline{E}[x_t])]$ can be written as:

$$E[(x^i_{1,t} - \overline{E}[x_t])^2] = \frac{[V + \sigma_\epsilon^2(\sigma_x^2 + \rho^2\sigma_z^2)]^2 + \rho^2\sigma_e^2\sigma_\epsilon^2\sigma_z^4 + \rho^2\sigma_e^2(\sigma_\epsilon^2 + \sigma_\mu^2)^2 W\sigma_z^2}{\Omega[\Omega - \sigma_e^2(\sigma_\epsilon^2 + \sigma_\mu^2 + \sigma_z^2)]}\text{Var}^C = \phi^C\text{Var}^C,$$

and

$$
\begin{aligned}
&E[(\mu^i_{1,t} - \overline{E}[\mu_t])]E[(x^i_{1,t} - \overline{E}[x_t])] \\
&= \frac{\sigma^2_\epsilon[V + \sigma^2_\epsilon(\sigma^2_x + \rho^2\sigma^2_z)] + \sigma^2_e[V + \sigma^2_e(\sigma^2_z + \sigma^2_\mu)] + \sigma^2_e\sigma^2_\epsilon(\sigma^2_x + \sigma^2_e)(\sigma^2_\epsilon + \sigma^2_\mu)W\sigma^2_z}{\Omega\sigma^2_e\sigma^2_\epsilon}\widetilde{\text{COV}} \\
&= \phi^{COV}\widetilde{\text{COV}}.
\end{aligned}
$$

Therefore, the forecast variance of $F_{i,t}y_{t+h}$ across all forecasters can be written as:

$$
Var(F_{i,t}y_{t+h}) = E[(F_{i,t}y_{t+h} - \overline{E}[F_{i,t}y_{t+h}])^2] = \rho^{2h}\text{Var}^C\phi^C + \text{Var}^T\phi^T + 2\rho^h\widetilde{\text{COV}}\phi^{COV},
$$

Take the derivative with respect to the forecast horizon h:

$$
\frac{\partial Var(F_{i,t}y_{t+h})}{\partial h} = 2\rho^h \ln\rho(\rho^h\text{Var}^C\phi^C + \widetilde{\text{COV}}\phi^{COV}).
$$

The forecast variance is increasing in h if and only if $\partial Var(F_{i,t}y_{t+h})/\partial h > 0$. That is,

$$
h > \underline{h} = \frac{1}{\ln\rho}\ln\frac{-\widetilde{\text{COV}}\phi^{COV}}{\text{Var}^C\phi^C}.
$$

Proof of Lemma 5.

When the public can observe the actual values of the trend and cyclical components, the agents would update their beliefs regarding the two components independently. Then the problem is exactly the same as the one in Morris and Shin (2002). The individual's prediction of the current inflation is given by:

$$
\begin{aligned}
F_{i,t}\pi_t &= E_{i,t}[(1-\alpha)\pi^*_t + \alpha\overline{E}[\pi_t]] \\
&= \frac{\sigma^2_\mu}{\sigma^2_\mu + (1-\alpha)^{-1}\sigma^2_\epsilon}s^\mu_{i,t} + \frac{(1-\alpha)^{-1}\sigma^2_\epsilon}{\sigma^2_\mu + (1-\alpha)^{-1}\sigma^2_\epsilon}\mu_{t-1} \\
&+ \frac{\sigma^2_x}{\sigma^2_x + (1-\alpha)^{-1}\sigma^2_e}s^x_{i,t} + \frac{(1-\alpha)^{-1}\sigma^2_e}{\sigma^2_x + (1-\alpha)^{-1}\sigma^2_e}\rho x_{t-1}
\end{aligned}
$$

And the average prediction of the current inflation is:

$$
\begin{aligned}
\overline{E}_{ob}[\pi_t] &= \frac{\sigma^2_\mu}{\sigma^2_\mu + (1-\alpha)^{-1}\sigma^2_\epsilon}\mu_t + \frac{(1-\alpha)^{-1}\sigma^2_\epsilon}{\sigma^2_\mu + (1-\alpha)^{-1}\sigma^2_\epsilon}\mu_{t-1} \\
&+ \frac{\sigma^2_x}{\sigma^2_x + (1-\alpha)^{-1}\sigma^2_e}x_t + \frac{(1-\alpha)^{-1}\sigma^2_e}{\sigma^2_x + (1-\alpha)^{-1}\sigma^2_e}\rho x_{t-1}
\end{aligned}
$$

Rearrange the term, we can get the first item.

When the public cannot observe the actual values of the trend and cyclical components, as shown in the benchmark model, the updating of the two components is not independent. Using the $\alpha - modified$ theorem provided by Huo and Pedroni (2020), that with the coordination motive, agents would place a lower weight on private information. We first guess that with the coordination motive, the forecast of agent i is given by:

$$F_{i,t}\pi_t = \boldsymbol{I}[(\boldsymbol{I} - \boldsymbol{\kappa^{un}})\boldsymbol{\theta^i_{2,t-1}} + \boldsymbol{\kappa^{un}}\boldsymbol{s_{i,t}}], \tag{A18}$$

where $\boldsymbol{\kappa^{un}}$ is given by:

$$\boldsymbol{\kappa^{un}} = \boldsymbol{\kappa}\begin{pmatrix} C^\mu & 0 \\ 0 & C^x \end{pmatrix} = \begin{pmatrix} \frac{V+\sigma_e^2(\sigma_z^2+\sigma_\mu^2)}{\Omega} & -\frac{\rho\sigma_\epsilon^2\sigma_z^2}{\Omega} \\ -\frac{\rho\sigma_e^2\sigma_z^2}{\Omega} & \frac{V+\sigma_\epsilon^2(\sigma_x^2+\rho^2\sigma_z^2)}{\Omega} \end{pmatrix}\begin{pmatrix} C^\mu & 0 \\ 0 & C^x \end{pmatrix}.$$

Then the average forecast is:

$$\overline{E}_{un}[\pi_t] = \boldsymbol{I}[(\boldsymbol{I} - \boldsymbol{\kappa^{un}})\overline{\boldsymbol{\theta}}_{\boldsymbol{t-1}} + \boldsymbol{\kappa^{un}}\boldsymbol{\theta_t}].$$

With the average forecast, individual forecast can be written as:

$$\begin{aligned} F_{i,t}\pi_t &= E_{i,t}[(1-\alpha)\pi_t^* + \alpha\overline{E}[\pi_t]] \\ &= (1-\alpha)\boldsymbol{I}\boldsymbol{\theta^i_{1,t}} + \alpha E_{i,t}\left[\overline{E}[\pi_t]\right] \\ &= (1-\alpha)\boldsymbol{I}\boldsymbol{\theta^i_{1,t}} + \alpha\left[\boldsymbol{I}(\boldsymbol{I} - \boldsymbol{\kappa^{un}})\boldsymbol{\theta^i_{2,t-1}} + \boldsymbol{\kappa}^{un}\boldsymbol{\theta^i_{1,t}}\right], \end{aligned} \tag{A19}$$

where $\boldsymbol{\theta^i_{1,t}}$ and κ are specified in Equation (8).

Match the coefficients in Equations (A18) and (A19), we can solve for C^μ and C^x:

$$C^\mu = \frac{(1-\alpha)\Omega[(1-r)V + \sigma_e^2(\sigma_\mu^2 + \sigma_z^2 - \rho\sigma_z^2)]}{[V + \sigma_e^2(\sigma_\mu^2 + \sigma_z^2 - \rho\sigma_z^2)][(1-\alpha)(\Omega - V) + \alpha\sigma_e^2\sigma_\epsilon^2]};$$

$$C^x = \frac{(1-\alpha)\Omega[(1-r)V + \sigma_\epsilon^2(\sigma_x^2 + \rho^2\sigma_z^2 - \rho\sigma_z^2)]}{[V + \sigma_\epsilon^2(\sigma_x^2 + \rho^2\sigma_z^2 - \rho\sigma_z^2)][(1-\alpha)(\Omega - V) + \alpha\sigma_e^2\sigma_\epsilon^2]};$$

It can be shown that when $\alpha = 1$, $C^\mu = C^x = 0$. In this case, the agents only care the average forecast, therefore would not use the private signals at all.

When $\alpha = 0$, $C^\mu = C^x = 1$. In this case, there's no coordination motive, the belief updating would be the same as our benchmark model. This shows the second item.

Proof of Proposition 4. Given the information structure, the central bank's beliefs

regarding the trend and cyclical components are given by:

$$F^{\mu}_{CB,t} = \frac{\sigma^2_{\mu}}{\sigma^2_{\mu}+\sigma^2_{\epsilon,c}} s^{\mu}_{c,t} + \frac{\sigma^2_{\epsilon,c}}{\sigma^2_{\mu}+\sigma^2_{\epsilon,c}} \mu_{t-1} \quad \text{and} \quad F^{x}_{CB,t} = \frac{\sigma^2_{x}}{\sigma^2_{x}+\sigma^2_{e,c}} s^{x}_{c,t} + \frac{\sigma^2_{e,c}}{\sigma^2_{x}+\sigma^2_{e,c}} \rho x_{t-1}.$$

Case 1: The public cannot observe the actual value of each components, and the central bank assume they cannot as well. The total social welfare loss in this case is:

$$\begin{aligned}
\mathcal{L}_1 &= E\left[\beta^2(\pi_t - \overline{E}[\pi_t])^2 + \omega(\pi_t - \pi^*_t)^2\right] \\
&= E\left[\beta^2[(1-\alpha)E_{CB}[\pi^*_t] + \alpha E^{un}_{CB}[\pi_t] - \overline{E}_{un}[\pi_t]]^2 + \omega[(1-\alpha)E_{CB}[\pi^*_t] + \alpha E^{un}_{CB}[\pi_t] - \pi^*_t]^2\right] \\
&= [\beta^2(1-\alpha)]E\left[(\overline{E}_{un}[\pi_t] - \pi^*_t)^2\right] + E\left[[(1-\alpha)(E_{CB}[\pi^*_t] - \pi^*_t) + \alpha(E^{un}_{CB}[\pi_t] - \overline{E}_{un}[\pi_t])]^2\right].
\end{aligned}$$

Case 2: The public cannot observe the actual value of each components, but the central bank mistakenly assume they can. The total social welfare loss in this case is:

$$\begin{aligned}
\mathcal{L}_2 &= E\left[\beta^2(\pi_t - \overline{E}[\pi_t])^2 + \omega(\pi_t - \pi^*_t)^2\right] \\
&= E\left[\beta^2[(1-\alpha)E_{CB}[\pi^*_t] + \alpha E^{ob}_{CB}[\pi_t] - \overline{E}_{un}[\pi_t]]^2 + \omega[(1-\alpha)E_{CB}[\pi^*_t] + \alpha E^{ob}_{CB}[\pi_t] - \pi^*_t]^2\right] \\
&= \beta^2 E\left[[(1-\alpha)(E_{CB}[\pi^*_t - \pi^*_t] + (1-\alpha)(\pi^*_t - \overline{E}_{un}[\pi_t]) + \alpha(E^{un}_{CB}[\pi_t] - \overline{E}^{un}[\pi_t]) + \alpha(E^{ob}_{CB}[\pi_t] - E^{un}_{CB}[\pi_t])]^2\right] \\
&+ \omega E\left[[(1-\alpha)(E_{CB}[\pi^*_t] - \pi^*_t) + \alpha(\overline{E}_{un}[\pi_t] - \pi^*_t) + \alpha(E^{un}_{CB}[\pi_t] - \overline{E}_{un}[\pi_t]) + \alpha(E^{ob}_{CB}[\pi_t] - E^{un}_{CB}[\pi_t])]^2\right] \\
&= [\beta^2(1-\alpha)]E\left[(\overline{E}_{un}[\pi_t] - \pi^*_t)^2\right] + E\left[[(1-\alpha)(E_{CB}[\pi^*_t] - \pi^*_t) + \alpha(E^{un}_{CB}[\pi_t] - \overline{E}_{un}[\pi_t])]^2\right] \\
&+ \alpha\beta^2 E\left[[E^{ob}_{CB}[\pi_t] - E^{un}_{CB}[\pi_t])]^2\right] + 2\alpha\omega E\left[cov(E^{ob}_{CB}[\pi_t] - E^{un}_{CB}[\pi_t], E_{CB}[\pi^*_t] - \pi^*_t)\right] \\
&+ 2\alpha\beta^2 E\left[cov(E^{ob}_{CB}[\pi_t] - E^{un}_{CB}[\pi_t], E^{un}_{CB}[\pi_t] - \overline{E}_{un}[\pi_t])\right].
\end{aligned}$$

Given the central bank's belief regarding the trend and cyclical components, it can be shown that:

$$E_{CB}[\pi^*_t] - \pi^*_t = (F^{\mu}_{CB,t} - \mu_t) + (F^{x}_{CB,t} - x_t).$$

$$E^{ob}_{CB}[\pi_t] - \overline{E}_{un}[\pi_t] = (\boldsymbol{\kappa}^{un}_{1,1} + \boldsymbol{\kappa}^{un}_{2,1})(F^{\mu}_{CB,t} - \mu_t) + (\boldsymbol{\kappa}^{un}_{1,2} + \boldsymbol{\kappa}^{un}_{2,2})(F^{x}_{CB,t} - x_t).$$

$$\begin{aligned}
E^{ob}_{CB}[\pi_t] - E^{un}_{CB}[\pi_t] = &(\frac{\sigma^2_{\mu}}{\sigma^2_{\mu} + (1-\alpha)^{-1}\sigma^2_{\epsilon}} - \boldsymbol{\kappa}^{un}_{1,1} - \boldsymbol{\kappa}^{un}_{2,1})(F_{c,t}\mu_t - \mu_{t-1}) \\
&+ (\frac{\sigma^2_{x}}{\sigma^2_{x} + (1-\alpha)^{-1}\sigma^2_{e}} - \boldsymbol{\kappa}^{un}_{1,2} - \boldsymbol{\kappa}^{un}_{2,2})(F_{c,t}x_t - \rho x_{t-1}) \\
&- (1 - \boldsymbol{\kappa}^{un}_{1,1} - \boldsymbol{\kappa}^{un}_{2,1} - \rho + \rho\boldsymbol{\kappa}^{un}_{2,2} + \rho\boldsymbol{\kappa}^{un}_{1,2})\overline{z}_{t-1}.
\end{aligned}$$

Note that $cov(F^{\mu}_{CB,t} - \mu_t, F^{\mu}_{CB,t} - \mu_{t-1}) = 0$, $cov(F^{x}_{CB,t} - x_t, F^{x}_{CB,t} - x_{t-1}) = 0$ and $cov(\overline{z}_{t-1}, F^{\mu}_{CB,t} - \mu_t) = cov(\overline{z}_{t-1}, F^{x}_{CB,t} - x_t) = 0$. Therefore, the total welfare loss in this

case is :

$$\mathcal{L}_2 = [\beta^2(1-\alpha)]E\left[(\overline{E}_{un}[\pi_t] - \pi_t^*)^2\right] + E\left[[(1-\alpha)(E_{CB}[\pi_t^*] - \pi_t^*) + \alpha(E_{CB}^{un}[\pi_t] - \overline{E}_{un}[\pi_t])]^2\right] + \alpha\beta^2 E\left[[E_{CB}^{ob}[\pi_t] - E_{CB}^{un}[\pi_t])]^2\right].$$

The difference of the social welfare loss in the two cases is:

$$\mathcal{L}_2 - \mathcal{L}_1 = \alpha\beta^2 E\left[[E_{CB}^{ob}[\pi_t] - E_{CB}^{un}[\pi_t]]^2\right] \geq 0.$$

Proof of Proposition 5. Using Equation (8), the individual level beliefs can be rewritten as:

$$\boldsymbol{\theta}_{1,t}^i = (\boldsymbol{I} - \boldsymbol{\kappa})\boldsymbol{\theta}_{2,t-1}^i + \boldsymbol{\kappa}\boldsymbol{s}_{i,t},$$

and therefore, the consensus level belief is:

$$\boldsymbol{\theta}_{1,t} = (\boldsymbol{I} - \boldsymbol{\kappa})\boldsymbol{\theta}_{2,t-1} + \boldsymbol{\kappa}\boldsymbol{\theta}_t.$$

Therefore, the error term $\boldsymbol{\theta} - \boldsymbol{\theta}_{1,t}$ is:

$$\begin{aligned}\boldsymbol{\theta} - \boldsymbol{\theta}_{1,t} &= (\boldsymbol{I} - \boldsymbol{\kappa})(\boldsymbol{\theta} - \boldsymbol{\theta}_{2,t-1}) \\ &= (\boldsymbol{I} - \boldsymbol{\kappa})(\boldsymbol{\theta} - \boldsymbol{\theta}_{1,t}) + (\boldsymbol{I} - \boldsymbol{\kappa})(\boldsymbol{\theta}_{1,t} - \boldsymbol{\theta}_{2,t-1}) \\ &= (\boldsymbol{I} - \boldsymbol{\kappa})(\boldsymbol{\theta} - \boldsymbol{\theta}_{1,t}) + (\boldsymbol{I} - \boldsymbol{\kappa})(\boldsymbol{\theta}_{1,t} - \boldsymbol{\theta}_{1,t-1}^t) + (\boldsymbol{I} - \boldsymbol{\kappa})(\boldsymbol{\theta}_{1,t-1}^t - \boldsymbol{\theta}_{2,t-1}),\end{aligned}$$

where $\boldsymbol{\theta}_{1,t-1}^t = [F_{1,t-1}\mu_{t-1} \quad \rho F_{1,t-1}x_{t-1}]'$.

At the consensus level, the forecast error and the consensus forecast revision are given by:

$$y_t - F_t y_t = \boldsymbol{I}(\boldsymbol{\theta} - \boldsymbol{\theta}_{1,t}) \quad \text{and} \quad F_t y_t - F_{t-1} y_t = \boldsymbol{I}(\boldsymbol{\theta}_{1,t} - \boldsymbol{\theta}_{1,t-1}^t).$$

Rearrange the terms, we can get:

$$y_t - F_t y_t = \boldsymbol{I}\boldsymbol{\kappa}^{-1}(\boldsymbol{I} - \boldsymbol{\kappa})\boldsymbol{I}'(F_t y_t - F_{t-1} y_t) - \boldsymbol{I}\boldsymbol{\kappa}^{-1}(\boldsymbol{I} - \boldsymbol{\kappa})\boldsymbol{I}'(F_{2,t-1} y_t - F_{t-1} y_t),$$

which is Equation (24) in the main text.

The estimated coefficient β_{CG}^{Trend} therefore is given by:

$$\begin{aligned}
\beta_{CG}^{Trend} &= \frac{cov(F_t y_t - F_{t-1} y_t, y_t - F_t y_t)}{var(F_t y_t - F_{t-1} y_t)} \\
&= \frac{cov(F_t y_t - F_{t-1} y_t, \boldsymbol{I}\boldsymbol{\kappa}^{-1}(\boldsymbol{I}-\boldsymbol{\kappa})\boldsymbol{I}'(F_t y_t - F_{t-1} y_t))}{var(F_t y_t - F_{t-1} y_t)} \\
&- \frac{cov(F_t y_t - F_{t-1} y_t, \boldsymbol{I}\boldsymbol{\kappa}^{-1}(\boldsymbol{I}-\boldsymbol{\kappa})\boldsymbol{I}'(F_{2,t-1} y_t - F_{t-1} y_t))}{var(F_t y_t - F_{t-1} y_t)} \\
&= \boldsymbol{I}\boldsymbol{\kappa}^{-1}(\boldsymbol{I}-\boldsymbol{\kappa})\boldsymbol{I}' - \boldsymbol{I}\boldsymbol{\kappa}^{-1}(\boldsymbol{I}-\boldsymbol{\kappa})\boldsymbol{I}' \frac{cov(F_t y_t - F_{t-1} y_t, F_{2,t-1} y_t - F_{t-1} y_t)}{var(F_t y_t - F_{t-1} y_t)} \\
&= \frac{1-\boldsymbol{\kappa}_{11}}{\boldsymbol{\kappa}_{11}} + \frac{1-\boldsymbol{\kappa}_{22}}{\boldsymbol{\kappa}_{22}} + \frac{\boldsymbol{\kappa}_{11}\boldsymbol{\kappa}_{12}(\boldsymbol{\kappa}_{21}-\boldsymbol{\kappa}_{22}) + \boldsymbol{\kappa}_{22}\boldsymbol{\kappa}_{21}(\boldsymbol{\kappa}_{12}-\boldsymbol{\kappa}_{11})}{\boldsymbol{\kappa}_{11}\boldsymbol{\kappa}_{22}(\boldsymbol{\kappa}_{11}\boldsymbol{\kappa}_{22}-\boldsymbol{\kappa}_{12}\boldsymbol{\kappa}_{21})} \\
&- \boldsymbol{I}\boldsymbol{\kappa}^{-1}(\boldsymbol{I}-\boldsymbol{\kappa})\boldsymbol{I}' \frac{cov(F_t y_t - F_{t-1} y_t, F_{2,t-1} y_t - F_{t-1} y_t)}{var(F_t y_t - F_{t-1} y_t)},
\end{aligned}$$

which is Equation (23) in the main text.

From the third equality, we observe that to show $\beta_{CG}^{Trend} > 0$, it is sufficient and necessary to show:

$$\frac{cov(F_t y_t - F_{t-1} y_t, F_{2,t-1} y_t - F_{t-1} y_t)}{var(F_t y_t - F_{t-1} y_t)} < 1.$$

The condition can then be rewritten as:

$$\begin{aligned}
&var(F_t y_t - F_{t-1} y_t) - cov(F_t y_t - F_{t-1} y_t, F_{2,t-1} y_t - F_{t-1} y_t) \\
&= cov(F_t y_t - F_{t-1} y_t, F_t y_t - F_{2,t-1} y_t) \\
&= \frac{1}{\Omega^2}\{[V + \sigma_e^2\sigma_\mu^2 + (1-\rho)\sigma_e^2\sigma_z^2]^2\sigma_\mu^2 + [V + \sigma_\epsilon^2\sigma_x^2 + \rho(\rho-1)\sigma_\epsilon^2\sigma_z^2]^2\sigma_x^2 \\
&+ [\sigma_\epsilon^2(\sigma_x^2+\sigma_e^2) - \rho\sigma_e^2(\sigma_\mu^2+\sigma_\epsilon^2)]^2\overline{\sigma}_z^2\} \\
&> 0,
\end{aligned}$$

where $\overline{\sigma}_z^2 = E[(\overline{E}[z_{i,t}])^2]$ is the variance of separation error at the consensus level.

The intuition follows from the first equality. Note that the term $F_t y_t - F_{t-1} y_t$ represents the revision in forecast between the current period and the previous period after observing the private signal. The term $F_t y_t - F_{2,t-1} y_t$ represents the revision in forecast between the current period and the forecast at the end of the previous period after observing the actual state y_{t-1}. Therefore, their covariance shall be positive.

Proof of Proposition 6. For those who correctly use the signals, their expectations

regarding the two components are:

$$E^c_{i,t}[\mu_t] = \frac{\sigma^2_\mu s^\mu_{i,t} + \sigma^2_\epsilon \mu_{t-1}}{\sigma^2_\mu + \sigma^2_\epsilon} \quad \text{and} \quad E^c_{i,t}[x_t] = \frac{\sigma^2_x s^x_{i,t} + \sigma^2_e \rho x_{t-1}}{\sigma^2_x + \sigma^2_e}.$$

The cross-forecaster mean beliefs regarding the two components of the group who correctly interpret the signals are:

$$E^C[\mu_t] = \mu_t - \frac{\sigma^2_\epsilon}{\sigma^2_\mu + \sigma^2_\epsilon}\gamma^\mu_t, \quad \text{and} \quad E^C[x_t] = x_t - \frac{\sigma^2_e}{\sigma^2_x + \sigma^2_e}\gamma^x_t.$$

For those who wrongly interpret the signals, their expectations regarding the two components are:

$$E^W_{i,t}[\mu_t] = \frac{\sigma^2_\mu s^x_{i,t} + \sigma^2_\epsilon \mu_{t-1}}{\sigma^2_\mu + \sigma^2_\epsilon} \quad \text{and} \quad E^W_{i,t}[x_t] = \frac{\sigma^2_x s^\mu_{i,t} + \sigma^2_e \rho x_{t-1}}{\sigma^2_x + \sigma^2_e}.$$

The cross-forecaster mean beliefs regarding the two components of the group who wrongly interpret the signals are:

$$E^W[\mu_t] = \frac{\sigma^2_\mu x_t + \sigma^2_\epsilon \mu_{t-1}}{\sigma^2_\mu + \sigma^2_\epsilon}, \quad \text{and} \quad E^W[x_t] = \frac{\sigma^2_x \mu_t + \sigma^2_e \rho x_{t-1}}{\sigma^2_x + \sigma^2_e}.$$

The forecast variance across all forecasters then is given by:

$$\begin{aligned} Var(F_{i,t}y_{t+h}) &= Var(\mu^i_{1,t}) + \rho^{2h} Var(x^i_{1,t}) + \rho^h E[(\mu^i_{1,t} - E[\mu_t])(x^i_{1,t} - E[x_t])] \\ &= \rho^{2h}[\tau\phi^C_w \text{Var}^C_w + (1-\tau)\phi^C_c \text{Var}^C_c] + [\tau\phi^T_w \text{Var}^T_w + (1-\tau)\phi^T_c \text{Var}^T_c] \\ &+ \rho^h(1-\tau)\tau\widetilde{\text{COV}}_m, \end{aligned}$$

where ϕ^C_w, ϕ^C_c, ϕ^T_w, and ϕ^T_c are positive scalars between 0 and 1:

$$\phi^C_w = \frac{\sigma^2_x \sigma^2_\epsilon}{\sigma^4_e + \sigma^2_x \sigma^2_\epsilon}; \qquad \phi^C_c = \frac{\sigma^2_x}{\sigma^2_e + \sigma^2_x};$$
$$\phi^T_w = \frac{\sigma^2_\mu \sigma^2_e}{\sigma^4_\epsilon + \sigma^2_\mu \sigma^2_e}; \qquad \phi^T_c = \frac{\sigma^2_\mu}{\sigma^2_\mu + \sigma^2_\epsilon}.$$

The first-order derivative of the $Var(F_{i,t}y_{t+h})$ regarding the forecast horizon h is:

$$\frac{\partial Var(F_{i,t}y_{t+h})}{\partial h} = 2\rho^{2h} \ln\rho \left[\tau\phi^C_w \text{Var}^C_w + (1-\tau)\phi^C_c \text{Var}^C_c\right] + (1-\tau)\tau\rho^h \ln\rho\widetilde{\text{COV}}_m.$$

The forecast variance is increasing in h, if and only if:

$$h > \underline{h}_m = \frac{1}{\ln \rho} \ln\left(-\tau(1-\tau)\right) \frac{\widetilde{\text{COV}}_m}{2[\tau \phi_w^C \text{Var}_w^C + (1-\tau)\phi_c^C \text{Var}_c^C]}.$$

C Supplemental materials

C.1 Common Shock

In this section, we analyze the case of correlated trend and cyclical components driven by a common shock, by following Delle Monache et al. (2024). They show the presence of a common shock influencing both the trend and cyclical components of GDP growth in the same direction.

This common shock assumption is widely used in the literature. It captures situations where economic shocks have both transitory and permanent effects. Many studies show that recessions impact the economy in both temporary and lasting ways. For example, Furlanetto et al. (2021) and Antolin-Diaz et al. (2017) show that supply shocks can negatively affect both the cyclical and permanent components of GDP. Similarly, Almeida et al. (2004) finds that an increase in firms' profitability can permanently elevate their cash flows while also boosting short-term cash flows by reducing potential losses.

In this section, we consider the following state generation process:

$$y_t = \mu_t + x_t,$$

$$\mu_t = \mu_{t-1} + \gamma_t^{\mu} + \delta_t \quad \text{and} \quad x_t = \rho x_{t-1} + \gamma_t^{x} + b\delta_t,$$

where δ_t is a common shock affecting both the trend and cyclical components. This shock is normally distributed with zero mean and variance σ_δ^2, and is independent across periods (i.e., $\delta_t \sim N(0, \sigma_\delta^2)$). The scalar b measures the relative importance of the shock to each of these components. Notably, following Delle Monache et al. (2024), we assume that b is positive, thereby capturing the common shock assumption.

To contrast with our benchmark model, we assume in this case that the trend component becomes observable at the end of each period. With the information structure, the belief updating process is given by:

$$\boldsymbol{\theta}_{1,t}^i = \boldsymbol{\theta}_{2,t-1}^i + \boldsymbol{\kappa}_{cor}(\boldsymbol{s}_{i,t} - \boldsymbol{\theta}_{2,t-1}^i), \tag{C20}$$

where $\boldsymbol{\theta}_{2,t-1}^i = (\mu_{t-1}, \rho x_{t-1})'$. Since forecasters are able to observe the actual trend and cyclical components at the end of each period, $\boldsymbol{\kappa}_{cor}$ is the corresponding Kalman gain

matrix given by:

$$\boldsymbol{\kappa}_{cor} = \begin{pmatrix} \frac{\tau_2^\mu}{\tau_1^\mu+\tau_2^\mu+\tau_3^\mu} & \frac{\tau_3^\mu}{b(\tau_1^\mu+\tau_2^\mu+\tau_3^\mu)} \\ \frac{b\tau_3^x}{\tau_1^x+\tau_2^x+\tau_3^x} & \frac{\tau_2^x}{\tau_1^x+\tau_2^x+\tau_3^x} \end{pmatrix}, \tag{C21}$$

where $\tau_1^\mu, \tau_2^\mu, \tau_3^\mu, \tau_1^x, \tau_2^x, \tau_3^x$ are the precisions of information:

$$\tau_1^\mu = \frac{1}{\sigma_\mu^2+\sigma_\delta^2}; \quad \tau_2^\mu = \frac{1}{\sigma_\epsilon^2}; \quad \tau_3^\mu = \frac{b^2}{b^2\sigma_\mu^2+\sigma_x^2+\sigma_e^2};$$

$$\tau_1^x = \frac{1}{\sigma_x^2+b^2\sigma_\delta^2}; \quad \tau_2^x = \frac{1}{\sigma_e^2}; \quad \tau_3^x = \frac{1}{b^2\sigma_\mu^2+b^2\sigma_\epsilon^2+\sigma_x^2}.$$

As shown in Equation (C21), the elements on the sub-diagonal is non-zero if $b \neq 0$. Given $b > 0$, the sub-diagonal elements are positive. This is because the surprise from the trend signal (i.e., $s_{i,t}^\mu - \mu_{t-1}$) contains information about the common shock, which also affects the cyclical components. Therefore, forecasters would use the trend signal to update their belief about the cyclical belief, and vice versa.

We show that in this case, the covariance between forecasters' trend beliefs and cyclical beliefs (i.e., $\widetilde{\text{COV}}_{cor}$) is always positive:

$$\widetilde{\text{COV}}_{cor} \propto b(\sigma_\delta^2+\sigma_\mu^2)[b^2(\sigma_\epsilon^2+\sigma_\mu^2)+\sigma_e^2+\sigma_x^2][\sigma_\delta^2(b^2\sigma_\epsilon^2+b^2\sigma_\mu^2+\sigma_e^2+\sigma_x^2)+\sigma_e^2(\sigma_\epsilon^2+\sigma_\mu^2)+\sigma_\epsilon^2\sigma_x^2]. \tag{C22}$$

With a positive covariance, predictions of this particular case would be similar to the special case discussed in Section 4.1, and therefore inconsistent with the observed empirical pattern.

C.2 Forecast of other forecasters

This section characterizes the case where forecasters not only observe the actual state value but also observe the forecasts from other forecasters. In our model, the individual forecast error comprises both the individual-specific forecast error and the common forecast error, while the consensus forecast includes only the common forecast error. Therefore, forecaster i would anchor to the consensus forecasts after observing the entire distribution.

That is, at the end of the period $t-1$, the individual separation error $z_{i,t-1}$ would be the same across different forecasters (i.e., $z_{t-1} = z_{i,t-1} = z_{j,t-1}$ for any i, j). Specifically, at the end of period t, forecasters observe the actual state value of the current period, y_{t-1}, and the forecasts, $F_{i,t-1}y_{t-1+h}$, from other forecasters. The separation error, z_{t-1}, is given by:

$$z_{t-1} = \frac{(\overline{\text{Var}}^T + \overline{\text{COV}})(x_{t-1} - x_{1,t-1}) - (\overline{\text{Var}}^C + \overline{\text{COV}})(\mu_{t-1} - \mu_{1,t-1})}{(\overline{\text{Var}}^T + \overline{\text{COV}}) + (\overline{\text{Var}}^C + \overline{\text{COV}})} \neq 0,$$

where $\mu_{t-1} - \mu_{1,t-1}$ and $x_{t-1} - x_{1,t-1}$ are the consensus forecast errors regarding the trend component and cyclical component:

$$\mu_{t-1} - \mu_{1,t-1} = \frac{\sigma_\epsilon^2(\rho^2\bar{\sigma}_z^2 + \sigma_x^2 + \sigma_e^2)}{\bar{\Omega}}\gamma_{t-1}^{\mu} + \frac{\rho\sigma_\epsilon^2\bar{\sigma}_z^2}{\bar{\Omega}}\gamma_{t-1}^{x} - \frac{\sigma_\epsilon^2(\sigma_x^2 + \sigma_e^2)}{\bar{\Omega}}z_{t-2},$$

$$x_{t-1} - x_{1,t-1} = \frac{\rho\sigma_e^2\bar{\sigma}_z^2}{\bar{\Omega}}\gamma_{t-1}^{\mu} + \frac{\sigma_e^2(\bar{\sigma}_z^2 + \sigma_\mu^2 + \sigma_\epsilon^2)}{\bar{\Omega}}\gamma_{t-1}^{x} + \frac{\rho\sigma_e^2(\sigma_\mu^2 + \sigma_\epsilon^2)}{\bar{\Omega}}z_{t-2}.$$

At the beginning of the current period t, after observing their private signals, individual forecasters' beliefs regarding the trend and cyclical components are still heterogeneous. Their beliefs are given by:

$$\mu_{1,t}^i = \frac{\sigma_\epsilon^2(\rho^2\bar{\sigma}_z^2 + \sigma_x^2 + \sigma_e^2)}{\bar{\Omega}}\mu_{2,t-1} + \frac{\bar{V} + \sigma_e^2(\bar{\sigma}_z^2 + \sigma_\mu^2)}{\bar{\Omega}}s_{i,t}^{\mu} - \frac{\rho\sigma_\epsilon^2\bar{\sigma}_z^2}{\bar{\Omega}}(s_{i,t}^{x} - \rho x_{2,t-1}),$$

$$x_{1,t}^i = \frac{\sigma_e^2(\bar{\sigma}_z^2 + \sigma_\mu^2 + \sigma_\epsilon^2)}{\bar{\Omega}}\rho x_{2,t-1} + \frac{\bar{V} + \sigma_\epsilon^2(\sigma_x^2 + \rho^2\bar{\sigma}_z^2)}{\bar{\Omega}}s_{i,t}^{x} - \frac{\rho\sigma_e^2\bar{\sigma}_z^2}{\bar{\Omega}}(s_{i,t}^{\mu} - \mu_{2,t-1}),$$

where $\bar{\sigma}_z^2$ is the variance of the common separation error. Note that $\mu_{2,t-1} = \mu_{t-1} + z_{t-1}$ and $\rho x_{2,t-1} = \rho x_{t-1} - \rho z_{t-1}$ are the common prior beliefs. Furthermore, $\bar{\Omega}$ and $\bar{V}$ are constants:

$$\bar{\Omega} = (\bar{\sigma}_z^2 + \sigma_\mu^2 + \sigma_\epsilon^2)(\sigma_x^2 + \sigma_e^2 + \rho^2\bar{\sigma}_z^2) - \rho^2\bar{\sigma}_z^4, \;\; \bar{V} = (\bar{\sigma}_z^2 + \sigma_\mu^2)(\sigma_x^2 + \rho^2\bar{\sigma}_z^2) - \rho^2\bar{\sigma}_z^4.$$

In summary, if forecasters can observe all the forecasts provided by other forecasters, the separation error across all forecasters would be common, which would be a weighted average of all historical state innovations. However, it is still non-zero, indicating that forecasters still cannot perfectly separate the two components. Therefore, our results obtained under the benchmark model still hold.

C.3 Misinterpretation of Signals

This subsection consider an alternative model that differs from our benchmark model in two ways. First, we assume that forecasters can observe not only the state value (i.e., y_{t-1}) at the end of each period but also the trend and cyclical components perfectly (i.e., μ_{t-1} and x_{t-1}). Consequently, there is no confusion about these components at the end of each period. Second, we introduce the possibility of forecasters misinterpreting the signals before they make forecasts. Specifically, there is a probability τ that a forecaster may interpret the trend signal as a cyclical one and, at the same time, treat the cyclical signal as a trend signal.

In this model, each forecaster updates their beliefs and forms expectations using

the Bayesian rule, even though there is a possibility of misinterpreting signals. That is,

$$\boldsymbol{\theta}_{1,t}^{i} = \boldsymbol{\theta}_{2,t-1} + \boldsymbol{\kappa} \times (\boldsymbol{s}_{i,t} - \boldsymbol{\theta}_{2,t-1}), \tag{C23}$$

where $\boldsymbol{\theta}_{2,t-1}$ is $(\mu_{t-1}, x_{t-1})'$ for all forecasters, as the actual value of the components from the previous period is perfectly observed and the Kalman gain matrix $\boldsymbol{\kappa}$ is standard:

$$\boldsymbol{\kappa} = \begin{pmatrix} \frac{\sigma_\mu^2}{\sigma_\epsilon^2+\sigma_\mu^2} & 0 \\ 0 & \frac{\sigma_x^2}{\sigma_e^2+\sigma_x^2} \end{pmatrix}.$$

For those who correctly interpret the signals, $\boldsymbol{s}_{i,t}$ is represented as $(s_{i,t}^{\mu}, s_{i,t}^{x})'$. And the variance-covariance matrix of their beliefs is given by:

$$\begin{pmatrix} \text{Var}_c^T & \widetilde{\text{COV}}_c \\ \widetilde{\text{COV}}_c & \text{Var}_c^C \end{pmatrix} = \begin{pmatrix} \frac{\sigma_\epsilon^2\sigma_\mu^2}{\sigma_\epsilon^2+\sigma_\mu^2} & 0 \\ 0 & \frac{\sigma_e^2\sigma_x^2}{\sigma_x^2+\sigma_e^2} \end{pmatrix}.$$

For those who wrongly interpret the signals, $\boldsymbol{s}_{i,t}$ is represented as $(s_{i,t}^{x}, s_{i,t}^{\mu})'$, the corresponding variance-covariance matrix of their beliefs is:

$$\begin{pmatrix} \text{Var}_w^T & \widetilde{\text{COV}}_w \\ \widetilde{\text{COV}}_w & \text{Var}_w^C \end{pmatrix} = \begin{pmatrix} \frac{\sigma_\mu^2(\sigma_\epsilon^4+\sigma_\mu^2\sigma_e^2)}{(\sigma_\epsilon^2+\sigma_\mu^2)^2} & 0 \\ 0 & \frac{\sigma_x^2(\sigma_e^4+\sigma_x^2\sigma_\epsilon^2)}{(\sigma_x^2+\sigma_e^2)^2} \end{pmatrix}.$$

We first examine the model's prediction about the covariance between the changes in the long term forecasts and cyclical forecasts. It is important to note that the Kalman gain matrix in Equation (C23) indicates that individuals' belief updating for the trend and cyclical components is independent. As a result, one's subjective beliefs regarding these components are also independent. Thus, we have $\widetilde{COV} = 0$. Therefore, the covariance of the changes in long term forecasts and cyclical forecasts becomes:

$$COV_F^h = (\rho^h - \rho^{3Y})\rho^{3Y} var(E[x_{i,t}] - E[x_{i,t-1}]) \geq 0.$$

In other word, the misinterpretation model always predicts a non-negative covariance between the changes in long term forecasts and cyclical forecasts, which is inconsistent with the fact documented in section 2.

Next, we examine the model's prediction of the forecast dispersion across forecast horizons. Proposition 6 summarizes our the result regarding the dispersion of forecasts over horizon.

Proposition 6. *If the individual forecaster may misinterpret the signals with a probability τ, the dispersion of forecasts across forecasters is increasing in the forecast horizon h, if and only*

if:

$$h > \underline{h}_m = \frac{1}{\ln \rho} \ln [\tau(1-\tau)] \frac{-\widetilde{COV}_m}{2[\tau \phi_w^C Var_w^C + (1-\tau)\phi_c^C Var_c^C]}, \tag{C24}$$

where $0 < \phi_w^C < 1$, $0 < \phi_c^C < 1$, $\widetilde{COV}_m = -\frac{(\sigma_\mu^2+\sigma_x^2)\sigma_x^2\sigma_\mu^2}{(\sigma_\epsilon^2+\sigma_\mu^2)(\sigma_\epsilon^2+\sigma_x^2)}$ *and* $\ln \rho < 0$.

Proposition 6 states that, similar to the benchmark model, the forecast variance increases as the forecast horizon extends when h is larger than a threshold $\underline{h}_m$. Interestingly, when everyone correctly interprets the signals (i.e., $\tau = 0$), or everyone misinterprets the signals (i.e., $\tau = 1$), the threshold $\underline{h}_m$ approaches infinity. This implies that the forecast variance decreases monotonically over the horizon. Furthermore, the threshold $\underline{h}_m$ could be negative if the value of τ falls within the intermediate range. This implies that the forecast variance increases monotonically over the horizon.

To understand this result, we examine the forecast variance, which can be decomposed as the dispersion of the cyclical beliefs across forecasters, the dispersion of the trend beliefs across forecasters, and their covariance:

$$\begin{aligned} Var(F_{i,t} y_{t+h}) = \rho^{2h}[\tau \phi_w^C \mathrm{Var}_w^C + (1-\tau)\phi_c^C \mathrm{Var}_c^C] + [\tau \phi_w^T \mathrm{Var}_w^T + (1-\tau)\phi_c^T \mathrm{Var}_c^T] \\ + \rho^h (1-\tau)\tau \widetilde{\mathrm{COV}}_m. \end{aligned} \tag{C25}$$

The covariance across forecasters (i.e., the third term) arises because forecasters can be divided into two groups in this model: those who misinterpret the signals and those who correctly use them. To illustrate, consider there is a positive strong trend signal. This signal would increase the trend forecasts of those who correctly interpret it and the cyclical beliefs of those who misinterpret it as a cyclical signal. As a result, due to the presence of individuals who misinterpret the signal, the trend forecast of the entire population, on average, is lower than it should be, while the cyclical belief is higher than it should be. This creates a negative covariance between mean forecaster beliefs about the trend and cyclical components, even though the beliefs of individuals regarding these components are independent.

As the forecast horizon extends, similar to the benchmark model, the dispersion of the cyclical beliefs decreases, and the covariance term increases. If the increase in the covariance term is more pronounced, the forecast variance would increase as the forecast horizon extends.